Relativistic Jets in Active Galactic Nuclei and Microquasars

**Gustavo E. Romero · M. Boettcher ·
S. Markoff · F. Tavecchio**

Abstract Collimated outflows (jets) appear to be a ubiquitous phenomenon associated with the accretion of material onto a compact object. Despite this ubiquity, many fundamental physics aspects of jets are still poorly understood and constrained. These include the mechanism of launching and accelerating jets, the connection between these processes and the nature of the accretion flow, and the role of magnetic fields; the physics responsible for the collimation of jets over tens of thousands to even millions of gravitational radii of the central accreting object; the matter content of jets; the location of the region(s) accelerating particles to TeV (possibly even PeV and EeV) energies (as evidenced by γ-ray emission observed from many jet sources) and the physical processes responsible for this particle acceleration; the radiative processes giving rise to the observed multi-wavelength emission; and the topology of magnetic fields and their role in the jet collimation and particle acceleration processes. This chapter reviews the main knowns and unknowns in our current understanding of relativistic jets, in the context of the main model ingredients for Galactic and extragalactic jet sources. It discusses aspects specific to active Galactic nuclei (especially

Gustavo E. Romero
Instituto Argentino de Radioastronoma (IAR), C.C. No. 5, 1894, Buenos Aires,
Argentina
E-mail: romero@iar-conicet.gov.ar

M. Boettcher
Centre for Space Research, Private Bag X6001, North-West University, Potchefstroom, 2520, South Africa
E-mail: Markus.Bottcher@nwu.ac.za

S. Markoff
Anton Pannekoek Institute for Astronomy, University of Amsterdam, 1098XH Amsterdam, The Netherlands
E-mail: s.b.markoff@uva.nl

F. Tavecchio
INAF-Osservatorio Astronomico di Brera, Via Bianchi 47, 23807 Merate, Italy
E-mail: fabrizio.tavecchio@brera.inaf.it

blazars) and microquasars, and then presents a comparative discussion of similarities and differences between them.

1 Introduction

Relativistic jets are collimated outflows of plasma and fields produced by accreting compact objects. The bulk motion of the plasma is close to the speed of light, so relativistic effects play an important role in the physical processes in these jets. The jet phenomenon appears to be common wherever mass accretion onto a central object occurs, and they become relativistic in the case of accretion onto compact objects, such as neutron stars or black holes, both in Galactic systems (neutron star and black-hole X-ray/γ-ray binaries, hereafter termed generically XRBs — termed microquasars when they exhibit prominent radio jets) and in extragalactic systems (active galactic nuclei [AGN], gamma-ray bursts [GRBs] and recently Tidal Disruption Events [TDEs]). Relativistic jets are ionized and produce non-thermal radiation from radio to gamma-rays in some cases. Observationally, in most cases, the presence of non-thermal radio emission has been the primary signature of relativistic jets, distinguishing jet-dominated radio-loud AGN from their radio-quiet counterparts (with very weak or absent jets), and microquasars (XRB states with prominent radio jets) from radio-quiet XRB states. In this chapter, we will focus on the relativistic jets from AGN and microquasars, while the physics of GRB and TDE jets is discussed extensively in chapters 6 – 8, and jets from pulsars in chapter 2.

The existence of jet-like structures was known as a peculiarity of some galaxies such as M87 since the early twentieth century (Curtis 1918). By the mid 1950s it was recognized that the extended radio emission in M87 was the result of synchrotron radiation (Burbidge 1956). The synchrotron hypothesis was soon applied to explain the extended radio lobes observed in some galaxies (Ginzburg 1961, Shklovskii 1961). After the discovery of quasars (Schmidt 1963) at large cosmological redshifts, it became clear that some of the radio sources were extremely distant and the size and total energy output of the radio emitting clouds was huge. The cooling time of the electrons responsible for the radiation is much shorter than the dynamical timescales, thus indicating a need for in-situ acceleration of relativistic particles along the jets and in the radio lobes. Fully non-thermal radio jets were soon detected in many radio galaxies using interferometric techniques. Structural time variations were also detected in these jets, and superluminal motions, originally predicted by Rees (1966) were found, first in the jet of the quasar 3C273, and later in many other sources (see Zensus and Pearson 1987, and references therein).

In our own galaxy, relativistic jets were associated with the emission line star SS433 (e.g., Abell and Margon 1979). The jets of this source, a compact object accreting from a companion star, precess with a 164-day period.

Only much later, in the 1990s, other X-ray binary sources mimicking the behaviour of extragalactic quasars were found (Mirabel et al. 1992) and superluminal motions observed within the Galaxy (Mirabel and Rodríguez 1994). XRBs with relativistic radio jets were dubbed "microquasars". About 15 such sources are currently classified as microquasars because of explicit measurements of relativistic proper motion, but $\sim$50 XRBs have by now been observed in the jet-dominated 'hard state' (Tetarenko et al. 2016, and see Section 4), and many more are suspected to exist in the Milky Way.

With the advent of orbiting X-ray observatories such as *Einstein*, *EXOSAT*, *ROSAT*, and more recently *RXTE*, *XMM-Newton*, *Chandra*, *Swift*, and *NuSTAR*, and the opening-up of the γ-ray sky especially with the Compton Gamma-Ray Observatory in the 1990s and more recently with *AGILE*] and the *Fermi* Gamma-Ray Space Telescope, it became soon clear that both Galactic and extragalactic jets are high-energy sources. Their spectral energy distribution (SED) is strongly dominated by non-thermal emission from radio up to γ-ray frequencies, and in many cases it is dominated by the γ-ray component that extends up to GeV and even TeV energies (see, e.g., Maraschi and Tavecchio 2001, Abdo et al. 2010). The emission from these objects tends to be highly variable at all wavelengths, with often complex — sometimes correlated, but sometimes also uncorrelated among different wavelength regimes — flux and spectral variability patterns, that may change character even within the same source among different eposides of activity. The study of these complex radiative features of relativistic jets is the only way to gain insight into the physical conditions of the outflowing plasma and the mechanisms that result in the jet launching and subsequent particle acceleration. However, even after over three decades of intensive multi-wavelength observing campaigns (including observations from the radio to γ-rays) and remarkable progress in general relativistic magnetohydrodynamic (GRMHD) and particle-in-cell (PIC) simulations of plasma phenomena relevant to jet launching, the dynamics, and particle acceleration, many fundamental aspects of the jet phenomenon are still very poorly understood or even constrained. This chapter attempts to summarize the cutting edge, as well as elucidate potential avenues for future research, in order to gain insight into the answers to these open questions:

— What is the primary physical mechanism powering the acceleration and collimation of the jet? Is the primary energy source the rotational energy of the black hole (Blandford and Znajek 1977), or is power released in the accretion flow the primary driver (Blandford and Payne 1982)? In the latter case, one would expect a tight connection between the observational signatures of the accretion flow and the presence/absence of relativistic jets, as is, indeed, observed in many Galactic systems, but also evidence for a correlation between black-hole spin and jet power has been claimed (e.g., McClintock et al. 2014, see Section 4 for a discussion). In general, what is the role of magnetic fields in the acceleration and collimation of relativistic jets?
— To what extent can the accretion and jet processes involving supermassive black holes in AGN be considered as simply scaled-up versions of the microquasar phenomenon? While the source of the accreted material

and thus the accretion-flow geometry is quite different, many aspects, such as mass-scaled short-term variability patterns and the characteristic two-component, non-thermal spectral energy distributions, appear to indicate a large degree of analogy between the two phenomena on different scales (e.g., Markoff et al. 2015).

– What is the strength and topology of magnetic fields along relativistic jets, and what role do they play in the collimation of jets out to tens of thousands of gravitational radii, as well as the acceleration of relativistic particles in-situ along the jets? What determines where particle acceleration begins, a region often modeled as a single zone for e.g., blazars (see Section 3), but also becoming a focus now for XRBs (see Section 4).

– What is the matter content of material flowing along the jets? Is it primarily an electron-positron pair plasma, or an ordinary electron-proton plasma (see, e.g., Sikora and Madejski 2000)? If protons are present in significant numbers, are they also subject to relativistic particle acceleration?

– What are the dominant radiation mechanisms leading to the observed two-component non-thermal emission seen from relativistic jet sources? Are these primarily leptonic processes, with protons (if present) not contributing to the radiative output, or are protons also accelerated to ultrarelativistic energies so that hadronic processes can make a significant contribution (see, e.g., Böttcher et al. 2013, for a comparative analysis of both types of models in the case of blazars)? If the latter is the case, then AGN may be the elusive sources of ultra-high-energy cosmic rays (UHECRs, i.e., cosmic-rays with energies $E > 10^{19}$ eV). Also, the acceleration of UHECRs in AGN environments is likely to result in charged-pion production, leading to the emission of PeV neutrinos, as recently confidently detected by the IceCube neutrino observatory (Aartsen et al. 2014).

In this chapter, we will discuss the physics and phenomenology that is common to relativistic jets on different size scales, from astronomical units to kiloparsecs. We will focus on the jets of microquasars and blazars, with emphasis on their radiative output. We will first introduce the basic, common model ingredients required for any model of relativistic jets of different sizes and velocities (Section 2). Against this background, we will offer an overview of the current knowledge about particle acceleration within the jets of blazars (Section 3) and microquasars (Section 4). The final section (5) provides a comparative discussion of the prevalent issues in blazar and microquasar jet physics, and an outlook towards future experiments that may shed light on these issues. The reader interested in extensive treatments of this subject may consult the recent monagraphs and collections by Beskin (2009), Belloni (2010), Böttcher (2010), Markoff (2010) and Romero and Vila (2014).

2 Basic Model Ingredients: Knowns and (Educated) Guesses

Wherever accretion of matter with angular momentum and magnetic fields into a gravitational well occurs, an accretion disk is formed, often accompanied by the expulsion of collimated outflows. When the gravitating object is compact (a weakly magnetized neutron star or a black hole), it is capable of launching relativistic outflows, although the exact mechanism is not yet clear. Models of relativistic jets were first developed for Active Galactic Nuclei (AGN) at the end of the 1970s and early 1980s (e.g., Blandford and Königl 1979, Marscher 1980a,b, Marscher and Gear 1985) and later adapted to microquasars (by then not known with this name) by Band and Grindlay (1986), Hjellming and Johnston (1988), Levinson and Blandford (1996).

In these early models for the broadband emission from jets, it is assumed that only leptons (electrons and positrons) are accelerated, and thus contributing significantly to the radiation, with protons (if present) not achieving sufficiently high energy. Such models are termed *leptonic models*, and they have achieved an increasing degree of sophistication over the past several decades, both for Galactic (e.g., Markoff et al. 2001a, 2005a, Georganopoulos et al. 2002, Kaufman Bernadó et al. 2002, Bosch-Ramon et al. 2006, Zdziarski et al. 2014) and extragalactic jets (e.g., Maraschi et al. 1992, Dermer and Schlickeiser 1993, Blandford and Levinson 1995, Levinson and Blandford 1995, Marcowith et al. 1995, Romero et al. 1995, Böttcher et al. 1997, Böttcher and Chiang 2002, Markoff et al. 2015).

Alternatively, if protons are accelerated to ultrarelativistic energies they may contribute significantly to the radiative output, and the corresponding class of models is termed *hadronic models* or *lepto-hadronic models*, to indicate that even in those models, relativistic leptons make a significant contribution to the SED, especially at low frequencies. For lepto-hadronic jet models for Galactic sources, see, e.g., Romero et al. (2003, 2005), Romero and Vila (2008), Vila and Romero (2010), Vila et al. (2012), Yan and Zhang (2015), Cerruti et al. (2015), Pepe et al. (2015) and for extragalactic sources, Mannheim (1993), Rachen and Biermann (1993), Mücke et al. (2003a), Reynoso et al. (2011, 2012), Böttcher et al. (2013).

As indicated in Section 1, many aspects of the jet geometry, magnetization, mode of particle acceleration and the location of the dominant energy dissipation and particle acceleration zone are currently still unknown, leaving a significant amount of freedom in the choice of model parameters. The various models of relativistic jets differ in the characteristics of the injection of relativistic particles, the properties of the region in the jet where the radiation is produced, the particles and physical interactions involved in the production of the radiation, the external conditions, the treatment of the transport of particles in the radiative zone, the inclusion of dynamical effects, the boundary and external medium conditions, the radiation reprocessing in the source, and many other factors.

The emission of high-energy and very-high-energy γ-rays requires the acceleration of particles to GeV and even TeV energies, which is likely to occur in relatively small, localized regions along the jet. Due to their short cooling time scale, those particles are expected to emit high-energy radi-

ation locally. The concept of a single, dominant, small emission region is further strengthened by the observed rapid variability which, due to the causality constraint, restricts the size of the emission region, in many cases, to the order of the gravitational radius of the central accreting object (e.g., Begelman et al. 2008). This gives credence to single-zone models, where the emitting region is considered to be homogeneous (usually assumed spherical but see, e.g. Giannios et al. 2009a) and the physical conditions uniform. Such models have been popular because of their relative simplicity. However, the often observed lack of strict correlations between variability patterns in different wavelength regimes demonstrates that they may be applicable primarily only to short-term, isolated flaring events in which the emission is likely to be dominated by a single, small emission region. Nevertheless, single-zone models may be characterized by a limited number of parameters, many of which can be reasonably well constrained from observables (for details on such observational parameter constraints, see Section 3 and 4). Hence, they have resulted in significant insight into the physical conditions and physical processes in the dominant high-energy emission region.

The necessity of inhomogenous (multi-zone) models has already been pointed out, e.g., by Ghisellini et al. (1985), but their implementation in a self-consistent way has been hampered by the large number of (poorly constrained) parameters required for such models. Only recently inhomogenous models with an adequate treatment of particle transport and all radiative processes have been developed. However these models have still not been made self-consistent with the magnetohydrodynamics (MHD) governing the plasma properties and flow characteristics, and which may determine how structures that accelerate particles are created. Ultimately the number of free parameters will be reduced once the macro- and microphysics can be linked, but this type of work is still in its early stages.

In what follows we will discuss the most important physical processes that enter relativistic jet models (both leptonic and lepto-hadronic) for both Galactic and extragalactic sources **in a generic model geometry as illustrated in Figure 1.** The discussion presented here rests upon the work by Markoff et al. (2005b), Vila et al. (2012), Pepe et al. (2015), Diltz and Böttcher (2014), Reynoso et al. (2012), Polko et al. (2014), Diltz et al. (2015), Zhang et al. (2014, 2015).

2.1 Energetics and geometry

A compact object (hereafter assumed to be a black hole) of mass M_{BH} accretes matter from its environment (in the case of a microquasars the accretion flow comes from a companion star). We write the accretion power L_{accr} in terms of the Eddington luminosity of the black hole as

$$L_{\mathrm{accr}} \equiv \dot{M}c^2 = q_{\mathrm{accr}}\, L_{\mathrm{Edd}} \approx 1.3 \times 10^{46} q_{\mathrm{accr}} \left(\frac{M_{\mathrm{BH}}}{10^8\, M_\odot} \right) \mathrm{erg\, s^{-1}}, \quad (1)$$
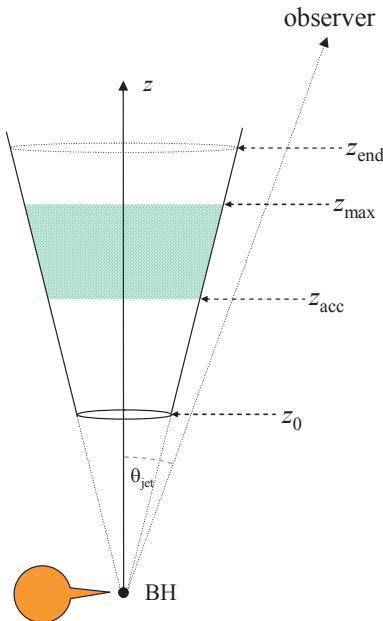
Fig. 1 Detail of a generic conical jet model, including the acceleration region (not to scale). Some relevant parameters are indicated.

where $\dot{M}$ is the mass accretion rate, $M_\odot$ is the solar mass, and q_{accr} is a dimensionless parameter. The accretion disk extends from an inner radius R_{in} to an outer radius R_{out}. For particularly lower luminosity (sub-Eddington) sources, within R_{in} the plasma is thought to become radiatively inefficient, "inflating" to form a hot, optically thin corona. The nature and geometry of this corona is a matter of significant debate (see, e.g. Nowak et al. 2011), however the existence of a population of hot electrons is necessary in any scenario.

A fraction of the accreted matter is ejected into two symmetrical jets, each carrying a power

$$L_{\mathrm{jet}} = \frac{1}{2} q_{\mathrm{jet}} \, L_{\mathrm{accr}}, \tag{2}$$

where $q_{\mathrm{jet}} < 1$. Note however that this assumption implicitly assumes the Blandford and Payne (1982) mechanism, thus if enhancement from the black hole spin is relevant (Blandford and Znajek 1977) this linear relationship with the accretion disk luminosity may no longer hold.

The jets are launched perpendicularly to the plane of the inner accretion disk at a distance z_0 from the black hole. The scale z_0 is the characteristic scale of the coronal plasma that is thought to surround the black hole (Romero et al. 2010). The jet might be the result of the evacuation of the corona by magnetocentrifugal effects, a hypothesis supported by the fact

that jets in XRBs are observed only in the hard state, when the accretion disk is truncated at a distance of the order of z_0. A spherical geometry for the corona seems to be the more appropriate on the basis of the intensity of the Compton reflection feature observed in some sources (e.g. Poutanen et al. 1997). It has been also suggested that the corona is essentially identical to the base of the jet (Markoff et al. 2005a). In any case, the full formation of the collimated outflow takes place at a distance z_0, and from there on the jet can be treated as a distinct physical component of the system.

The jet axis makes an angle $\theta_{\rm jet}$ with the line of sight to an observer on Earth. The exact geometry of the jet will be determined by the balance of internal and external pressure, and thus strongly depends on the plasma properties at launch, which are currently undetermined. There is evidence, e.g. in the case of M87, that the jet base is described by an approximately paraboidal shape, transitioning to a conical structure (Asada and Nakamura 2012, Potter and Cotter 2013) consisistent with predictions of a collimated, magnetically-dominated flow that is converted to a kinetically dominated flow. At large distances ($z \gg 10^5 \, r_g$, where $r_g = GM_{\rm BH}/c^2$ is the gravitational radius of the black hole), jets appear to be well collimated in a quasi-cylindrical structure. The simplest assumption, often adopted in the literature, is thus a constant jet radius over the section of the jet responsible for the majority of the radiative output. Alternatively, a conical geometry is often assumed, so that the jet cross-sectional radius grows as

$$r(z) = r_0 \left(\frac{z}{z_0} \right). \tag{3}$$

If magnetic energy is the primary driver of the outflow (i.e., the plasma is ejected by some magnetocentrifugal mechanism or driven by Poynting flux), the magnetic energy density at the base of the jet must be enough to set the plasma in motion. This requires at least as much energy in the magnetic field as kinetic energy the jet will achieve. In this case, the value B_0 of the magnetic field at z_0 may be constrained by the condition of equipartition between the magnetic and the kinetic energy densities, $U_{\rm mag}(z_0) \geq U_{\rm kin}(z_0)$. Then, assuming magnetic-flux conservation, the magnetic energy density decreases as the jet expands. One may parameterize the dependence on z of the magnetic field strength as

$$B(z) = B_0 \left(\frac{z_0}{z} \right)^m, \tag{4}$$

where the index $m \geq 1$ depends on the magnetic-field topology (e.g. Krolik 1999). In the case of a conical jet and a purely poloidal magnetic field (i.e., $B = B_z$), $m = 2$, whereas for a purely toroidal B-field (i.e., $B = B_\phi$), $m = 1$.

However, in the case of an MHD-driven outflow, such conservation is likely not valid. In a widely accepted model of jet acceleration (see, for example, Spruit 2010), a fraction of the magnetic energy is converted into kinetic energy of the plasma. The bulk Lorentz factor of the jet, $\Gamma_{\rm jet}$, then increases up to a maximal value. The behavior of $\Gamma_{\rm jet}$ with the distance to the black hole has been studied both analytically and numerically in

the context of ideal MHD (e.g., Lyubarsky 2009, Tchekhovskoy et al. 2008, 2010, Polko et al. 2014).

In the context of this simple model we parameterize dissipation in the region $z_{\rm acc} \leq z \leq z_{\rm max}$, where some fraction of the jet power is transformed into kinetic energy of relativistic electrons (and protons in the case of lepto-hadronic models). Possible acceleration mechanisms include diffusive shock acceleration (DSA, see, e.g., Summerlin and Baring 2012) or, in particular for jets with high magnetization, fast magnetic reconnection in presence of turbulence (e.g., Lazarian et al. 2015). If DSA is the dominant acceleration mechanism, the value of $z_{\rm acc}$ is constrained by the fact that, for shock waves to develop, the magnetic energy density of the plasma must be in sub-equipartition with the kinetic energy density (Komissarov et al. 2007). The power transferred to the relativistic particles is parameterized as

$$L_{\rm rel} = q_{\rm rel} L_{\rm jet}, \tag{5}$$

where $q_{\rm rel} < 1$. The value of $L_{\rm rel}$ is the sum of the power injected in both protons and electrons

$$L_{\rm rel} = L_p + L_e \equiv (1 + a)\, L_e \tag{6}$$

where we have defined an energy partion parameter a such that $L_p = a\, L_e$. If $a > 1$ the jet is proton-dominated (i.e., hadronic or lepto-hadronic models), whereas for $a < 1$ most of the power is injected in relativistic electrons (i.e., leptonic models).

2.2 Microphysical particle treatment

The relativistic particles in the jet lose energy by radiation and also adiabatic losses in the case of an expanding jet. Several processes contribute to the radiative cooling, since particles can interact with the magnetic, radiation, and matter fields of the jet.

The most important interaction channel with the magnetic field of the jet is synchrotron radiation. For a charged particle of mass m, energy $E = \gamma m c^2$, and charge $q = Z\,e$, the synchrotron energy-loss rate is (e.g., Blumenthal and Gould 1970)

$$\left. \frac{d\gamma}{dt} \right|_{\rm synchr} = -\frac{4}{3} \left(\frac{m_e}{m} \right)^3 \frac{c\sigma_{\rm T}\, U_{\rm mag}}{m_e c^2}\, Z^4\, \gamma^2, \tag{7}$$

where c is the speed of light, m_e is the electron mass, $\sigma_{\rm T}$ is the Thomson cross-section, and $U_{\rm mag}$ is the magnetic energy density. The ratio $(m_e/m)^3$ in Eq. (7) makes synchrotron cooling particularly efficient for the lightest particles.

Relativistic electrons also cool through inverse Compton (IC) scattering off the jet and potentially also external radiation fields. Writing the characteristic photon energy of the target photon field as $\epsilon = h\nu/(m_e c^2)$, the Compton scattering process with electrons is elastic in the electron

rest frame if $\epsilon\gamma \ll 1$, which denotes the Thomson regime. In this regime, the Compton cooling rate is identical to Equation 7, except for replacing the energy density U_{rmmag} by the energy density of the target radiation field, $U_{\rm rad}$. Due to the same suppression factor $(m_e/m)^3$, Compton scattering is very inefficient for particles heavier than electrons/positrons, and is therefore usually considered only for leptons. Only in cases where extreme energies for protons are possible, this channel must be taken into account also for heavier particles (e.g., Aharonian 2000, 2002)). For the more general case, in which the Thomson condition is not fulfilled (i.e., including the Klein-Nishina regime with $\epsilon\gamma \gtrsim 1$), the energy-loss rate needs to be evaluated considering recoil in the rest frame, using the full Klein-Nishina cross section, e.g. following Blumenthal and Gould (1970); see Böttcher et al. (1997), Dermer and Menon (2009), Böttcher et al. (2012) for detailed calculations of the Compton loss rates specific to blazars.

An important and ubiquitous target photon field is the synchrotron radiation co-spatially produced within the jet. This is referred to as the synchrotron-self-Compton (SSC) process, which often dominates the X-ray (and sometimes also γ-ray) emission in relativistic jet models. In a homogeneous single zone of radius R in steady-state, the radiation energy density $U_{\rm rad}$ is related to the emissivity $j_{\rm synchr}$ (i.e., the energy production rate per unit volume in synchrotron radiation) by

$$U_{\rm synchr}^{\rm homog} = \frac{3}{4}\frac{R}{c}\,j \qquad (8)$$

In more complex geometries, a convenient treatment lies in the "local approximation" of Ghisellini et al. (1985):

$$U_{\rm synchr}^{\rm local}(z) \approx j_{\rm synchr}(z)\,\frac{r_{\rm jet}(z)}{c}, \qquad (9)$$

Additional target photon fields for Compton scattering can originate outside the jet and include the radiation field from the accretion disk and of the stellar companion, in the case of microquasars, as well as line-dominated radiation from the Broad Line Region, Narrow Line Region, and a dusty torus around the central accretion flow in the case of AGN (see Sections 3 and 4 for more details).

The interaction of relativistic protons with radiation can create electron-positron pairs ("photopair" production via the Bethe-Heitler process)

$$p + \gamma \rightarrow p + e^- + e^+. \qquad (10)$$

The photon threshold energy for this process is ~ 1 MeV in the rest frame of the proton. At higher energies, proton-photon collisions can also yield pions ("photomeson" production). The two main channels are

$$p + \gamma \rightarrow p + a\pi^0 + b\left(\pi^+ + \pi^-\right) \qquad (11)$$

and

$$p + \gamma \rightarrow n + \pi^+ + a\pi^0 + b\left(\pi^+ + \pi^-\right), \qquad (12)$$

where the integers a and b are the pion multiplicities. Both channels have approximately the same cross-section, and a photon threshold energy of ~ 145 MeV in the proton rest-frame, corresponding to a proton energy, in the laboratory frame, of

$$E_p^{\text{thr}} = \frac{m_p c^2 \, m_\pi c^2}{2 \, E_{\text{ph}}} \left(1 + \frac{m_\pi}{2 \, m_p}\right) \sim 7 \times 10^{16} \, E_{\text{eV}}^{-1} \text{ eV} \qquad (13)$$

where E_{eV} is the characteristic photon energy of the target photon field in units of eV. The subsequent decay of charged pions injects leptons and neutrinos

$$\pi^+ \to \mu^+ + \nu_\mu, \quad \mu^+ \to e^+ + \nu_e + \overline{\nu}_\mu, \qquad (14)$$

$$\pi^- \to \mu^- + \overline{\nu}_\mu, \quad \mu^- \to e^- + \overline{\nu}_e + \nu_\mu, \qquad (15)$$

whereas neutral pions decay into two photons,

$$\pi^0 \to \gamma + \gamma. \qquad (16)$$

For photomeson and photopair production, the proton energy-loss rate can be calculated as in Begelman et al. (1990). Hadronic / lepto-hadronic models involving photo-meson production require protons to be accelerated to energies of at least the threshold energy given in Equation (13). Confining protons of this energy to the small emission region sizes inferred from rapid variability, typically requires magnetic fields of $B \gtrsim 10 - 100$ G. In the presence of such strong magnetic fields, the electron-synchrotron radiation field is expected to be strongly dominant over any potential external radiation fields. Therefore, one typically only considers the synchrotron photons of primary electrons as the target photon field for photo-pair and photo-pion production. γ-rays are produced through the $p\gamma$ interaction channels primarily by synchrotron radiation of charged secondaries ($e^\pm$, $\mu^\pm$, $\pi^\pm$), and the decay of neutral pions.

High-energy protons can also interact with thermal particles in the jet plasma. Due to the low densities present in extragalactic jet sources, proton-proton interactions are usually negligible in AGN jets, but they can make a significant contribution to the proton loss rate and radiation output in the case of the much denser Galactic jet sources. If the energy of the relativistic proton is higher than the threshold value for π^0 production (≈ 1.22 GeV), the collision with a thermal proton can create pions

$$p + p \to p + p + a\pi^0 + b\left(\pi^+ + \pi^-\right), \qquad (17)$$

$$p + p \to p + n + \pi^+ + a\pi^0 + b\left(\pi^+ + \pi^-\right). \qquad (18)$$

As in proton-photon interactions, proton-proton collisions inject photons by means of the decay of neutral pions. Charged pions inject electron-positron pairs and neutrinos through the decay chains of Eqs. (14) and (15).

The energy-loss rate for a proton of energy E is given by (e.g., Begelman et al. 1990)

$$\frac{dE}{dt}\bigg|_{pp} = -n_p \, c \, E \, \kappa_{pp}\sigma_{pp}, \qquad (19)$$

where n_p is the number density of thermal protons in the co-moving frame[1] , σ_{pp} is the proton-proton cross-section, and $\kappa_{pp} \approx 0.5$ is the total inelasticity of the interaction. A convenient parametrization for σ_{pp} is presented in Kelner et al. (2006). Taking the assumptions about distribution of jet power above, we can calculate the value of n_p in the comoving frame (see also Bosch-Ramon et al. 2006):

$$n_p = (1 - q_{\text{rel}}) \frac{L_{\text{jet}}}{\Gamma_{\text{jet}}^2 \pi r_{\text{jet}}^2 v_{\text{jet}} m_p c^2}, \qquad (20)$$

where m_p is the proton mass.

Finally, in the case of an expanding jet, particles also lose energy due to adiabatic cooling. The corresponding adiabatic energy loss rate is given by

$$\frac{dE}{dt}\bigg|_{\text{ad}} (E, z) = -\frac{E}{3}\frac{dV}{dt}. \qquad (21)$$

which obviously depends on the jet geometry (see, e.g., Bosch-Ramon et al. 2006).

The total energy-loss rate is simply the sum of the relevant loss rates for the particle species in consideration

$$\frac{dE}{dt}\bigg|_{\text{tot}} (E, z) = \sum_i \frac{dE}{dt}\bigg|_i (E, z). \qquad (22)$$

For particles whose gyro-radii are smaller than the acceleration / radiation region (this is typically always the case for electrons/positrons), the maximum energy of primary electrons and protons can be estimated by equating the total energy-loss rate to the acceleration rate

$$-\frac{dE}{dt}\bigg|_{\text{tot}} (E_{\max}) = \frac{dE}{dt}\bigg|_{\text{acc}} (E_{\max}). \qquad (23)$$

However, for protons, the confinement condition (i.e., the gyro-radius equalling the size of the acceleration region) is sometimes the dominant factor limiting the maximum energy, rather than radiative cooling. The magnitude and energy dependence of the particle acceleration rate obviously depends on the dominant acceleration mechanisms. However, it is often convenient to parameterize diffusive shock acceleration processes through an acceleration efficiency parameter $\eta < 1$ so that the acceleration time scale is a multiple $\eta^{-1} > 1$ of the gyro-timescale. Consequently, the acceleration rate is then given by (e.g., Aharonian 2004).

---

[1] Henceforth, we refer to as "comoving" or "jet frame" the reference frame fixed to the jet plasma, where the outflow bulk velocity is zero. The "observer frame" corresponds to the frame in which the jet bulk velocity is v_{jet}.

$$\frac{dE}{dt}\bigg|_{\text{acc}} = \eta\, e\, c\, B(z), \qquad (24)$$

Pions and muons can also interact before decaying. This effect becomes important when particles are very energetic and the physical conditions in the jet are such that the cooling time is shorter than the mean lifetime (Reynoso and Romero 2009). Pion and muon synchrotron radiation (and cooling) may be neglected if the maximum primary proton Lorentz factor and the magnetic field satisfy the conditions (Böttcher et al. 2013):

$$B\,\gamma_p \ll \begin{cases} 7.8 \times 10^{11}\ \text{G} & \text{for pions} \\ 5.6 \times 10^{10}\ \text{G} & \text{for muons} \end{cases} \qquad (25)$$

The injection of secondary particles is not a consequence of diffusive shock acceleration, but a by-product of the interaction of primary protons and electrons. The maximum energy of pions, muons, and secondary electron-positron pairs is then not fixed by Eq. (23). It is instead determined by the characteristics of the particular process through which the different particles were injected, and by the maximum energy of the primary particles (which is constrained by Eq. 23).

The injection of primary particles into the emission region may represent either the entrainment of external material by the flow, or a very rapid (e.g., first-order Fermi) acceleration process, on a time scale much shorter than all other relevant time scales. Such injection is thus usually trated as a phenomenological source term $Q(E,z)$ in the co-moving jet frame, which is often parameterized either as a δ function in particle energy,

$$Q(E,z)\big|_{\text{entrainment}} = Q_0\,\delta(E - \Gamma_{\text{jet}}\,mc^2) \qquad (26)$$

in the case of entrainment by the relativistic flow of Lorentz factor Γ_{jet} (e.g., Pohl and Schlickeiser 2000), or as a power-law in energy multiplied by an exponential cutoff,

$$Q(E,z) = Q_0\,E^{-p}\exp\left[-E/E_{\text{max}}(z)\right]\,f(z). \qquad (27)$$

in the case of diffusive shock acceleration. In the latter case, the value of the spectral index is typically in the range $1.5 \lesssim p \lesssim 2.4$. The cutoff energy E_{max} depends on z, and is calculated according to Eq. (23). The function $f(z)$ describes the injection profile along the jet that defines the length of the acceleration region.

In most studies in the literature, the form of the injection function $Q(E)$ — especially the spectral index p — is left as a free parameter, whose value may be used as an indication of the dominant particle acceleration mechanism. In the case of $p \sim 2$, non-relativistic shocks present themselves as a standard solution to achieve such a particle spectrum, while very hard spectra (down to $p \sim 1$) have been shown to be possible in the case of magnetic reconnection (e.g., Sironi and Spitkovsky 2014, Guo et al. 2016). Diffusive shock acceleration at relativistic parallel shocks produces particle spectra with $\alpha \sim 2.2 - 2.3$ (e.g., Kirk and Duffy 1999). Mildly relativistic,

oblique shocks are capable of producing spectral indices in a wide range, from $p \sim 1$ to very steep spectra, depending primarily on the obliquity, i.e., the angle of the ordered component of the magnetic field with respect to the shock normal (Summerlin and Baring 2012). Thus, unfortunately, the diagnostic of determining p from model fitting of spectral energy distributions of jet sources, is not sufficient to pin down the dominant particle acceleration mechanism, one of the fundamental unknowns in our understanding of relativistic jets (but see some additional discussion in Section 5).

Finally, the value of the normalization constant Q_0 is obtained from the total power injected in each particle species

$$L_i = \int_V d\mathbf{r} \int_{E_{\min}}^{E_{\max}} dE\, E\, Q_i(E, z),$$ (28)

where the index i runs over protons and electrons. The interaction of relativistic protons with matter and radiation injects charged pions, muons, and secondary electron-positron pairs. Electron-positron pairs are also created through photon-photon annihilation. These processes define the specific expressions for $Q(E, z)$ for the respective secondary particles.

The sources of charged pions are proton-photon and proton-proton interactions. Suitable expressions for the corresponding pion injection functions were presented in Atoyan and Dermer (2003), Kelner et al. (2006), and Kelner and Aharonian (2008), while expressions for the consequent muon injection may be found in Lipari et al. (2007). Finally, electrons and positrons are injected through muon decay, photopion production, and $\gamma\gamma$ absorption. Convenient expressions for the electron/positron injection rate from muon decay are presented in Schlickeiser (2002). Expressions for the pair injection rate from photopair production may be found in Chodorowski et al. (1992) and Mücke et al. (2000). The rate of pair production from photon-photon annihilation

$$\gamma + \gamma \rightarrow e^+ + e^-.$$ (29)

is derived in Böttcher and Schlickeiser (1997). Two-photon annihilation is also a photon sink. Its effect on the escape of photons from the jet is discussed below (Section 2.3).

The evolution of the particle distributions is governed by transport equations of the form

$$\frac{\partial N(E,t,z)}{\partial t} + \frac{\partial \left(\Gamma_{\text{jet}} v_{\text{jet}} N(E,t,z)\right)}{\partial z} + \frac{\partial \left(b(E,t,z) N(E,t,z)\right)}{\partial E}$$

$$-\frac{\partial}{\partial E}\left[\frac{E^2}{(a+2)\, t_{\text{acc}}} \frac{\partial N(E,t,z)}{\partial E}\right] + \frac{N(E,t,z)}{T_{\text{dec}}(E)} + \frac{N(E,t,z)}{T_{\text{esc}}(E)} = Q(E,t,z)$$
(30)

The second term on the l.h.s. of Eq. (30) represents particle convection along the jet, the third term describes systematic energy losses/gains, where $b(E,z) = -dE/dt|_{\text{tot}}$ encompasses all energy loss plus first-order acceleration terms. The fourth term on the l.h.s. represents diffusion in momentum

space and describes second-order (stochastic) shock acceleration on a characteristic time scale t_{acc}. Here, $a = v_s^2/v_A^2$ is the square of the ratio of shock speed to the Alfvén speed in the co-moving jet plasma. T_{dec} is the decay time scale. This term vanishes for stable particles. However, a corresponding term should be included for electrons and positrons to account for the loss of pairs due to pair annihilation. T_{esc} is the particle escape time scale.

This equation is appropriate for a very general case of a spatially extended, inhomogeneous jet, in which the physical parameters may vary in time and space along the jet. In time-independent (steady-state) models, the first term $\partial N/\partial t$ is set to zero. Homogeneous, single-zone models neglect the second (convection) term. In many treatments, momentum diffusion (and, thus, stochastic acceleration) is also neglected, thus leaving out the fourth term on the l.h.s. Note that Eq. (30) still assumes that the jet is homogeneous across the jet cross section (i.e., no radial dependence) and that the particle distributions are locally isotropic in the co-moving jet frame. Also, spatial diffusion has been neglected (see, e.g., Chen et al. 2015, 2016, for a blazar jet model that includes spatial diffusion).

2.3 Radiative output

We now proceed to calculate the total radiative spectrum of all particle species produced by each of the interaction processes described in Sect. 2.2. In this exposition, we will restrict ourselves to quoting simple, δ-function approximations for the respective emissivities. Detailed expressions for the emissivities can be found, e.g., in Atoyan and Dermer (2003), Romero and Vila (2008), Reynoso and Romero (2009), Dermer and Menon (2009), Böttcher et al. (2012), and references therein.

The emissivities $j(\epsilon) = dE/(dV\,dt\,d\epsilon\,d\Omega)$ [erg cm^{-3} s^{-1}] at photon energy $h\nu = \epsilon\,m_e c^2$ are commonly first evaluated in the co-moving jet frame, and then transformed to the observer frame. The relevant transformations are governed by the Doppler factor

$$D = \left[\Gamma_{\mathrm{jet}}\left(1 - \beta_{\mathrm{jet}}\cos\theta_{\mathrm{jet}}\right)\right]^{-1} \tag{31}$$

where θ_{jet} is the jet viewing angle and $\beta_{\mathrm{jet}} = v_{\mathrm{jet}}/c$.

Relativistic Doppler effects then result in photon energies being blue/red shifted as $\epsilon_{\mathrm{obs}} = D\,\epsilon$, and variability time scales appear contracted as $\delta t_{\mathrm{obs}} = \delta t/D$. The relativistic boosting of radiative flux depends on the geometry (see, e.g., Lind and Blandford 1985). In the case of a continuous, extended jet, the flux will be enhanced by a factor of D^2 so that the observed flux can be calculated as

$$F_{\epsilon_{\mathrm{obs}},\mathrm{ext}} = \frac{1}{d_L^2}\int_{z_{\mathrm{acc}}}^{z_{\mathrm{max}}} r_{\mathrm{jet}}^2(z)D^2(z)\,j(\epsilon_{\mathrm{obs}}/D, z)\,dz. \tag{32}$$

where d_L is the luminosity distance to the source.

In the case of single emission zone with co-moving volume V, the flux transformation is determined by a factor D^3, i.e.,

$$F_{\epsilon_{\text{obs}},\text{zone}} = \frac{V\,j(\epsilon_{\text{obs}}/D)\,D^3}{d_L^2} \tag{33}$$

where the additional factor of D originates from the volume integration (which is taken over z in the laboratory frame in Eq. 32), taking into account Lorentz contraction and light-travel-time effects.

The dominant radiation mechanisms resulting from high-energy, accelerated particles are: synchrotron radiation (of primary electrons and protons as well as secondary pions, muons, and electrons/positrons), inverse Compton scattering (relevant only for electrons and positrons), and π^0 decay.

The synchrotron spectrum from an ensemble of charged particle of mass m, charge $q = Z\,e$, and energy $\gamma\,mc^2$ moving at random directions with respect to a magnetic field $B = B_{\text{G}}$ G peaks at a frequency

$$\nu_c^{\text{sy}} = \frac{3qB}{4\pi mc}\,\gamma^2 \equiv \nu_0\,\gamma^2 \approx 4.2 \times 10^6\,B_{\text{G}}\gamma^2\,Z\,\frac{m_e}{m}\text{ Hz} \tag{34}$$

Based on a simple δ-function approximation for the synchrotron emissivity of a single particle, the synchrotron spectrum of an ensemble of particles with energy distribution $n(\gamma)$ can be evaluated as[2]

$$j_\nu^{\text{sy},\delta} = \frac{4}{9}\,c\,\left(\frac{q^2}{m\,c^2}\right)^2\,U_{\text{mag}}\,\nu_0^{-3/2}\,\nu^{1/2}\,n\left(\sqrt{\frac{\nu}{\nu_0}}\right). \tag{35}$$

In the Thomson regime ($\epsilon\,\gamma \ll 1$), a target photon of energy ϵ will be scattered to higher energies by an isotropic ensemble of relativistic electrons of energy $\gamma\,m_ec^2$ to an average scattered photon energy $\epsilon_s \approx \gamma^2\,\epsilon$. **The Compton emissivity resulting from Compton scattering of a target photon field with photon number distribution $n_{\text{ph}}(\epsilon)$ by a relativistic electron distribution $n_e(\gamma)$ in the Thomson regime can be approximated as**

$$j_\nu^{\text{Thomson},\delta}(\epsilon_s) \approx \frac{h\,c\,\sigma_T\,\epsilon_s^2}{8\pi}\int\limits_{\epsilon_s}^{\infty} d\gamma\,\frac{n_e(\gamma)}{\gamma^4}\int\limits_{\epsilon_s/(2\gamma^2)}^{\infty} d\epsilon\,\frac{n_{\text{ph}}(\epsilon)}{\epsilon^2} \tag{36}$$

where a simple δ function approximation for the Compton cross section has been employed. More general expressions for the synchrotron and Compton emissivities, including Compton scattering in the Klein-Nishina regime, may be found, e.g., in Blumenthal and Gould (1970), Rybicki and Lightman (1979), Dermer and Menon (2009), Böttcher et al. (2012).

In the decay of a π^0 meson of energy $E_{\pi^0} = \gamma_{\pi^0}m_\pi c^2$, two photons with energy $E_\gamma \approx (1/2)E_{\pi^0}$ are produced, while the production of π^0 mesons depends on the (energy-dependent) $p\gamma$ cross section, branching ratio (i.e., fraction of $p\gamma$ pion production events resulting in the production of a π^0) and inelasticity (i.e., the fraction of the proton's energy transferred to the

---

[2] note a typo in Eqs. (3.38) and (3.39) in Böttcher et al. (2012), where a factor c is missing

newly produced pion). A convenient approximation for the calculation of the resulting photon production spectrum can be found in Atoyan and Dermer (2003), Romero and Vila (2008).

The photon emission spectrum must be corrected for various absorption processes. At low (radio) frequencies, synchrotron-self absorption (SSA) will be dominant (see, e.g., Rybicki and Lightman 1979, Böttcher et al. 2012), while at high energies ($E \gg 1$ GeV) γ-ray absorption can be caused by photon-photon annihilation into electron-positron pairs (see Eq. (29)). The $\gamma\gamma$ opacity for a photon of energy ϵ_γ in a target photon field $n_{\mathrm{ph}}(\epsilon)$ is

$$\kappa_{\gamma\gamma}(\epsilon_\gamma) = \frac{1}{2} \int\limits_{-1}^{1} d\mu \int\limits_{\epsilon_{\mathrm{th}}}^{\infty} d\epsilon \, \sigma_{\gamma\gamma}(\epsilon_\gamma, \epsilon, \mu) \, n_{\mathrm{ph}}(\epsilon) \, (1 - \mu) \qquad (37)$$

where μ is the cosine of the collision angle, and $\sigma_{\gamma\gamma}$ is the annihilation cross-section (e.g., Gould and Schréder 1967), and ϵ_{th} is the threshold energy,

$$\epsilon_{\mathrm{th}} = \frac{2}{\epsilon_\gamma \, (1 - \mu)}. \qquad (38)$$

The $\gamma\gamma$ optical depth $\tau_{\gamma\gamma}$ is then evaluated as the length integral over $\kappa_{\gamma\gamma}$ along the photon propagation direction. Eq. (37) is simplified when the target photon distribution is isotropic. A convenient expression for $\tau_{\gamma\gamma}$ in this particular case is obtained in Gould and Schréder (1967).

If the absorbing photon field is located outside the emission region (as, e.g., in the case of VHE γ-ray absorption by the Extragalactic Background Light, see Section 3), the $\gamma\gamma$ opacity simply leads to a correction factor $exp(-\tau_{\gamma\gamma})$ with respect to the unabsorbed flux spectrum, $F_{\mathrm{intr}}(\epsilon)$. However, in case emission and absorption are taking place co-spatially, the solution to the radiative transfer equation becomes more involved. In the case of a homogeneous source, this solution is given by

$$F_{\mathrm{obs}}^{\mathrm{int}}(\epsilon_\gamma) = F_{\mathrm{intr}}(\epsilon_\gamma) \, \frac{1 - e^{-\tau_{\gamma\gamma}(\epsilon_\gamma)}}{\tau_{\gamma\gamma}(\epsilon_\gamma)} \qquad (39)$$

In the optically-thin limit ($\tau_{\gamma\gamma} \ll 1$), Eq. (39) simply reduces to $F_{\mathrm{obs}}^{\mathrm{opt.\,thin}} = F_{\mathrm{intr}}$, as expected, while in the optically-thick limit ($\tau_{\gamma\gamma} \gg 1$), it becomes $F_{\mathrm{obs}}^{\mathrm{opt.\,thick}} = F_{\mathrm{intr}}/\tau_{\gamma\gamma}$. If the target photon field has a power-law spectrum $n_{\mathrm{ph}}(\epsilon) \propto \epsilon^{-(\alpha_t + 1)}$ (i.e., an energy index of α_t), then the opacity also has a power-law depencence on energy, $\tau_{\gamma\gamma}(\epsilon_\gamma) \propto \epsilon_\gamma^{\alpha_t}$. Consequently, internal $\gamma\gamma$ absorption leads to a spectral break by $\Delta\alpha_\gamma = \alpha_t$ around the photon energy where $\tau_{\gamma\gamma}(\epsilon_\gamma) = 1$. The presence or absence of such spectral breaks in the γ-ray spectra of relativistic jet sources can be used to constrain the bulk Lorentz factor of the emission region (e.g., Baring 1993, Dondi and Ghisellini 1995, Böttcher et al. 2012). As we will elaborate on in Section 3.3, $\gamma\gamma$ absorption in the immediate environment (especially, the Broad Line Region) of powerful blazars also provides constraints on the location of the γ-ray emission region in those objects.

In addition to photons, if hadronic charged-pion production processes are relevant, also electron and muon neutrinos at $\sim$ TeV – PeV energies

are produced. The detection of astrophysical neutrinos and their unique identification with relativistic jet sources would therefore uniquely identify sites where protons are being accelerated to ultrarelavisitic energies exceeding the pion production threshold (see Eq. 13), possibly even reaching the energies of ultra-high-energy cosmic rays (UHECRs) with energies $E \gtrsim 10^{19}$ eV.

Convenient templates for the pion production spectra from relativistic $p\gamma$ and $p - p$ interactions in the case where pion and muon synchrotron losses may be neglected, can be found in Kelner and Aharonian (2008), Kelner et al. (2006), respectively. If pion and muon synchrotron emission can not be neglected, their energy losses prior to decay need to be taken into account. A formalism to evaluate the secondary-particle production rates in this more general case, has been developed in Hümmer et al. (2010).

2.4 Polarization

Relativistic jets are expected to produce polarized synchrotron radiation. Such radiation is observed from radio to X-rays. At higher energies, inverse Compton upscattering of the polarized synchrotron photons can yield polarized X/gamma-rays (e.g., Bonometto and Saggion 1973), and also anisotropic Compton scattering of unpolarized radiation fields by non-relativistic or mildly relativistic electrons can introduce polarization (e.g., Poutanen 1994, Krawczynski 2012). Evidence for polarization in high-energy radiation from relativistic jet sources has been found, e.g., in Cygnus X-1 (Laurent et al. 2011, Romero et al. 2014), and there are several developments for X-ray and γ-ray polarimeters currently on-going and proposed, such as the X-Ray Imaging Polarimeter Experiment (XIPE, Soffitta et al. 2013), or the Polarization Spectroscopic Telescope Array (PolSTAR, Krawczynski et al. 2016).

Both in the case of optically-thin synchrotron and synchrotron-self-Compton scattering, the preferred polarization direction indicates the predominant orientation of the magnetic field, as the Electric Vector Position Angle (EVPA) is perpendicular to the projection of the B-field onto the plane of the sky. A non-vanishing synchrotron polarization therefore clearly indicates an at least partially ordered magnetic field. If the B-field is perfectly ordered, then optically-thin synchrotron radiation by a non-thermal power-law particle distribution with index p yields a degree of polarization Π of

$$\Pi_{\mathrm{Sy}} = \frac{p + 1}{p + \frac{7}{3}} \tag{40}$$

corresponding to polarization degrees of $\Pi \sim 70 - 75$ % for typical spectral indices of $p \sim 2 - 3$ (e.g., Rybicki and Lightman 1979). The measured degree of optical polarization in relativistic jet sources is typically in the range $\Pi \lesssim 30$ %, and often significantly smaller than that. This indicates that the emission must originate from regions with partially disordered magnetic fields.

Especially in the case of blazars, it is known that the polarization properties are highly variable, both in degree of polarization and polarization angle (PA). Paritcularly noteworthy in this context are large swings in the PA (Romero et al. 1995), which sometimes correlate with multi-wavelength flares (Marscher et al. 2008a, 2010, Abdo et al. 2010, Blinov et al. 2015, 2016). Such PA swings naturally suggest the existence of helical fields (e.g., Zhang et al. 2014, 2016). Models based on random fluctuations in a turbulent field have been also proposed (Marscher 2014).

Time-dependent multiwavelength polarization measurements diagnose the topology of the magnetic field in the emission region and its change during variability events. Such observations may therefore be a unique tool to identify the role of magnetic fields in the formation of jets and in the relativistic particle acceleration processes leading to the emission of high-energy radiation. The diagnostic power of (time-dependent) polarization signatures in blazars will be discussed in more detail in Section 3.

At low (radio) frequencies, the propagation of polarized emission through a magnetized medium leads to a rotation of the EVPA, known as Faraday Rotation (e.g. Pacholczyk 1963). This may occur even within the source, and thus lead to effective Faraday depolarization (e.g., Burn 1966), as the EVPAs of radiation produced in different locations along the line of sight within the source appear rotated by different amounts. The amount of Faraday rotation, $\Delta\psi$, i.e., the angle by which the EVPA is rotated, depends on the electron density n_e, the projection of the magnetic field $\overrightarrow{B}$ along the line of sight $\overrightarrow{s}$, and the radiation wavelength λ as

$$\Delta\psi \propto \lambda^2 \int n_e(s)\overrightarrow{B}(s) \cdot d\overrightarrow{s} \tag{41}$$

Due to the λ^2 scaling, this effect is generally only relevant at radio frequencies and is negligible at optical or higher frequencies.

3 Blazars

The class of peculiar extragalactic sources dubbed *blazars* represents a quite small, but remarkably interesting fraction of the entire population of AGN (e.g. Urry and Padovani 1995). While a formal definition is difficult to establish, the canonical features used in their classification include the presence of a compact radio core, with flat or even inverted spectrum, extreme variability (both in timescale and in amplitude) at all frequencies, and a high degree of optical and radio polarization. More recently, intense gamma-ray emission (although not ubiquitous, but in many cases dominating the total bolometric radiative power output) has also been used for blazar selection. A recent census counts about 3000 known blazars (Massaro et al. 2009).

Phenomenologically, blazars are further divided in two subgroups depending on special observational characteristics: 1) *BL Lacertae* objects are characterized by an extreme weakness (equivalent width < 5 Å) or even

absence of emission lines in their optical spectra, a feature generally attributed to a low accretion rate onto the central supermassive black hole and an environment largely depleted of potential fuel for black-hole accretion, not exhibiting a prominent broad-line region; 2) if the optical spectra display broad emission lines typical of quasars (or QSOs = Quasi Stellar Objects), blazars will be instead classified as *Flat Spectrum Radio Quasars* (FSRQ). FSRQs are generally more powerful than BL Lacs. The FSRQ population follows a positive cosmological evolution close to that of normal quasars, being quite rare in the local Universe and with a density peaking around $z \sim 2$ (e.g., Dunlop and Peacock 1990). The BL Lac population, instead, displays a quite different trend. In particular, the less powerful high-frequency peaked BL Lacs (HBL), follow a *negative* cosmological evolution (Rector et al. 2000, Ajello et al. 2014), i.e. they tend to be more numerous in the local Universe, with their density decreasing with redshift. The different evolutions could be related to a generic connection between FSRQs and BL Lacs, the latter representing the final stage of the FSRQ activity, after the fuel for black-hole accretion has been exhausted (Cavaliere and D'Elia 2002, Böttcher and Dermer 2002).

Relativistic beaming offers a simple explanation for the peculiarities displayed by blazars (Blandford and Rees 1978, Blandford and Königl 1979), in particular the inverted radio spectrum, the huge brightness temperature, the existence of superluminal moving features, the short variability timescale and the powerful γ-ray emission. Different methods agree to determine typical Doppler factors of localized emission regions in blazar jets in the range $D \simeq 10 - 20$ (but reaching in some cases values as large as 50), implying a similar bulk Lorentz factor for the plasma outflowing in the jet (Lister et al. 2013, Ghisellini and Tavecchio 2015, and references therin) and a viewing angle as small as few degrees. Blazars, therefore, represent radio sources in which the jet velocity points almost along the line of sight. In this geometry, the relativistically beamed non-thermal continuum produced within the jet easily outshines any other emission component from the active nucleus or the host galaxy. In the view of the *unification scheme*, BL Lacs and FSRQ are considered the beamed counterparts of the FRI (low power) and FRII (high power) radiogalaxies, respectively (e.g., Urry and Padovani 1995).

The remarkably smooth continuum emission of blazars, extending over the entire electromagnetic spectrum, from the radio band to γ-ray energies (see Fig.2 for an example), is characterized in the $\nu F(\nu)$ representation (the so-called spectral energy distribution, SED) by a typical "double humped" shape (e.g., Sambruna et al. 1996, Fossati et al. 1998). While the characteristics of the low energy component were already well known and fairly well understood as synchrotron radiation of relativistic electrons in the 1980s (e.g., Marscher and Gear 1985), it was realized only after the advent of the γ-ray telescope EGRET (Energetic Gamma-Ray Experiment Telescope) onboard the *Compton Gamma-ray Observatory* in the 1990s (Fichtel et al. 1994) that many blazars exhibit significant γ-ray emission, often dominating the SEDs. Including the γ-ray output, the apparent bolometric luminosities of blazars reach, in some cases, $L_\gamma = 10^{49}$ erg s^{-1} (e.g.,
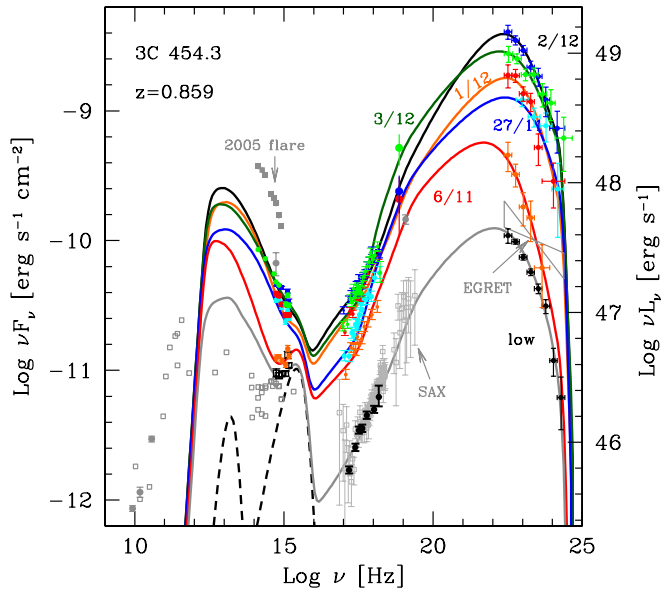
Fig. 2 Spectral energy distributions of the FSRQ 3C454.3 during different activity states in 2012 (coloured) and a quiescent phase (gray). The data clearly show the typical "double humped" shape of the SED. Curves show the result of a one-zone leptonic emission model. The reader can appreciate the extreme variability, especially in the γ-ray band. From Bonnoli et al. (2011).

Bonnoli et al. 2011). These extreme luminosities, combined with the observed short (often intra-day) variability, provide one line of evidence for relativistic beaming in blazars (see, e.g., Schlickeiser 1996, for a review).

Improved γ-ray instruments in space (*Fermi* and *AGILE*) and the development of Cherenkov telescope facilities on the ground (H.E.S.S., MAGIC, VERITAS, and the future CTA), together with intense multifrequency coordination efforts provide increasingly complete coverage of the rapidly changing SEDs, which is instrumental in the understanding of the physical processes shaping the blazar phenomenon. The Cherenkov telescopes, sensitive to very high energy (VHE) γ-rays ($E > 50$ GeV), have revealed an important population of blazars (BL Lacs, in particular) characterized by an intense emission at TeV energies which, besides jet physics, can be exploited as a probe for cosmic backgrounds and intergalactic magnetic field.

3.1 Emission models: the standard scenario

As clearly indicated by the high degree of radio and optical polarization, the low-energy spectral component of blazars is produced through the syn-

chrotron mechanism, most likely by a population of highly relativistic electrons. The origin of the high-energy component is still debated. Two general scenarios for the production of high energy radiation are discussed (see also Sec. 2), namely *hadronic* or *leptonic* models (e.g., Böttcher et al. 2013).

3.1.1 Leptonic models

The most popular class of models adopts the leptonic scenario, in which the high-energy component is the result of the inverse Compton scattering of soft photons by the same electrons responsible for the synchrotron emission. Different sources of soft photons can be considered; the emission will be dominated by inverse Compton scattering of the photon component with the largest energy density (as measured in the co-moving jet frame). Depending on the nature of soft photons dominating the IC process, the leptonic high-energy emission is comprised of SSC or *External Compton* (EC) radiation.

In the SSC model (e.g., Maraschi et al. 1992, Tavecchio et al. 1998) it is assumed that target photons are dominated by the synchrotron photons themselves. In this class of models synchrotron and IC emission are strongly coupled. This affords the possibility to derive robust constraints on the basic physical quantities of the jet from the observed SED (Tavecchio et al. 1998). In the EC model one assumes that the low energy radiation produced in the central regions of the AGN (directly emitted by the accretion disk or reprocessed by the gas in the Broad Line Region or by the parsec-scale molecular torus) dominates over the synchrotron radiation. However, even in this case, SSC emission is still expected to make a non-negligible contribution, especially at X-ray energies. A possibility (Dermer and Schlickeiser 1993) is thus to consider the direct UV emission from the accretion disk; however for sufficiently large distances from the disk, the de-beaming suffered by the radiation directly coming from the disk causes a strong depression of this contribution in the jet frame. The primary disk radiation is partly reflected/reprocessed by the gas of the BLR and beamed in the jet frame, providing a strong contribution to the emission (Sikora et al. 1994). Błażejowski et al. (2000) pointed out that IC scattering of the thermal near-infrared radiation ($T \simeq 10^3$ K) emitted by the dust of the parsec-scale torus expected to surround the central AGN region could provide the dominant contribution to the high energy emission, especially in the energy band 10 keV – 100 MeV. This could be the case especially for FSRQ detected above few tens of GeV (see below), however for BL Lacs this component is less likely to be important as recent evidence suggests the dusty torus dwindles at lower accretion rates (Plotkin et al. 2012a).

Not only the optical/UV emission from the accretion disk, but also the beamed synchrotron emission from the jet can be "reflected" by the BLR and thus serve as target photon field for Compton scattering. The double change of frame (source → lab frame → source) leads to a great amplification of the energy density of the soft radiation (Ghisellini and Madau 1996, Tavani et al. 2015). However, as discussed by Böttcher and Dermer (1998) and Bednarek (1998), when the constraints posed by the travel time of the

radiation are taken into account, the relative contribution of this mechanism to the total emission may be severely suppressed.

The question of the dominant target photon field is intimately linked to the location of the emission region along the jet, which will provide additional clues towards the dominant particle acceleration mechanism. This aspect will be discussed in more detail in Section 3.3
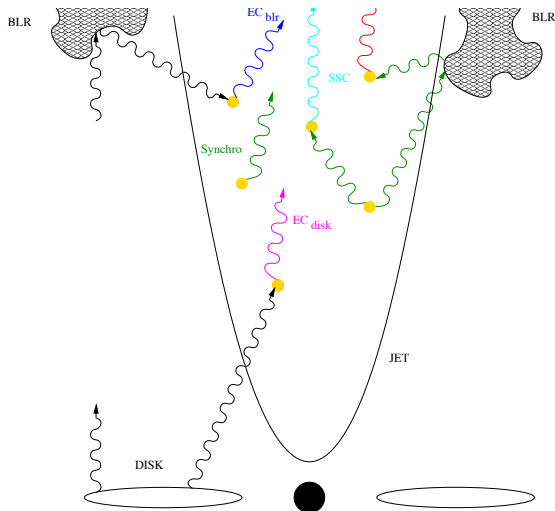
Fig. 3 Sketch illustrating the basic emission model for blazars. Relativistic electrons in the jet produce radiation through synchrotron emission and IC scattering. Soft target photons for the IC process are the synchrotron photons themselves (*SSC radiation*) and those produced in the external environment (*EC radiation*), namely produced in the disk, or reprocessed in the BLR. A third class of models (*the mirror model*) consider also the synchrotron photons "reflected" by the BLR. Further out also the IR radiation emitted by the molecular torus can be scattered.

The general set-up of leptonic blazar emission models is sketched in Fig.3. The jet flow is expected to become dissipative around 10^2 – 10^3 Schwarzschild radii (corresponding to about 0.01 – 0.1 parsec for a BH mass of 10^9 M$_\odot$), likely through shocks or magnetic reconnection events which can accelerate particles to ultrarelativistic energies (sometimes this is defined as the "blazar zone"). Typical variability timescales of $\delta t_{\rm var} \sim$ few hours (although shorter timescales events have been occasionally observed), together with typical Doppler factors of $D \sim 10$ – 20, limit the size of the emission region to $R \lesssim \delta t_{\rm var} \, c \, D/(1 + z) \sim 10^{15}$ – 10^{16} cm.

SED modeling of a large number of blazars (e.g., Ghisellini et al. 2010) suggests that SSC and EC processes dominate the high energy emission of different types of blazars: in the case of FSRQ, which display bright thermal features (emission lines and the *blue bump*), γ-ray production is likely dominated by EC (often with a contribution from SSC in the X-ray
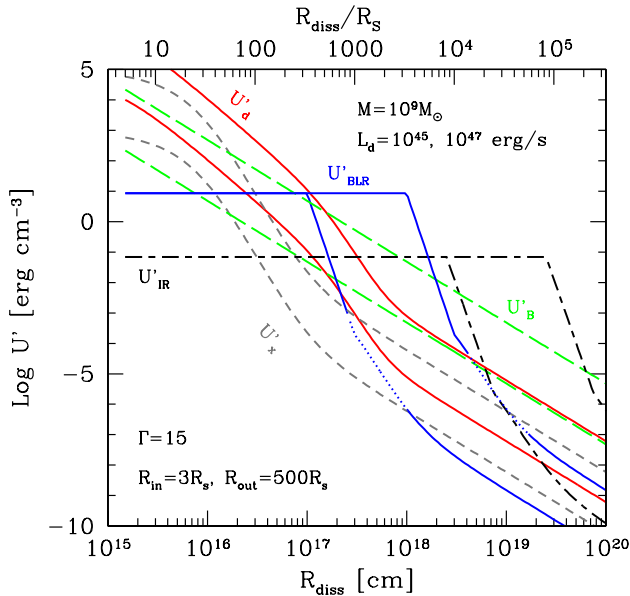
Fig. 4 Comparison of different energy densities as measured in the jet reference frame. The jet is assumed to have a bulk Lorentz factor $\Gamma = 15$ and the black hole mass is assumed to be $M = 10^9 M_\odot$. The two sets of lines correspond to two disk luminosities: $L_d = 10^{45}$ and 10^{47} erg s^{-1}. The magnetic energy density (long dashed lines) is calculated assuming that a fraction $\epsilon = 0.1$ of the jet power is carried as magnetic field. From Ghisellini and Tavecchio (2009).

band), while in high-frequency peaked BL Lac objects (characterized by very weak or even absent thermal components) the SSC process dominates. However, the situation is less straightforward for intermediate (relatively powerful) BL Lac objects, in which the EC emission could play some role (Böttcher 2010). Moreover, for FSRQ, the actual external radiation field ruling the EC emission depends on the position of the emitting region along the jet. This is shown in Fig. 4, in which the energy densities of the various radiation fields (in the rest frame of the jet) are plotted as a function of the distance from the central engine. Within the radius marking the distance where the BLR clouds are located[3] the energy density is dominated by the constant BLR radiation field. Beyond the BLR radius, U_{BLR} falls rapidly with distance and the radiation from the torus starts to dominate. The great majority of FSRQs can be modelled assuming that the emitting region is at distances smaller than the BLR radius (e.g., Ghisellini et al. 2010, 2014), thus considering only EC with the BLR photons. However, for FSRQ

---

[3] For simplicity we are assuming that the clouds producing the broad lines are located at the same distance. In reality, different emission lines are likely produced in a stratified BLR, in which the ionization factor decreases with distance (Netzer 2008).

detected at VHE, the emission likely occurs beyond this radius due to $\gamma\gamma$ absorption constraints (see Section 3.3).

3.1.2 Hadronic models

Even in the case of the leptonic models described above, protons are expected to be present in the jet in order to ensure charge neutrality, **unless a pure electron-positron pair plasma is assumed.** However, in order to contribute significantly to the radiative output (through proton synchrotron and $p\gamma$ pion production), they need to be accelerated to energies $E_p \gg 10^{16}$ eV (see Section 2.2). In order for such acceleration to be possible within the constrained size of the blazar emission region, large magnetic fields of $B \gtrsim 10$ G are required.

If the acceleration of protons to the required energies does happen in blazar jets, the hadronic radiation processes discussed in Sections 2.2 and 2.3 become relevant. Due to the high magnetic fields, the radiative output from leptons in the emission region will then be strongly dominated by synchrotron radiation, so that the high-energy (X-ray through γ-ray emission is likely dominated by proton synchrotron radiation and synchrotron emission of secondaries resulting from photopion production. Such models are termed *hadronic* or *lepto-hadronic* models (e.g., Mannheim 1993, Mannheim and Biermann 1992, Mücke and Protheroe 2001, Mücke et al. 2003b, Reynoso et al. 2011, Petropoulou and Mastichiadis 2012, Böttcher et al. 2013, Petropoulou et al. 2015)

As the particle densities in blazar jets are very low ($n \lesssim 10^3$ cm^{-3}), pion production processes are strongly dominated by $p\gamma$ interactions, in which case the secondary particles (pions, muons, electrons/positrons) are produced with large Lorentz factors of $\gamma \gtrsim 10^7$. π^0 decay photons and synchrotron photons from electrons/positrons at these energies emerges at $\gg 1$ TeV energies, where the emission region is highly opaque to $\gamma\gamma$ absorption, producing additional electron/positron pairs in a cascading process. Due to the extreme energies in protons and the relatively low radiative efficiency of protons compared to leptons, as well as the increased bulk mass to accelerate, hadronic jet models of blazars typically require several orders of magnitude larger jet powers than leptonic models for the same blazars. In some cases, the required jet powers even exceed the Eddington luminosity of the central supermassive black hole, thus requiring a revision of our current understanding of the formation of relativistic jets and related energy considerations (see, e.g., Section 2.1; Zdziarski and Böttcher 2015).

In terms of fitting SEDs of blazars, hadronic models have met with similar sucess as leptonic models (see, e.g., Fig. 5). Hence, SED modeling is generally not sufficient to distinguish leptonic from hadronic models and, thus, to constrain the jet energetics, and additional diagnostics need to be developed. One possibility lies in the different variability patterns expected in leptonic and hadronic models, due to the vastly different radiative cooling times of protons compared to electrons/positrons. Due to the complexity of hadronic models (including 8 different particle species + photons, with a rather complicated energy dependence of pγ pion production processes),
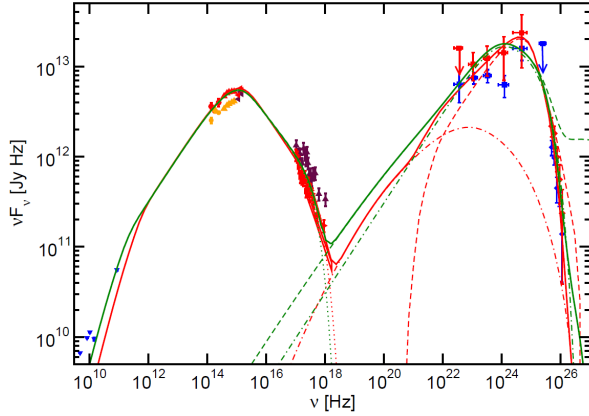
Fig. 5 Leptonic (red) and hadronic (green) fits to the simultaneous SED of the intermediate BL Lac object 3C66A. Different line styles indicate different radiation components: solid = total SED, including correction for EBL absorption; dotted = primary electron synchrotron; red dashed = EC(torus); red dot-dashed = SSC; green dot-dashed = proton synchrotron; green dashed = total proton synchrotron + cascade emission

the development of time-dependent hadronic models has only recently made significant progress (e.g., Mastichiadis et al. 2013, Diltz et al. 2015, Weidinger and Spanier 2015).

Another alternative to distinguish leptonic from hadronic models consists of the fact that only hadronic processes result in the production of high-energy neutrinos (e.g., Petropoulou et al. 2015). Thus, the identification of blazars with the sources of astrophysical TeV – PeV neutrinos, as now confidently detected by IceCube (Aartsen et al. 2014) would unamibguously prove the presence of ultrarelativistic protons in blazar jets. However, unfortunately, the angular resolution of IceCube (and other neutrino observatories) is currently too poor to provide such a unique identification (but see, e.g., Kadler et al. 2016).

In light of current developments of X-ray and γ-ray observatories with polarimetry capabilities, high-energy polarization may also be considered as a distinguishing diagnostic of leptonic and hadronic models. In particular, Zhang and Böttcher (2013) have shown that the X-ray and γ-ray emission from blazars in the case of a hadronic origin is expected to be polarized with polarization degrees similar to those observed in the optical band (i.e., $\Pi \lesssim$ a few tens of percent). On the other hand, in leptonic models, the X-ray emission of most (non-HBL) blazars is expected to be dominated by SSC emission, which is expected to exhibit a degree of polarization of about half that of the target photon field, i.e., $\Pi_X \sim \Pi_{\rm opt}/2$. In the case of EC dominated γ-ray emission, those γ-rays are expected to be essentially unpolarized, in stark contrast to the prediction of hadronic models. Thus, X-ray and γ-ray polarimetry of blazars may serve as a powerful diagnostic to distinguish leptonic and hadronic emission models.

3.2 One-zone *vs* multizone/structured jets

In the previous section we discussed the emission scenarios without specifying in detail the nature and the geometry of the emission region. Unfortunately, our knowledge of the geometry and even the composition of jets is still rather poor. Therefore in the modeling of blazars even the specific characteristics of the region responsible for the emission should be considered as a free parameters.

Blazar models can generally be divided in inhomogeneous (or jet) and homogeneous models. In the first class of models (Blandford and Königl 1979, Ghisellini et al. 1985) one assumes that the observed emission is produced in an extended volume along the jet and a particular geometry (e.g. conical, parabolical) for it (see also Section 2.1). Moreover one needs to specify the evolution of the main physical quantities (magnetic field, particle density, particle energy) along the jet: this necessarily introduces a great number of free parameters.

Most of the recent discussions in the literature consider a single, homogeneous emission region. The most direct support to these *one-zone* models comes from the correlated variability at different frequencies (Ulrich et al. 1997), although deviations from this behavior (e.g. the so-called orphan flares, Krawczynski et al. 2004) are sometimes observed. It is clear that this is an over-simplification of the actual geometry and physics involved in jets, but with the advantage to drastically reduce the unknown parameters of the model. This approach is valid to approximate the very compact region where high-energy radiation is produced. Consequently, such models do typically not reproduce the low-frequency radio emission from blazars, which is known to emerge in larger-scale ($\gg$ pc) jet structures, as evidenced by the drastically different radio variability time scales compared to optical through γ-ray variability, and consistent with the fact that such one-zone model configurations are optically thick to synchrotron self-absorption at radio frequencies.

Emission models typically assume a-priori that the jet contains high energy particles. An evident problem to consider is the identification of the physical processes able to energize particles to such high energies. Clearly, the problem of the nature of the emission region and that concerning the acceleration process(es) are coupled. A "paradigm" popular until recent years is the so-called *shock-in-jet* model (Marscher and Gear 1985, Spada et al. 2001). It is assumed that, due to instability in the flow, an internal shock can form in the jet. Particles are then accelerated at the shock front through diffusive shock acceleration (Fermi I) processes. This scenario is supported by the observations of traveling "knots" at VLBI ($\approx$ pc) scale. In this scheme the emitting region can be identified with the region downstream the shock, where particles injected from the front radiatively cool and emit (Kirk et al. 1998, Chiaberge and Ghisellini 1999, Sokolov et al. 2004, Böttcher and Dermer 2010, Joshi and Böttcher 2011, Chen et al. 2011)).

However, several criticisms to this view have been advanced. In fact several observational and theoretical arguments seem to challenge the shock

model, at least in its simplest form. Among them, the observation of episodes of ultra-rapid variability in γ rays both in BL Lacs and FSRQ, with timescales down to few minutes (Aharonian et al. 2007, Albert et al. 2007, Arlen et al. 2013, Aleksić et al. 2011a), implies, through the causality argument, very compact emission regions ($R < ct_{\mathrm{var}}D \approx 10^{14}[t_{\mathrm{var}}/1\,\mathrm{min}]\,D/10\,\mathrm{cm}$) incompatible with the expected size of a shock. Also, detailed fits often reveal that a model with a unique region is not able to provide a good representation of the SED and more than one component is required (Aleksić et al. 2015, Barres de Almeida et al. 2014, Tavecchio et al. 2011). From a more fundamental perspective, it is expected that, at the typical distance of the "blazar zone", the flow is still dominated by the Poynting (i.e. magnetic) flux (e.g., Komissarov et al. 2007). In these circumstances diffusive particle acceleration by shocks is expected to be quite inefficient (Kennel and Coroniti 1984, Sironi et al. 2015).

All these issues bring stimulated new proposals for the structure of the emission region. Rapid variability suggests that (at least occasionally) the radiation is produced in very compact regions embedded in the jet. This have been identified with turbulent cells (Narayan and Piran 2012, Marscher 2014) or with large plasmoids resulting from efficient magnetic reconnection in a relativistic regime (Giannios et al. 2009b, Giannios 2013, Sironi et al. 2015). In both cases, the compact regions are thought to move relativistically in the jet reference frame. The resulting beaming of the emitted radiation in the observer frame (which is the combination of the beaming factor of the compact region in the jet frame and that of the jet flow with respect to the observer) can be very large, with Doppler factors easily reaching $D \sim 50$.

In the framework of the Turbulent Extreme Multi-Zone (TEMZ) model (Marscher 2014), the turbulence also reproduces variations of the linear polarization angle (PA), possibly including large-angle PA swings occasionally observed during FSRQ monitoring (e.g., Marscher et al. 2010). An alternative explanation for such PA swings, correlated with multi-wavelength flares, was suggested by Zhang et al. (2014, 2015), in the context of an inhomogeneous shock-in-jet model. They have shown that such a model, in which the emission region is pervaded by a helical magnetic field, naturally produces PA swings of 180° (or multiples thereof in the case of multiple disturbances propagating through the jet) associated with multiwavelength flares, when carefully accounting for all light travel time effects, without the need for any asymmetric jet structures (such as bends or helical motions of plasmoids along the jet). In Zhang et al. (2015), this model was successfully applied to model, for the first time, snap-shot SEDs, multiwavelength light curve *and* time-dependent optical polarization signatures (Π and PA) of 3C279 during the correlated PA swing $+ \gamma$-ray flare (Abdo et al. 2010) of 2009, in one coherent model (see Figure 6). In a follow-up study, this model was more self-consistently coupled to the results of MHD simulations of relativistic shocks in blazar jets in order to constrain, from first principles, the particle energetics and magnetic-field topology (Zhang et al. 2016).

The magnetic reconnection scenario also appears rather promising. Dedicated Particle in Cell plasma simulations (Sironi and Spitkovsky 2014)
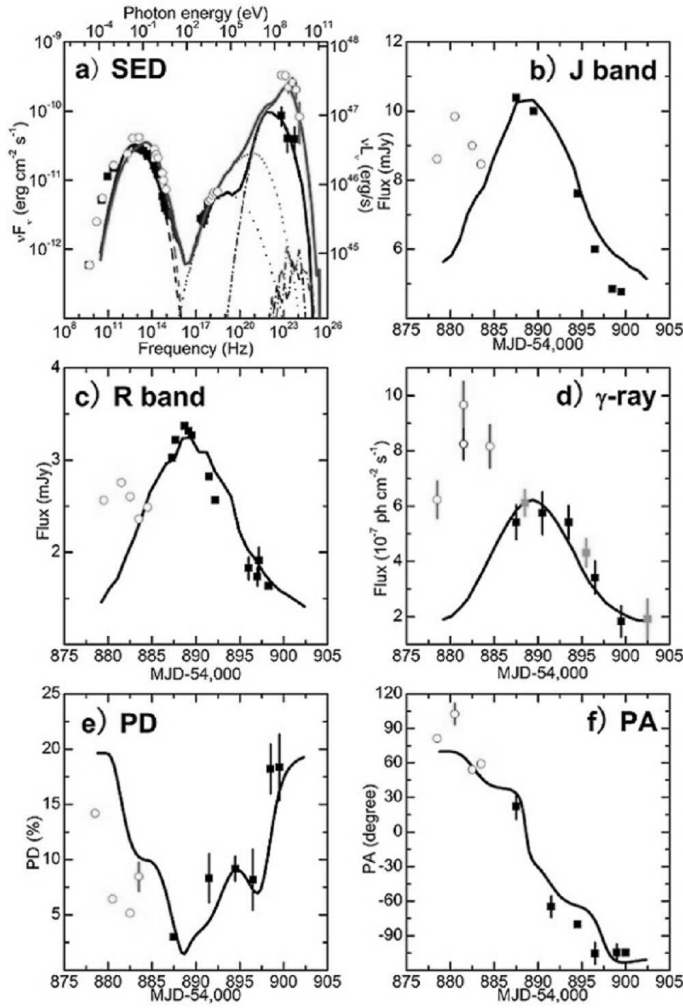
Fig. 6 Simultaneous fits to flux and polarization signatures of the FSRQ 3C279 during the correlated PA swing + multiwavelength flare of 2009 (Abdo et al. 2010), using the polarization-dependent shock-in-jet radiation transfer model of Zhang et al. (2014). (a) Snap-shot SEDs in quiescence and at the peak of the flare; (b – d) flux light curves in the IR (J-band), optical (R-band) and γ-rays (Fermi-LAT); (e) time-dependent optical polarization degree; (f) time-dependent polarization angle, reproducing the observed PA swing. From Zhang et al. (2015).

indicate that the combined action of acceleration at X-points and the subsequent Fermi-II like acceleration from the magnetic islands could provide an efficient way to rapidly accelerate electrons (and ions). A possible problem for this scenario is that BL Lac jets (in which most of the ultra-fast events have been recorded) appear to be weakly magnetized when the SED is reproduced by standard emission models (Tavecchio and Ghisellini 2016).

Even if in the process of magnetic reconnection, the original magnetic energy density is reduced in the reconnection zones, much of the radiative energy dissipation of accelerated particles is expected to occur in the remaining magnetic islands, in which the magnetization still has to be high for magnetic reconnection to occur.

Another possible multi-zone model especially relevant for BL Lac jets is the so-called *spine-layer* model (Ghisellini et al. 2005, Tavecchio and Ghisellini 2008). In this picture, the jet is thought to be composed by two regions, an inner spine, moving with bulk Lorentz factor $\Gamma_s = 10 - 20$, surrounded by a slower ($\Gamma_l \simeq 5$) layer. This kind of structure could result naturally from the jet acceleration mechanism itself (McKinney 2006) or due to the interaction with the external environment (Rossi et al. 2008). If both structures produce radiation, the energy density of the radiation produced by one component is relativistically amplified in the rest frame of the other component by the square of the relative Lorentz factor, $\Gamma_{\mathrm{rel}} = \Gamma_s \Gamma_l (1 - \beta_s \beta_l)$. In this way the IC emission of the spine (which, having a much larger Lorentz factor, will preferentially dominate the emission at small viewing angles) receives a contribution from this kind of EC process. This structure could also be important in the possible production of high-energy neutrinos from BL Lac jets (Tavecchio et al. 2014) and to unify BL Lacs with the misaligned parent population of FRI radio galaxies (Chiaberge et al. 2000).

3.3 Location of the emitting region

Therefore the location of the emitting region in the jet is still quite hotly debated, especially for the case of γ rays. The problem is more acute for FSRQs for which the radiative environment of the jet changes significantly along the jet. As we have pointed out above, most of the models in the past assumed that the emission occurs within the BLR radius. Indeed, this is consistent with the variability timescale (down to a few hours, Tavecchio et al. 2010) and, importantly, the large radiative energy density ensures a large efficiency of the EC power, allowing one to minimize the total jet power (Ghisellini et al. 2014). However there is independent evidence that, at least occasionally, the emission occurs beyond the BLR radius, possibly even at several parsecs from the center (e.g., Agudo et al. 2011).

Important (almost model independent) evidence comes from the detection of VHE γ-ray photons from a handful of FSRQs (3C 279, PKS 1510-089, PKS 1222+216, PKS 1441+25, B0218+357) during active flaring states. The discovery of FSRQ as VHE sources was quite surprising since, in the standard scenario, a huge opacity for gamma rays with energies above few tens of GeV is expected (e.g., Donea and Protheroe 2003, Liu and Bai 2006). The UV radiation from the BLR (lines and continuum) is a target for $\gamma\gamma$ pair production, whose energy threshold is $E_{\gamma,\mathrm{th}} = 25/(E_{\mathrm{le}}/10\,\mathrm{eV})$ GeV. The optical depth starts to be important at an energy corresponding to the intense H Lyα line, $E_{\mathrm{le}} \sim 10$ eV, that is for $E_\gamma \sim 25$ GeV. The detection of photons with $E > 30$ GeV therefore, especially in powerful sources – for which the optical depth should be particularly large, naively increasing

as $\tau \approx L_{\mathrm{disc}}^{0.5}$ – immediately leads to the inference that the emission should occur beyond (or very close to) R_{BLR} (Pacciani et al. 2014, Boettcher and Els 2016, Coogan et al. 2016). Models for the VHE emission from FSRQs adopt this view, and generally assume that the observed high-energy radiation is produced through the IC scattering of the IR radiation field of the molecular torus (Tavecchio et al. 2011, Aleksić et al. 2011b, Pacciani et al. 2014, Aleksić et al. 2014, Ackermann et al. 2014, Ahnen et al. 2015).

For quiescent states there is no evidence of VHE emission from FSRQs (although this conclusion is clearly influenced by sensitivity limits). Therefore, it is not clear whether the quiescent emission should also originate outside the BLR. Through the analysis of long-term *Fermi*/LAT data of bright FSRQs, Poutanen and Stern (2010) claimed that the spectra show a well-defined and sharp break close to 6 GeV, which can be readily interpreted as induced by absorption through the interaction with the He II Lyα line/recombination continuum, expected from highly ionized clouds. On the other hand, such a break could also be intrinsic to the emitted spectrum, arising from the combination of two components, namely, the Compton-upscattered disk and BLR radiation fields (Finke and Dermer 2010), or from Klein-Nishina effects and a curving electron distribution (Cerruti et al. 2013). Further investigations showed that the amount $\Delta\alpha_\gamma$ of the break is variable, with also the indication of a possible anti-correlation between the column density of the He II Lyα continuum and the gamma-ray flux (Stern and Poutanen 2011). A possible way to interpret this complex phenomenology is to assume a stratified BLR, with lines of decreasing ionization produced at increasing distances from the central engine and with the emission region changing position with time (Stern and Poutanen 2014).

3.4 A blazar sequence?

Soon after the discovery of the intense gamma ray emission from blazars, Fossati et al. (1998) reported the existence of a trend between the radio luminosity (at 5 GHz) of a blazar and the position of the two SED peaks (see Fig. 7). This trend was dubbed the *blazar sequence*. According to the basic scheme, the SEDs of powerful sources (FSRQs) peak in the mm and MeV bands. Considering sources of lower luminosity, the two peaks progressively shift to higher frequency, reaching the X-ray band and the TeV band, respectively, in the case the low-luminosity BL Lac objects. Together with this trend, one can also observe a decreasing *Compton dominance*, defined as the ratio of the luminosity of the high-energy bump with respect to the low energy one (see also Finke 2013).

The SED modeling (Ghisellini et al. 1998) shows that the *spectral* blazar sequence is accompanied by a correlation between two physical quantities, namely the energy (or the Lorentz factor) of the electrons emitting at the SED peaks γ_{p} and the sum of the energy density in magnetic field and radiation, $U = U_{\mathrm{mag}} + U_{\mathrm{rad}}$ of the form $\gamma_{\mathrm{p}} \propto U^{-1/2}$ (Fig.8). This led Ghisellini et al. (1998) to heuristically propose that the main agent ruling the blazar sequence is the radiative cooling of the relativistic electrons. In fact,
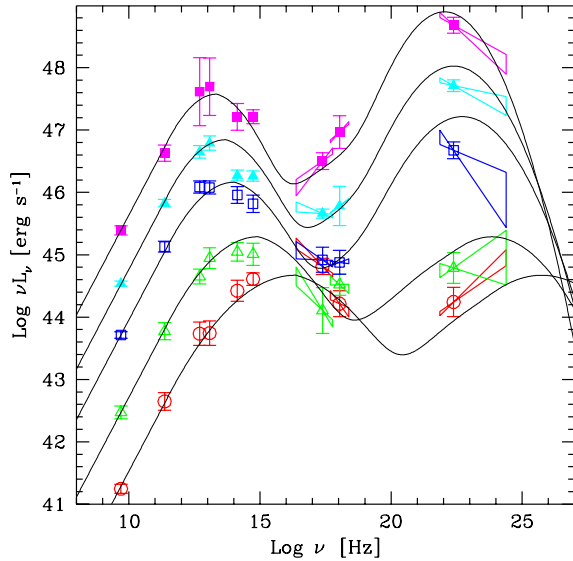
Fig. 7 The data-points show the average SED of blazars in bins of different radio (5 GHz) luminosity. The polynomial fitting curves (black lines) mark an inverse trend connecting the radio luminosity and the peak frequency of the two spectral component (the *blazar sequence*). From Donato et al. 2001.

assuming a universal acceleration mechanism acting in all jets ensuring a characteristic acceleration rate per particle $\dot{\gamma}_{acc}$, the equilibrium between acceleration gain and radiative losses $\dot{\gamma}_{acc} = |\dot{\gamma}_{cool}| \propto \gamma^2 U$ would naturally lead to the derived correlation. While the first work included only a few objects, with quite sparse data, subsequent studies using larger samples, more complete SED and better γ-ray data, confirmed the existence of the trend (Ghisellini et al. 2010, Ghisellini and Tavecchio 2015). The above *cooling scenario* has been further extended in Ghisellini and Tavecchio (2008), to include scaling laws between black hole mass, AGN luminosity, jet power and BLR radius. In this scheme the ultimate parameter determining the blazar appearance could be the accretion rate onto the central supermassive black hole in Eddington units (Ghisellini et al. 2009).

Still not clear is the connection between the general trend shown by the sequence (peaks shifting towards lower frequency for increasing emitted power) and the behavior of single sources which, instead, generally follow the opposite pattern between quiescent and flaring states. A possibility is that the evolution is still dictated by the equilibrium between cooling and acceleration rate, with the latter increasing during active states. This seems to be the case in the well studied BL Lac Mkn 421 (Mankuzhiyil et al. 2011), for which the SED fits of different states reveal that the magnetic field in the emitting region and the energy of the electrons emitting at the SED
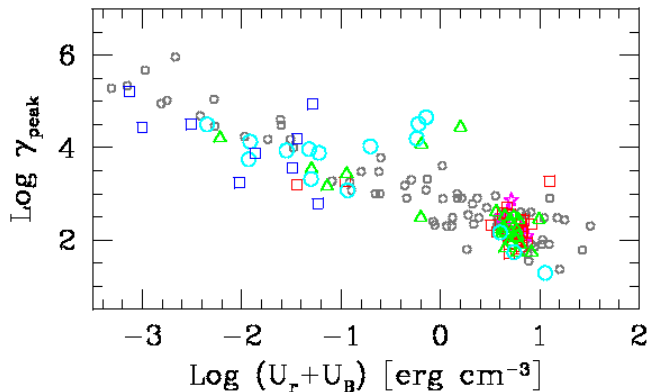
Fig. 8 Lorentz factor of relativistic electrons emitting at the SED peak versus the total energy density (magnetic plus radiative) for a sample of blazars. From Ghisellini et al. (2010).

peaks are related by the expected relation $B \propto \gamma^{-2}$. On the other hand, for the other prototypical VHE BL Lac, Mkn 501, the evidence suggests that only the electron energy is changing (Tavecchio et al. 2001, Mankuzhiyil et al. 2012). In this case a possibility is that the parameter regulating the SED is the acceleration efficiency.

The actual existence of the blazar sequence is the subject of a lively debate. Most of the criticisms focus on the fact that observational biases could severely affect the selection of these sources, possibly introducing spurious trends. For instance, about $40 - -50$ % of the known BL Lac objects lack a reliable redshift measurement (made difficult by the weakness of their emission lines) and this could hamper the identification of far, powerful BL Lacs, which would patently violate the SED sequence. As a way to circumvent this limitation, Finke (2013) suggested to use the Compton dominance instead of luminosity as the quantity to correlate with the SED peak frequencies, which does not require the knowledge of redshifts (with only a negligibly small error introduced by a lack of knowledge in the redshift of the peak frequencies). Using this new correlation discriminant, he found renewed evidence for the existence of a sequence, in agreement with the original Fossati et al. (1998) sequence for BL Lac objects, especially at high peak frequencies, but essentially no correlation for blazars with synchrotron peak frequencies below $\sim 10^{14}$ Hz, with Compton dominance parameters spreading over ~ 3 orders of magnitude without any correlation with the synchrotron peak frequency. The efforts devoted to investigate the sequence at low luminosities also start to show possible deviations from the expectations (e.g., Caccianiga and Marchã 2004, Padovani et al. 2007, Raiteri and Capetti 2016), although the situation is particularly delicate since low luminosity non-blazar AGNs, misaligned (hence less beamed) blazars or blazars with (relatively) low mass black holes could "pollute" the samples. These criticisms have been condensed by Giommi et al. (2012) (see also

Giommi et al. 2013, Giommi and Padovani 2015) into a simplified view aiming at demonstrating that, even without any real trend in the intrinsic SED, selection effects alone can be responsible for the observed spectral sequence.

It is important to remark that, in discussing these issues, one should always clearly distinguish between the (observational) blazar sequence, in the sense of Fossati et al. (1998), and the (theoretical) cooling scenario (and its extensions). In fact, even if the spectral sequence could be affected by selection effects, the latter is a more general physical scheme which, in fact, can accomodate or even envisages the existence of possible outliers from the canonical blazar sequence (e.g., Ghisellini and Tavecchio 2008, Ghisellini et al. 2012, 2013). Note also that, according to the general scenario developed in Ghisellini and Tavecchio (2008), the observed sequence could just be the "tip of the icerberg" of the blazar population, representative only of the most massive and powerful blazars. Sources with smaller black hole masses or slightly misaligned jets are expected to produce low-luminosity jets with, however, a SED shape similar to that of the powerful FSRQ, thus appearing as outliers from the blazar sequence. In this sense the observed sequence could just be the upper edge of an envelope of progressively misaligned blazars (Meyer et al. 2011).

4 X-Ray Binaries — Microquasars

Over the last decades, it has become clear that many aspects of accretion physics are mirrored across the black hole mass scale, irregardless of the size difference and accretion environment. The extent of this 'mass-scaling' suggests the relative importance of mechanisms within the inner accretion flow rather than those dictated by fueling and/or outer disk geometry, and gives clues about the nature of jet launching. Although our theoretical understanding still lags the quality of the precision, broadband data in many cases, we are starting to find empirical trends that allow an urgently needed reduction in the number of free parameters.

In isolation, the modeling of jets and particle acceleration in XRBs is subject to the same uncertainties and avalanch of free parameters as discussed in the above Sections for AGN. However because XRBs evolve on much faster timescales, they offer a unique perspective, where an individual can traverse a wide variety of behaviors that only large samples of AGN can equally populate. This has opened a new window on one of the more persistent problems to solve in jet physics: the coupling between bulk dynamical properties (or macrophysics), and the microphysics of processes like particle acceleration and radiation. In this Section we will summarize some of the recent progress in this area and its extension to AGN.

XRBs come in several flavors, high and low mass (with respect to the companion star), and with black holes or neutron stars as the compact object. In order to compare with AGN we will be limiting ourselves to discussing black hole XRBs. The complicated phenomenology of XRBs has been covered in several papers and reviews (see e.g., McClintock and Remillard 2006, Fender 2006, Belloni 2010) to which we refer the interested reader.
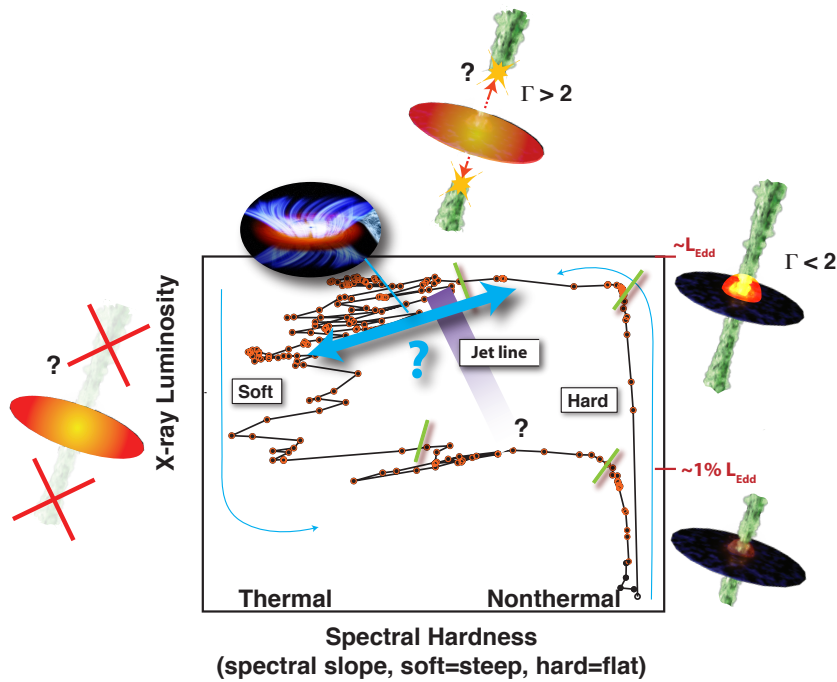
Fig. 9 The hardness-intensity diagram (HID) for an outburst of XRB GX339−4, with schematics of the corresponding inflow/outflow configuration per state. Only the two canonical states (hard and soft) are indicated.

Here we will only summarize the most relevant properties, in order to focus the discussion on comparisons with jetted AGN with a focus on breaking model degeneracy and better understanding particle acceleration.

Low mass XRBs (LMXBs) are black holes with a main-sequence companion star whose mass is smaller than the compact object, typically on the order of a solar mass. The star fills its Roche lobe and thus feeds material to the black hole via its L1 Lagrangian point, which leads to a well defined entry point for material to populate an accretion disk in the orbital plane. LMXBs go through transient outbursts, likely driven by thermal instabilities in the accretion disk (e.g. Lasota 2001), which initiate a sequence of distinct states, originally classified in terms of X-ray and spectral timing properties. Fig. 9 shows a schematic view of this pattern of cyclic behavior, using actual data from the Galactic LMXB GX339−4, which has been a great boon for our understanding because it experiences a full outburst cycle approximately every 1-2 years. The figure shows the outburst pattern in a commonly used phase space of X-ray luminosity (related to, not necessarily linearly) the accretion rate $\dot{M}$ onto the black hole, and the X-ray spectral hardness. The latter indicates the relative dominance of thermal (soft spectrum) versus nonthermal (hard power law) processes. This type of diagram is referred to a hardness-intensity (HID) diagram.

During a typical outburst, a LMXB rises out of quiescence (off the plot in the lower right corner in Fig. 9), a state which is quite difficult to study by definition because of the very low luminosity. The weakest sources seen in quiescence so far are XTE J1118+480, A0620−00, and Swift J1357.2−0933, all with $L_{\mathrm{X}} \leq 10^{-8} L_{\mathrm{Edd}}$ (e.g. Gallo et al. 2007, 2014, Plotkin et al. 2016). At some point the rising X-rays trigger a monitoring instrument such as *SWIFT* or *MAXI* (in the past it was typically *RXTE*) and these facilities then send out alerts, allowing further multiwavelength coverage. At the point that a source is bright enough to trigger facilities, it is already in the so-called hard state. This state is associated with compact, steady jets which are synchrotron self-absorbed, resulting in the classical flat/inverted spectrum associated also with the compact cores of AGN (Blandford and Königl 1979). The hard state is the longest lasting of the LMXB states and, while quiescence has been argued to be a separate state, the latest observational evidence supports the persistence of jets smoothly down into quiescence, as well as other properties (see, e.g., Plotkin et al. 2015).

As the source luminosity increases (assumedly driven by a rising accretion rate), somewhere around $\sim 0.5 L_{\mathrm{Edd}}$ the spectrum begins to soften and the source moves counter-clockwise around the upper right corner in the diagram, beginning a transition into a state often referred to as the Hard Intermediate State (HIMS). These transitions are harder to categorize based on radio or X-ray spectra, but are clearly demarcated via changes/features in the power density spectra (e.g., Belloni 2010), that we will not discuss in detail here, but that include the presence of quasi-periodic oscillations (QPOs) and various types of broadband variability. The hard-to-HIMS transition occurs very quickly and within a day or days, the jets are seen to radically transform from steady flow to a transient state with brighter, discrete ejecta at a distinct point often referred to as the "jet line" in the HID. The jets appear now as discrete optically thin blobs moving with superluminal motion; it was on this state that the original argument for the nickname "microquasar" was based (Mirabel and Rodríguez 1994). After the flaring ends, the source is in the Soft Intermediate State (SIMS) and the jets essentially deconstruct: the radio and IR synchrotron radiation vanishes and the source proceeds into the left side of the diagram, into a soft thermal state that is almost entirely disk dominated, with a multi-temperature black body. As the luminosity decreases (assumedly along with $\dot{M}$), the spectrum begins to harden again and the jets reform, at a luminosity around an order of magnitude or more below the hard-to-soft transition. This hysteresis effect is not well understood, but it seems clear that something besides the accretion rate, likely magnetic field topology, is an important driver. With renewed steady jets, the hard state recedes down into quiescence and the outburst is over. A typical outburst can last from months to $\sim$ a year.

In contrast to LMXBs, HMXBs tend to be persistent, with Cyg X-1 seen as the "prototypical" source of its class. Cyg X-1 does show state changes, but with a much lower range in luminosity, and because it does not go into quiescence it never undergoes the full hysteresis loop (e.g. Gleißner et al. 2004, Wilms et al. 2006). Mostly it varies between soft and hard states. In

contrast to LMXBs, only a few HMXBs are known in our Galaxy (Tetarenko et al. 2016).

The two states that can be associated with particle acceleration via the presence of jets are thus the hard and HIMS. Interestingly, the discovery of jets in XRBs came over 30 years after their discovery as a class via X-ray observations, at which point a paradigm based entirely on accretion disk phenomena was already well established. The X-ray hard state SED is typically comprised of a nonthermal power law with $\Gamma \sim 1.5 - 1.8$, and an exponential cutoff around 100 keV. Sometimes there are also weak reflection features such as an iron fluorescent line and a "Compton bump" leading to hardening above ~ 15 keV (Lightman and White 1988, Fabian et al. 1989). The hard state SED can be explained in terms of a moderately optically thick ($\tau \lesssim 1$), static region of hot electrons existing near the black hole and disk. The existence of this region, named the corona, was inferred in order to explain the hard X-ray power-law via unsaturated inverse Compton scattering. In this scenario, the corona upscatters the weaker disk thermal photons (not usually visible in the spectrum, but assumed present because of the clear thermal disk signature in the soft state). This type of scenario seems natural, because the temperature that gives both the spectral index (for some optical depth) and cutoff is consistent with the Virial temperature for a compact region within 10s of r_g from the black hole (see, e.g., Titarchuk 1994, Magdziarz and Zdziarski 1995).

As is common in astrophysics, however, increasing precision in the observations tends to provide challenges. More extensive monitoring after the launch of $RXTE$ revealed significant variability in the cutoff over relatively short timescales (e.g., Rodriguez et al. 2003, Wilms et al. 2006), suggesting a more dynamic region than originally envisioned. Another complication was the relatively weak reflection signatures in many observations. In order to reduce the amount of coronal emission intercepted by the cooler disk, many variations of geometry were developed, including a recessed disk, a patchy corona, magnetic flares, etc. (see, e.g., Haardt 1997, Merloni and Fabian 2002). One paper in particular suggested that a magnetic corona could be accelerated to moderately relativistic speeds away from the disk, thus providing an explanation for the relatively weak reflection signatures in Cyg X-1 (Beloborodov 1999). This latter scenario is especially relevant in the context of integrating jets into the existing coronal picture.

The problem is that relativistic jets need dynamically important, ordered magnetic fields theading the disk near the black hole, in order to launch (e.g. McKinney 2006, Beckwith et al. 2008). The need for these fields creates two main complications to the original picture: first, the coronal electrons will want to follow the magnetic fields lines and the static picture breaks down. Secondly, the introduction of a strong magnetic field means that the electrons will also radiate (and thus cool) via synchrotron emission, and those photons can also be inverse Compton upscattered (SSC) along with those from the disk.

The presence of jets thus requires some rethinking of the original picture, and highlights the need to find a self-consistent link between the three types of flow: inflowing disk, corona, and outflowing jets. The problem is

that multiple regions introduces degeneracy for the interpretation of the hard X-ray spectrum, which can now be from a thermal corona, a hybrid thermal/nonthermal corona, an isolated nonthermal corona or a magnetized corona comprising the base of the jets, as well as direct synchrotron emission (Markoff et al. 2005b). In the meantime, more recent studies of reflection suggest that the data are more consistent with a source of disk illumination that lies on the axis above the disk, and changes its height ("lamppost" reflection, see, e.g., Miniutti and Fabian 2004, Dauser et al. 2013). This idea further supports a hybrid corona/jet base, where the effect of even mildly relativistic acceleration of the jets away from the disk means that IC/SSC from the jet base will dominate over synchrotron emission in the reflected component, unless particle acceleration starts within 10s of r_g of the black hole (see, e.g., Markoff and Nowak 2004).

In an attempt to rule out one or more of the various hard state emission scenarios, Nowak et al. (2011) carried out an extensive, simultaneous campaign on Cyg X-1 using *Suzaku*, *RXTE* and *Chandra-HETG*. Instead, they found that all main (Compton-dominated) scenarios provided equally good statistical descriptions of the new data sets. On the other hand, the fact that XRB jets clearly emit synchrotron radiation up to the mm/IR bands, depending on the observation (e.g. Fender 2006), presents a way to probe the connection between the components. For instance, coordinated multi-wavelength observations can help to isolate the jet-related components, as well as build a picture of the jet properties in XRBs compared to AGN (content, particle acceleration, etc.).

Thus in parallel with some of the developments in ideas about the corona, the era of coordinated, quasi-simultaneous observations of XRBs really began to take off at the start of this century, particularly between the radio and X-ray bands (but see also Motch et al. 1982). Soon after, a tight, nonlinear correlation was discovered between the radio and X-ray luminosities of GX339−4, holding over many orders of magnitude, and repeated during different outbursts (Fig. 10 and, e.g., Corbel et al. 2000, 2003, 2013). This correlation was soon found to extend to other sources (e.g. Gallo et al. 2003), as well as between the IR and X-ray bands (Russell et al. 2006).

Because the different configurations of disk vs jet dominance in the HID are also seen among the various AGN classifications, the idea soon arose that AGN may be undergoing XRB-like state changes, just over much longer timescales. This idea of trying to "pair" XRB states to AGN classes, often referred to as 'mass scaling' in accretion, has been the topic of much exploration in the last ~ 13 years. The most successful pairings to date involve the longer-lasting hard and soft states. For instance, there is a compelling mass-dependent scaling between the power spectra of the soft/intermediate state and that of Seyferts (e.g., McHardy et al. 2006). However, in the context of jets and particle acceleration, the most interesting scaling is the so-called Fundamental Plane (FP) of black hole accretion.

The FP is an empirical relation, essentially a 2D plane linking all sub-Eddington, jetted black hole types in the 3D space of X-ray luminosity, radio luminosity and mass. After the discovery of the radio/X-ray correlation in
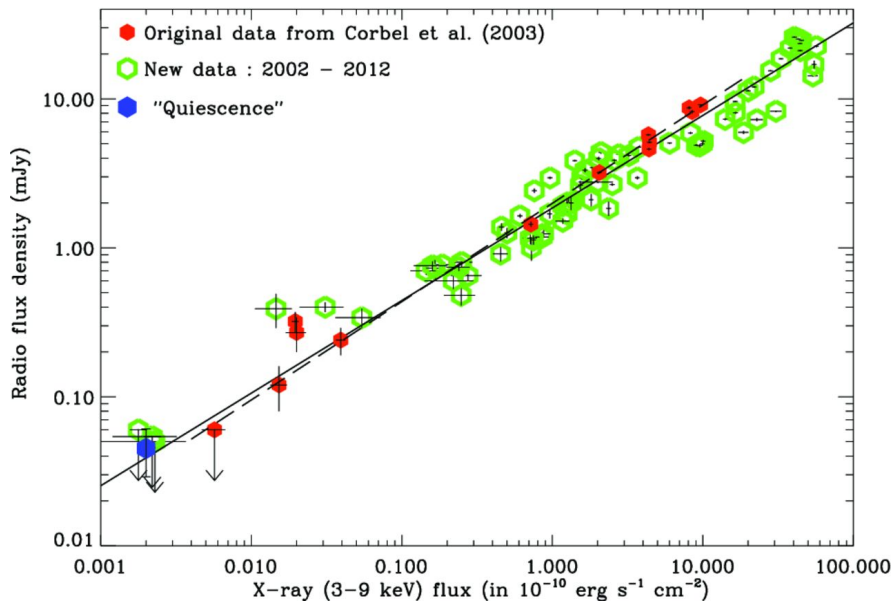
Fig. 10 Radio vs. X-ray correlation in the hard state of GX 339−4, with the original correlation shown in red from Corbel et al. (2003), and the newer outbursts. The dashed line illustrates the original radio/X-ray correlation from the 19971999 period, while the solid line corresponds to a fit to the new whole sample. The blue point shows the source close to quiescence. From Corbel et al. (2013).

individual XRBs, it was quickly realized that this correlation represents the ratio of the efficiencies for the two radiative processes. For instance Markoff et al. (2003) considered the scaling in the context of synchrotron emission from the jets. Using a Blandford-Königl-like jet model (Blandford and Königl 1979), one can show that the self-absorbed, flat/inverted radio-through-IR part of the spectrum will scale as $\sim \dot{M}^{17/12-2/3\alpha_{\mathrm{RIR}}}$, where α_{RIR} is the spectral index of the self-absorbed part of the jet and is close to 0 (see also Falcke and Biermann 1995). The measured slope of the correlation is $L_{\mathrm{X}} \propto L_{\mathrm{R}}^{0.6-0.7}$ (Corbel et al. 2013), which constrains the dependence of $L_{\mathrm{X}} \propto \dot{M}^{2-2.3}$, ruling out radiatively efficient processes for the hard X-ray spectrum. This result was generalized by Heinz and Sunyaev (2003), expressing all physical scales in terms of M_{BH} (via r_g) and all powers in terms of $\dot{m} \sim L_{\mathrm{Edd}}/(c^2) \propto M_{\mathrm{BH}}$. This mass scaling effectively introduces a normalization term into the radio/IR/X-ray correlations. In other words, if compact jets and accretion disks are self-similar structures across the immense mass and power scales seen by "hard state-like" black holes, then all black holes should show a similar coupling of X-ray and radio luminosity as a function of relative accretion rate, once "corrected" by the mass.

This idea was explored and tested empirically by two different groups, using large samples of AGN Merloni et al. (2003), Falcke et al. (2004). If the AGN follow a similar correlation as hard state XRBs over much longer timescales, this trend would be revealed statistically by looking at snap-
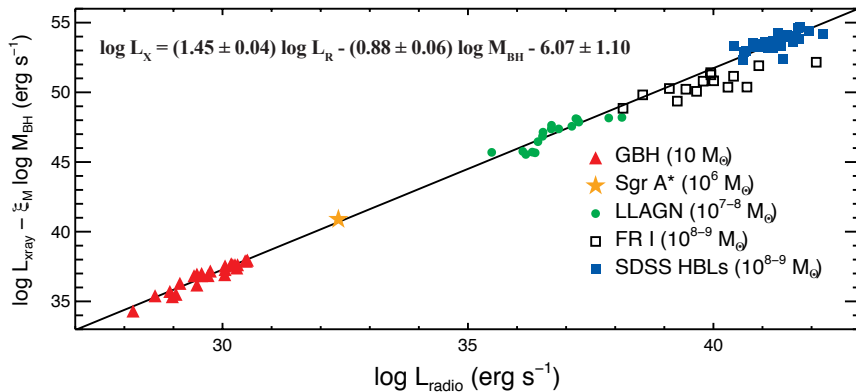
Fig. 11 A projection in mass of the Fundamental Plane for black hole accretion onto the radio and X-ray luminosity plane, using a Bayesian regression technique on data from hard state XRBs and a sample of sub-Eddington accreting AGN (Plotkin et al. 2012b).

shots of a large number of objects. Both groups, using different approaches, found that such a correlation indeed seems to extend to AGN, and in the subsequent years more discussion and exploration of the statistics has ensued. A good summary can be found in Plotkin et al. (2012b), as well as the most robust derivation of the FP, for the first time also including BL Lacs (see Fig. 11). While there is still some debate over exactly which AGN classes fit on the FP, it is pretty clear that sub-Eddington, steady jetted sources such as **Low Louminosity AGN (LLAGN) or Low-Ionization Emission-Line Regions (LINERs),** FRIs and BL Lacs do, and perhaps also **Narrow-Line Seyfert-1 (NL Sy1)** with radio detections (e.g. Gültekin et al. 2009).

The extension of the broadband correlations found in XRBs to AGN has therefore opened up a new pathway to study the disk/jet coupling in black holes. The X-rays probe the conditions near the black hole, in a corona or near the launchpoints of the jet, and its intimate connection to the transfer of energy into accelerated particles further out in the jets, responsible for the radio/IR parts of the FP correlation.

Having established that mass-scaling seems to hold in the disk/jet coupling, we can now consider how to use it in order to better understand the power and acceleration properties of the jets in the hard state (for all black hole masses).

4.1 Origin of the high-energy emission

Returning to the question of the origin of the hard state emission, the degeneracy between synchrotron and inverse Compton processes (and for the latter, also between different contributing photon fields) exists at both ends of the mass range. In XRBs, the lower Lorentz factor of the jets limits EC

to two contributions: the accretion disk or the companion star. In LMXBs the companion star is not bright enough to compete with the disk, reducing the possible source of the X-rays to direct synchrotron radiation, SSC emission, EC of disk photons, or some combination. In most scenarios all of these could give the correct scalings for the FP, thus the next step is to move beyond correlations and look at modeling the broadband SEDs.

The original suggestion that synchrotron could contribute significantly to the hard X-ray spectrum in XRBs came from Markoff et al. (2001a), for one of the first quasi-simultaneous broadband (radio through X-ray) SEDs compiled (Hynes et al. 2000). The hard X-ray spectrum shows little to no reflection, nor a high energy cutoff, in contrast to what would be expected for a thermal corona model. Furthermore, jets can account for all the nonthermal components in the spectrum, as long as the particle acceleration initiates somewhat offset from the black hole, at around $50r_g$. This requirement of having a transition from primarily thermal plasma in the jets (similar to Sgr A*, see, e.g., Markoff et al. 2001b) to a region where a powerlaw of particles is accelerated implies a break in the spectrum where this enhanced emission transitions from optically thick to thin. This feature is not always possible to detect because it often falls in the IR band where the companion star and/or disk can contribute, but it can be seen explicitly in GX339$-$4 (see Fig. 12, and, e.g. Corbel and Fender 2002), and detected or constrained in many other observations (Russell et al. 2010, 2013b, Koljonen et al. 2015).

We will come back to the break in Section 4.2, but its location in the SED provides a hard limit on how much synchrotron emission can contribute to the hard X-ray spectrum. Unlike the SED for XTE J1118+480, most hard state XRBs, particularly at higher luminosity, do show evidence for some reflection and thus a contribution in SSC/EC from the corona, or jet base. However synchrotron emission can still contribute at the $\sim 10\%$ level, which has implications for particle acceleration in XRBs. Even when the break is not visible, there are independent methods to gauge the jet synchrotron contribution. For instance Russell et al. (2010) studies the evolution of an outburst in the XRB XTE J1550$-$564 in three IR bands. During the decline from outburst in the disk-dominated soft state, a clear exponential decay is visible. Upon transition to the hard state, an excess emission above this monotonic decrease appears, corresponding to the jets re-activating. Extracting this excess allows an independent determination of the jet synchrotron contribution to the IR band, and its spectral index, which is found to match that of the X-rays in both slope and normalization.

Another independent constraint on the contribution and geometry of the jets comes from fast IR/optical and X-ray variability studies. One of the first examples of such a spectro-timing study is presented for XTE J1118+480 in Hynes et al. (2003), where they extract the broadband SED of the rms variability in IR, UV and X-ray, and find it follows a $\nu^{-0.6}$ powerlaw, consistent with optically thin synchrotron emission. More recently, Kalamkar et al. (2016) detect the first IR QPO during a hard state of GX339$-$4 (at half the frequency of the X-ray QPO, and the same frequency as that found in optical/UV/Xray from Hynes et al. 2003 for XTE J1118), as well
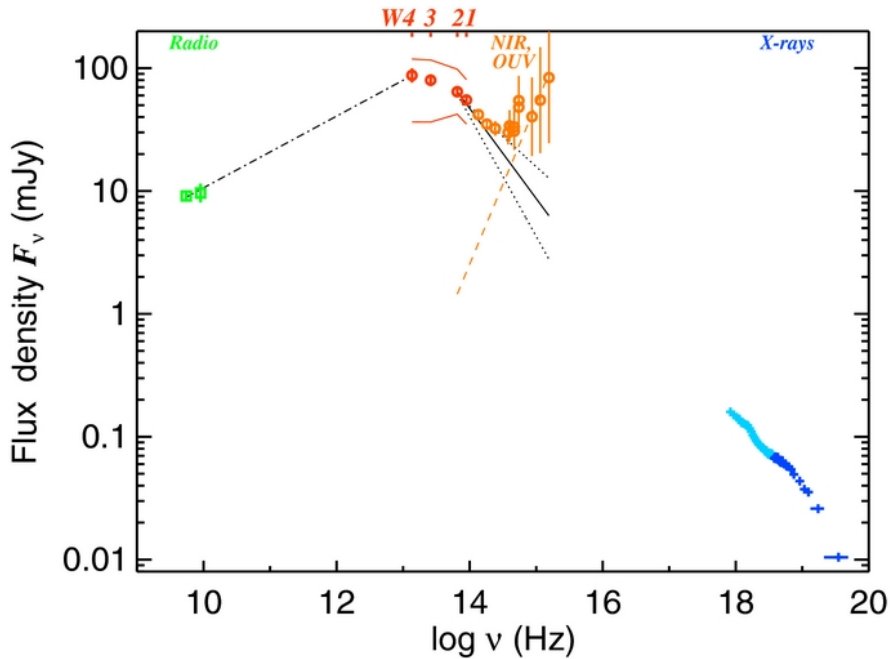
Fig. 12 Average dereddened SED of GX 339−4, including WISE data points for the first time (in red). Red curves represent the envelope of extreme variations over 13 WISE epochs. The near-infrared and optical/ultraviolet (OUV) points are plotted in orange and radio in green, and the break from optically thick to optically thin is apparent, see (Gandhi et al. 2011).

as strongly correlated sub-second variability, with the IR lagging the X-rays by 111ms. The direction of the lag, as well as brightness temperature and size arguments, effectively rules out reprocessing or hot-inflow models, similar to argumentation in Hynes et al. 2003. The timescale for the lag corresponds to a light-travel distance of $3700r_g$ for $\sim 6M_\odot$, consistent with the distance of the IR-emitting region based on the location of the break in the spectrum of Gandhi et al. (2011) (Fig 12). The first detection of a QPO in the IR further suggests a picture where oscillations rooted in the accretion flow are conveyed with the plasma into the jets, perhaps via ordered magnetic field lines.

Of all microquasars, Cygnus X-1 is the most extensively observed. This source has been the target of monitoring campaigns that allowed to estimate the parameters of the binary and to obtain detailed spectra at all wavelengths. Cygnus X-1 is located at 1.86 kpc from Earth. A high-mass stellar companion of spectral type O9.7 Iab and mass $\sim 20\ M_\odot$ and a black hole of 14.8 $M_\odot$ (Orosz et al. 2011) form the binary system.

In the X-ray band Cygnus X-1 switches between the typical hard and soft states of X-ray binaries. The soft state is characterized by a blackbody component of $kT \lesssim 0.5$ keV from an accretion disk, and a soft power-law with spectral photon index $\Gamma \sim 2 - 3$. The source, however, spends most

of the time in its hard state, in which the spectral energy distribution is well described by a power-law of spectral index $\Gamma \sim 1.7$ that extends up to a high-energy cutoff at ~ 150 keV (e.g. Dove et al. 1997, Poutanen et al. 1997). The origin of this power-law is the Comptonization of disk photons by thermal electrons in the hot corona that partially covers the inner region of the disk. The detection of a Compton reflection bump and the Fe Kα line at ~ 6.4 keV support the presence of the corona during the low/hard state. Additionally, intermediate spectral states have also been reported (Belloni et al. 1996).

Persistent and transient jets have been resolved at radio wavelengths in Cygnus X-1 during the hard state (e.g. Stirling et al. 2001, Rushton et al. 2011). The outflow is extremely collimated (aperture angle $\sim 2°$, Stirling et al. 2001) and propagates at an angle of $\sim 29°$ with the line of sight (Orosz et al. 2011). The radio emission is modulated by the orbital period of the binary because of absorption in the wind of the companion star (e.g. Brocksopp et al. 2002).

Cygnus X-1 is one of the two confirmed MQs that is a gamma-ray source.[4] The first detection of soft gamma rays up to a few MeV was achieved with the instrument *COMPTEL* aboard the *Compton Gamma-Ray Observatory* (McConnell et al. 2002). Emission in the same energy range was later observed with *INTEGRAL* (e.g. Laurent et al. 2011). The *INTEGRAL* detections represented a breakthrough since it was found that the ~ 400 keV - 2 MeV photons were highly polarized.

At higher energies Cygnus X-1 is fundamentally a transient source on timescales of 1-2 d. Episodes of gamma-ray emission have been detected with the satellite *AGILE* between 100 MeV and a few GeV in the hard state (Sabatini et al. 2010, and marginally during the hard-to-soft transition (Sabatini et al. 2013). The analysis of *Fermi*-Large Area Telescope (LAT) data at 0.1-10 GeV revealed weak flares (three of them quasi-simultaneous with *AGILE* detections; Bodaghee et al. 2013, and weak steady emission (Malyshev et al. 2013).

Finally, Cygnus X-1 has been observed in the very high energy band (≥ 100 GeV) with the Major Atmospheric Gamma Imaging Cherenkov (MAGIC) telescope during the hard state (Albert et al. 2007). During inferior conjunction a flare (duration of less than a day, rising time ~ 1 h) was likely detected with a significance of 4.0σ (3.2σ after trial correction). Only upper limits could be obtained for the steady emission.

The broadband spectral energy distribution (SED) of Cygnus X-1 in the hard state displays several components. The radio emission is synchrotron radiation of relativistic electrons accelerated in the jets. This component is observed up to its turnover at infrared frequencies, where the stellar continuum takes over. The emission of the disk/corona dominates up to the hard X-rays, but the origin of the MeV tail observed with *COMPTEL* and *INTEGRAL* is still disputed. Its high degree of polarization (¿65%) suggests this component is emitted in an ordered magnetic field such as is expected to exist in the jets, a result supported by the fact that the polarized X-ray emission is only clearly detected during the hard state (Ro-

---

[4] The other one is Cygnus X-3.

driguez et al. 2015). In this scenario the MeV tail would be the cutoff of the jet synchrotron spectrum, see for example the fits to the data obtained by Malyshev et al. (2013), Zdziarski et al. (2012), Zdziarski et al. (2014), and Zhang et al. (2014). An alternative model was introduced by Romero et al. (2014), where the MeV tail is synchrotron radiation of secondary non-thermal electrons in the corona. This model predicts significant polarization also during intermediate spectral states, something that cannot be presently ruled out from the data (Rodriguez et al. 2015).

All known gamma-ray binaries host a high-mass donor star, a fact that points to a fundamental role played by the stellar wind and/or radiation field in the mechanisms that produce the high-energy photons. In leptonic models for MQs gamma rays are produced by inverse Compton (IC) scattering of the stellar radiation off relativistic electrons, whereas in hadronic models gamma-rays are generated by the decay of neutral pions injected in the interactions of non-thermal protons in the jets with cold protons of the stellar wind (Romero et al. 2003, 2005).

The inclusion of relativistic protons in the jets brings about a feature absent in purely leptonic models, namely the production of secondary particles (neutrinos, electron-positron pairs, muons, pions) in high-energy hadronic interactions. The cooling of charged secondaries may contribute to the radiative spectrum of the jets. In Cygnus X-1 the effects of the impact of the jets in the interstellar medium suggest that they carry a significant amount of kinetic energy in cold protons (Gallo et al. 2005, Heinz 2006).

In Fig. 13 we show the results of the modeling of the broadband non-thermal emission reported by Pepe et al. (2015). In this model, the emission from 1 to ~ 150 keV is produced by Comptonization of disk photons in the coronae around the black hole (see, nevertheless, Georganopoulos et al. 2002). The synchroron radiation extends up to soft gamma-rays. The high-energy and very high-energy gamma-rays are the result of a combination of SSC, pp, and $p\gamma$ interactions. The dominant source of thermal protons for pp is the wind of the star. Since these winds tend to be clumpy, flaring behaviour is expected around 1 TeV (Romero et al. 2010).

4.2 Particle acceleration

Thus due to a wide range of simultaneous broadband monitoring campaigns and spectro-timing campaigns over the last decades, a picture is emerging of a linked inflow/outflow system where both "sides" of the flow can contribute to the broadband spectrum. Contrary to the original picture of XRBs which focused exclusively on the accretion disk, these small accreting black holes are fully capable of launching relativistic jets, and those jets accelerate particles just as in blazars. Because of their relatively higher compactness, and thus stronger magnetic fields, jet synchrotron from moderately high-energy particles easily reaches the X-ray band and can compete with IC processes for the hard state spectrum. Finally, the detection of strong linear polarization in the soft gamma-rays from Cyg X-1 (Laurent et al. 2011), and more recently the *Fermi* detection of a hard power law (Zanin et al. 2016) seems to clinch the question about particle acceleration in XRB jets. Orbital
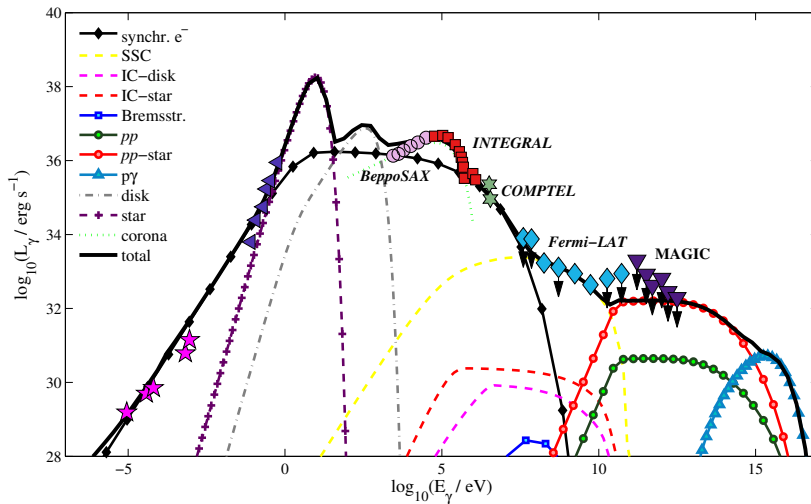
Fig. 13 Spectral energy distribution of the jet of the galactic microquasar Cygnus X-1. From Pepe et al. (2015).

modulations hint that for this source the GeV γ-ray emission occurs further out in the jets upon interaction with the stellar winds. A few detections of X-ray lines suggest hadronic content as well (e.g., Migliari et al. 2002, Díaz Trigo et al. 2013), though it is not clear if this is entrained or directly accelerated.

The question now becomes, can we learn something new from XRBs that will help us understand particle acceleration in jets in general, and help reduce the large number of free parameters in the various models? Many of the free parameters come from a lack of constraints on the jet bulk (M/HD driven) properties, and how they couple to particle acceleration properties (the macro-microphysics connection). XRBs offer a distinct advantage to AGN in this sense, given the realtime evolution displayed in this coupling. We will end this Section by discussing some new explorations of this connection.

The spectral break from the flat/inverted synchrotron spectrum to a power-law (e.g., Fig. 12 is the canonical signature of the transition from self-absorbed to optically thin regimes. The power-law at higher frequencies reveals an accelerated particle distribution, and the compactest part of the jet where particle acceleration is present will dominate the emission at the break itself. In AGN (see Sections 3.2 and 3.3) this region is offset from the black hole, and often modeled de-facto by a single zone where dissipation of magnetic bulk energy into particle kinetic energy occurs via acceleration. In XRBs, the break location in the spectrum also corresponds to an offset from the black hole and may correspond to a similar dissipation zone.

Unlike AGN, XRB jets can barely be imaged with VLBI, however their smaller sizes allow for much more causality between the launch point and
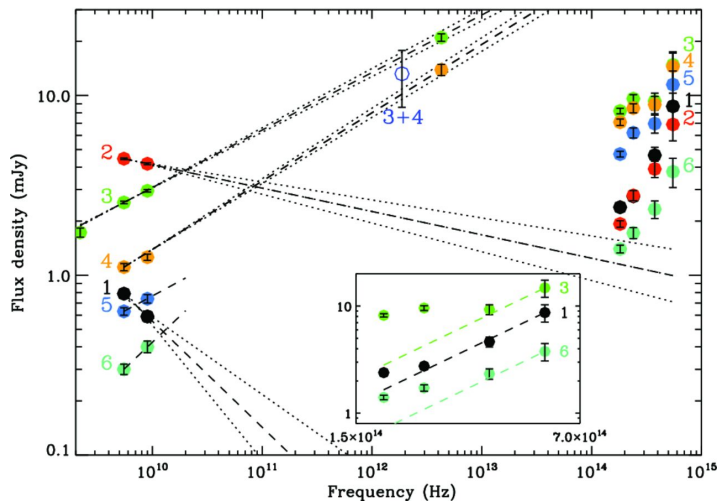
Fig. 14 Evolution of the radio to OIR SED during the soft to hard state transition as the jets reform, and become optically thick. The numbers (and associated colours) refer to sequential epochs, and the dashed lines correspond to the extrapolation of the radio spectra. Inset: zoom of the OIR spectra # 1, 3 and 6. From Corbel et al. (2013).

the outermost regions. Assuming a conservatively low plasma velocity of $0.3c$, the time for flow to travel from the black hole to the outermost regions of impact on the ISM at scales on the order of a pc (Corbel et al. 2002) is ~ 10 years, and most of the intrinsic broadband SED seems to be emitted within scales > 100 times smaller (e.g. Markoff et al. 2005b). Thus an observing campaign covering the broadband emission from radio to X-ray can easily track the direct response of the steady jets to changes in the inner accretion flow in real time. However XRB jets are also seen to dismantle and reconfigure on timescales of weeks during state changes. During these times, multiwavelength monitoring reveals the buildup of the accelerated particle distribution, the transition from optically thin to self-absorbed (see Fig. 14), and the evolution in the spectrum including the spectral break, all as a function of changes in the accretion flow (Fig. 15).

Focusing now on the spectral break, if this feature originates in the *same* region for all sources (i.e., at some fixed number of r_g), then the dependence on M_{BH} and $\dot{m}$ can be derived for various standard accretion scenarios (see, e.g., Falcke and Biermann 1995, Markoff et al. 2003, Heinz and Sunyaev 2003). For the case of low-luminosity sources that fit on the FP, the slope of the correlation makes clear that these are in a radiatively inefficient state, as explained above. Briefly summarizing arguments presented in Heinz and Sunyaev (2003), this state is gas pressure dominated and the pressure is directly related to the particle density, which in turn is typically defined as $\rho = \dot{M}/(4\pi RHv)$. Since all physical scales for black holes can be expressed in terms of r_g, which is lin-

ear in mass, and $\dot{m} \equiv \dot{M}/M_{\rm BH}$, the pressure thus depends on the ratio $\dot{m}/M_{\rm BH}$. MRI-driven turbulence (Balbus and Hawley 1998) implies that the magnetic pressure is closely bound to the gas pressure, which means $B^2 \propto \dot{m}/M_{\rm BH}$ as well. If the jet is launched from the disk and shares the same scalings, one can solve for the photosphere where $\tau_{\rm SSA} = 1$, and show that for a fixed plasma β and a particle index of $p = 2$, the break frequency in the SED will scale as $\sim \dot{m}^{2/3}$, for objects of same mass and spin. *Thus in an individual XRB, this dependence on accretion rate can be isolated and tested.*

If the particle index p is significantly steeper, or the particle distribution is quasi-thermal, the scaling of $\dot{m}$ will be moderated slightly to $\sim 5/8$, while if the jet were launched from a non-advective disk (this seems ruled out by the FP, however for completeness we include it) the scaling for all particle distributions is $\sim 1/2$. The point is that for any reasonable set of physical conditions for jet launching, the internal pressure provided by the gas and magnetic field would be expected to increase with $\dot{m}$ (for fixed spin and $M_{\rm BH}$), giving a positive scaling of the break frequency with $\dot{m}$ as the jet becomes optically thick at increasingly compacter scales.

However, already early monitoring of single sources like GX 339−4 indicated that the spectral break seems to move in the opposite direction expected from purely optical depth scalings as explained above (Markoff et al. 2003). By now there are a few well-observed outbursts from other sources that reveal the evolution of the SED (see, e.g., Fig. 15). These clearly show the spectral break increasing in frequency as the power in the thermal disk spectrum, and thus accretion rate, decreases. Broader compilations of multiple measurements from several XRBs Russell et al. (2013b) show a similar trend in the location of the dissipation region.

The current best interpretation of these campaigns is that the location of the dissipation region that defines the break is itself moving, likely driven by changes in the jet itself. This evolution can also be seen in a correlation between break frequency and spectral index, indicating a blazar-sequence like relationship for XRBs (Koljonen et al. 2015). One important clue is that the break seems to be relatively stable within individual sources, and from source to source, for a given (relative) luminosity in Eddington units. Fits to multiple SEDs from many XRBs also show that the range of values for the break within a given source corresponds to a range of distance within the total length of the jets of $\sim 10 - 10^4 \, r_g$.

Similar to other FP properties, the location of the break seems to be related more to the relative power (in, e.g., $\dot{m}$) than the size of the black hole. For instance in the few hard state-like LLAGN where quasi-simultaneous and/or high-spatial resolution data are available, the implied break occurs within a similar range as seen in XRBs (Markoff et al. 2008, and see Fig.16). In fact, the same self-similar model (where all distances and powers are expressed in mass-scaling units of r_g and $L_{\rm Edd}$, or $\dot{m}$, can be used to fit the
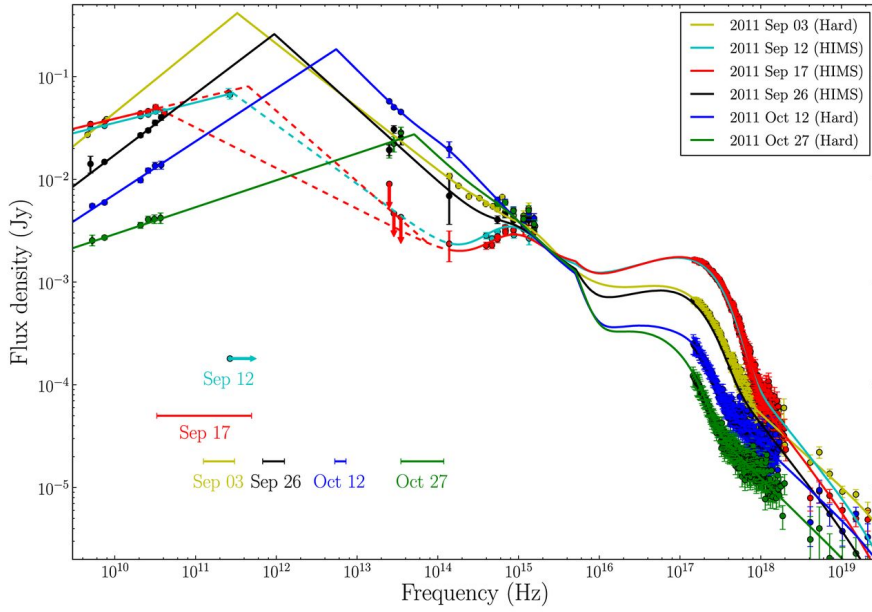
Fig. 15 Broadband radio to X-ray SED of MAXI J1836-194 taken during its 2011 outburst. Dashed lines indicate possible ranges of parameters, with the horizontal bars showing the uncertainty range for the optically thick-to-thin spectral break. Only four epochs of X-ray observational data are depicted to avoid crowding. The jet spectral break moves to higher frequency following the transition back to the hard state from the HIMS during a failed state transition, and is anticorrelated with accretion rate as indicated by the disk component. From Russell et al. (2014).

broadband SEDs of two black holes at opposite ends of the mass scale at similar accretion power, with all physical scales tied (see Fig. 17). Together these results suggest that the location of the particle acceleration zone is a direct consequence of conditions in the base of the jets, or in turn, the accretion flow. This opens the door to an exploration of whether the zone (and associated SED break) could be a predictive property of, e.g., an MHD outflow, providing a means to drastically reduce the number of free parameters currently employed.

In a series of papers, Polko et al. (2010, 2013, 2014) have derived a self-similar (following on prescriptions in Vlahakis et al. 2000 and Vlahakis and Königl 2003), relativistic MHD flow solution, including a pseudo-Newtonian treatment of gravity. These models can be used as intermediaries between special relativistic MHD and GRMHD simulations and observations, and also to explore potential drivers of the correlations observed in XRBs. For instance, if the break location is associated with particle acceleration at a disruption such as a recollimation shock (e.g., Marscher et al. 2008b) or turbulent instabilities that form from shear once the bulk plasma velocity exceeds the fast magnetosonic speed, the scaling with other properties can be explored and used to rule out various launching scenarios. Thus the
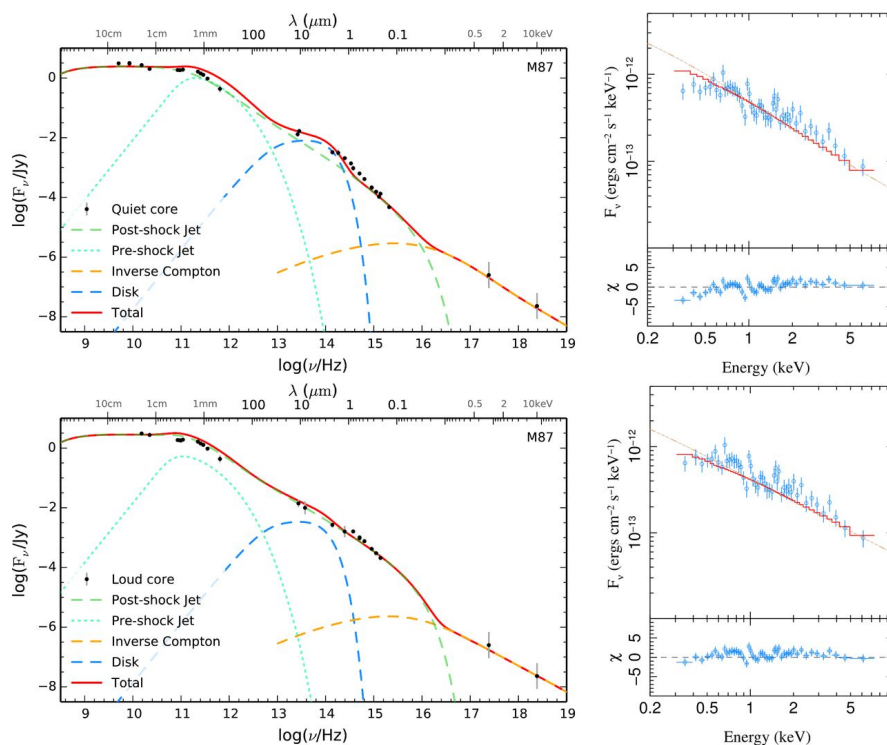
Fig. 16 An outflow-dominated model fit to the SED of M87, where all data are from within a 0.4 arcsec aperture radius (32pc). The top panel shows the result for the quiescent state, the bottom panel for the active one. The X-ray spectrum used in the model for both states is the 2002 Chandra spectrum, the fit for which is shown as a separate plot. The data are fit using the model in Markoff et al. (2005b) that is also applied to XRBs, and a location of the break implies an acceleration region of 10s of r_g, similar to XRBs as well. From Prieto et al. (2016).

spectral breaks potentially provide an important new pivot for connecting inflow properties to the outflows, a longstanding issue in the field.

4.3 Clues about particle acceleration efficiency

XRBs have thus taught us that the location of particle acceleration may depend on the jet bulk properties, and that this property seems to extend to AGN, similar to the radio/X-ray correlations. Another indication from recent MWL campaigns is that there is a dependence of particle acceleration efficiency on accretion power. This phenomena was actually first noticed in Sgr A*, where the linearly polarized "submm bump" synchrotron feature in the spectrum (e.g., Bower et al. 2015) corresponds to emission from very close to the black hole and assumedly connects to a weak jet. No evidence for a spectral break or an optically thin power-law exists in the quiescent spectrum of Sgr A*, whose synchrotron and SSC spectrum can be
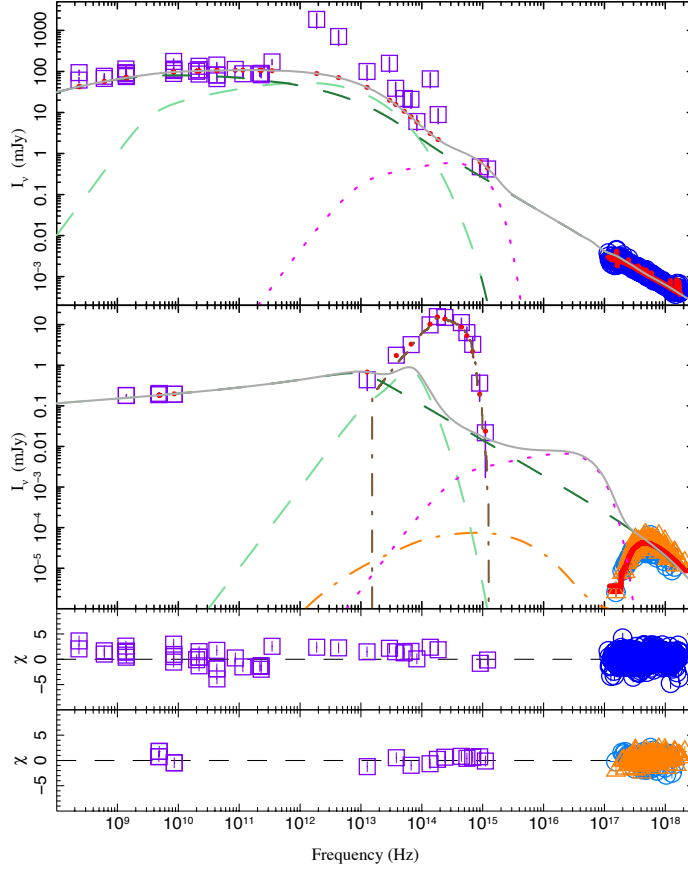
Fig. 17 Best joint-fit model with all physical free parameters tied to SEDs of similar accretion power (based on L_X/L_{Edd} from the LLAGN M81 (top) and hard state XRB V404 Cyg (bottom). Lines show the individual model components (light green/dashed: thermal synchrotron, dark green/dashed: non-thermal synchrotron, orange/dasheddotted: synchrotron self-Compton, magenta/dotted: multicolor blackbody disk, and gray/dasheddotted: stellar component in the case of V404), all absent absorption. The gray/solid line shows the total model, while the red/solid line and dots show the model after forward folding through detector space, including absorption. The IR/optical part of the M81 SED also includes a galactic stellar and dust contribution (not fitted). The spectral break in both sources implies a particle acceleration region in the jets starting at $300r_g$. From Markoff et al. (2015).

explained by a mildly relativistic thermal distribution of particles in both the corona as well as jets. However Sgr A* also experiences a nonthermal flaring in the X-rays approximately daily, often accompanied by IR flaring, and models of this process suggest the appearance of sporadic and weak particle acceleration at the level of less than 1% of the thermal peak (e.g., Yuan et al. 2003, Dibi et al. 2014, Dibi et al. 2016).

Now that there are several observations of XRBs in a similar state of quiescence as Sgr A*, with $L_X < 10^{-8}L_{Edd}$, it seems that the lack of a strong power law in the emitting particles may be a universal hallmark of this state. For instance, the SEDs of A0620−00 (Gallo et al. 2007, Froning et al. 2011), XTE J1118+480 (Plotkin et al. 2015), and Swift J1357.2−0933 (Shahbaz et al. 2013) can all be explained with a dominant thermal synchrotron bump, and if any power-law is present it is consistent with being very weak and/or produced relatively far out in the jets. The physics of this dependence of particle acceleration on accretion rate is not yet understood, but may point to a jet power threshold below which the structures needed to accelerate particles cannot form or (as in the case of Sgr A*) be maintained.

One final note is that two distinct types of jets are seen in XRBs, at different accretion powers, and also radio-quiet states are seen. These can all occur in a single outburst of a source, thus ruling out spin as a driver for these states. The relationship between spin and jet power is also being explored for XRBs, but to date the jury is still out on this issue, due to disagreements about both how to measure the total jet power as well as the spin (e.g., Narayan and McClintock 2012, Russell et al. 2013a).

In summary, XRBs are ideal testbeds for our understanding about black hole accretion and jet launching in general. Specifically they can reveal details about how particle acceleration is linked to the bulk plasma properties of the jets, in ways that cannot be as directly probed in AGN due to the longer timescales. XRB jets clearly accelerate particles, but the same questions about leptonic vs hadronic content still exist for these sources as for AGN. Similar to AGN, particularly blazars, there seems to be a dissipation/acceleration region offset from the black hole some distance down the jets, and a sequence in power and break frequency that may reveal the nature of the structures providing acceleration. The strong evidence for mass-scaling in the accretion physics around black holes makes XRBs valuable tools for probing these questions. The possibility that XRBs can accelerate hadrons to PeV energy is an interesting prospect, and something that near-future instruments like CTA will be able to test. Their energy budgets are smaller than supernovae, but there are many more of them, meaning that XRBs could be an important contributing source for the Galactic CR population. **Some models, for instance the one by Pepe et al. (2015) some of whose predictions are illustrated in Fig. 13, can accommodate proton acceleration up to 10^{15} eV at the base of the jet and reach 10^{16} eV at distances $\sim 10^{12}$ cm from the compact object. These might be among the most energetic protons accelerated in the Galaxy**.

5 Discussion

Galactic and extragalactic jets present many similarities, and also many differences. Both seem to be powered by accretion of magnetized matter with angular momentum onto a compact object; they both can display apparent superluminal motions; they seem to present a correlation of causal significance between the accretion and ejection processes; they display variability along the whole electromagnetic spectrum. These and other similarities are often stressed. The differences, however, are also important, and frequently overlooked. We emphasize the following ones:

– Galactic jets seem to be slower. In some cases, where the bulk motions are directly measured through emission lines, the plasma velocity is $\sim 0.3c$. There are some exceptional objects, however, such Sco X-1, with Lorentz factors up to 10.
– Galactic jets become dark not far from the central source. Typical lengths are ~ 1000 AU.
– They are heavy (have hadronic content) and produce thermal emission at their termination regions.
– They interact with stellar winds (in the case of microquasars with high-mass donor stars).
– The size of the accretion disk is constrained by the presence of the donor star.
– Gravitational and radiative effects of the donor star can be important to jet formation and propagation.
– The disk and corona are hotter than in active galactic nuclei; magnetic fields are also higher close to the jet base.

These differences can yield, however, opportunities for observational and theoretical studies of physical situations that can be applied, with suitable modifications, to extragalactic jets. In this review we have seen how a relatively simple model can easily be adapted to a quantitative description of both types of outflows.

Because of the proximity of Galactic jets, many physical processes that take place in mechanisms operating also in AGNs can be observationally probed in great detail and on vastly shorter timescales. The use of VLBI radio observations to resolve jets during simultaneous X-ray and gamma-ray monitoring of microquasars remains to be fully explored. The implementation of this kind of multiwavelength studies would facilitate the construction of refined models that can be later extrapolated to AGNs and larger scales. Testing the new predictions of such models in a very different scenario would strengthen our understanding of the underlying physics.

References

M.G. Aartsen, M. Ackermann, J. Adams, J.A. Aguilar, M. Ahlers, M. Ahrens, D. Altmann, T. Anderson, C. Arguelles, T.C. Arlen, et al., Observation of High-Energy Astrophysical Neutrinos in Three Years of IceCube Data. Physical Review Letters **113**(10), 101101 (2014). doi:10.1103/PhysRevLett.113.101101

A.A. Abdo, M. Ackermann, I. Agudo, M. Ajello, H.D. Aller, M.F. Aller, E. Angelakis, A.A. Arkharov, M. Axelsson, U. BACH, et al., The Spectral Energy Distribution of Fermi Bright Blazars. ApJ **716**, 30–70 (2010). doi:10.1088/0004-637X/716/1/30

G.O. Abell, B. Margon, A kinematic model for SS433. Nature **279**, 701–703 (1979). doi:10.1038/279701a0

M. Ackermann, M. Ajello, A. Allafort, E. Antolini, G. Barbiellini, D. Bastieri, R. Bellazzini, E. Bissaldi, E. Bonamente, J. Bregeon, et al., Multifrequency Studies of the Peculiar Quasar 4C +21.35 during the 2010 Flaring Activity. ApJ **786**, 157 (2014). doi:10.1088/0004-637X/786/2/157

I. Agudo, S.G. Jorstad, A.P. Marscher, V.M. Larionov, J.L. Gómez, A. Lähteenmäki, M. Gurwell, P.S. Smith, H. Wiesemeyer, C. Thum, J. Heidt, D.A. Blinov, F.D. D'Arcangelo, V.A. Hagen-Thorn, D.A. Morozova, E. Nieppola, M. Roca-Sogorb, G.D. Schmidt, B. Taylor, M. Tornikoski, I.S. Troitsky, Location of γ-ray Flare Emission in the Jet of the BL Lacertae Object OJ287 More than 14 pc from the Central Engine. ApJ **726**, 13 (2011). doi:10.1088/2041-8205/726/1/L13

F.A. Aharonian, TeV gamma rays from BL Lac objects due to synchrotron radiation of extremely high energy protons. New A **5**, 377–395 (2000). doi:10.1016/S1384-1076(00)00039-7

F.A. Aharonian, Proton-synchrotron radiation of large-scale jets in active galactic nuclei. MNRAS **332**, 215–230 (2002). doi:10.1046/j.1365-8711.2002.05292.x

F.A. Aharonian, *Very high energy cosmic gamma radiation : a crucial window on the extreme Universe* 2004

F. Aharonian, A.G. Akhperjanian, A.R. Bazer-Bachi, B. Behera, M. Beilicke, W. Benbow, D. Berge, K. Bernlöhr, C. Boisson, O. Bolz, V. Borrel, T. Boutelier, I. Braun, E. Brion, A.M. Brown, R. Bühler, I. Büsching, T. Bulik, S. Carrigan, P.M. Chadwick, A.C. Clapson, L.M. Chounet, G. Coignet, R. Cornils, L. Costamante, B. Degrange, H.J. Dickinson, A. Djannati-Ataï, W. Domainko, L.O. Drury, G. Dubus, J. Dyks, K. Egberts, D. Emmanoulopoulos, P. Espigat, C. Farnier, F. Feinstein, A. Fiasson, A. Förster, G. Fontaine, S. Funk, S. Funk, M. Füßling, Y.A. Gallant, B. Giebels, J.F. Glicenstein, B. Glück, P. Goret, C. Hadjichristidis, D. Hauser, M. Hauser, G. Heinzelmann, G. Henri, G. Hermann, J.A. Hinton, A. Hoffmann, W. Hofmann, M. Holleran, S. Hoppe, D. Horns, A. Jacholkowska, O.C. de Jager, E. Kendziorra, M. Kerschhaggl, B. Khélifi, N. Komin, K. Kosack, G. Lamanna, I.J. Latham, R. Le Gallou, A. Lemière, M. Lemoine-Goumard, J.P. Lenain, T. Lohse, J.M. Martin, O. Martineau-Huynh, A. Marcowith, C. Masterson, G. Maurin, T.J.L. McComb, R. Moderski, E. Moulin, M. de Naurois, D. Nedbal, S.J. Nolan, J.P. Olive, K.J. Orford, J.L. Osborne, M. Ostrowski, M. Panter, G. Pedaletti, G. Pelletier, P.O. Petrucci, S. Pita, G. Pühlhofer, M. Punch, S. Ranchon, B.C. Raubenheimer, M. Raue, S.M. Rayner, M. Renaud, J. Ripken, L. Rob, L. Rolland, S. Rosier-Lees, G. Rowell, B. Rudak, J. Ruppel, V. Sahakian, A. Santangelo, L. Saugé, S. Schlenker, R. Schlickeiser, R. Schröder, U. Schwanke, S. Schwarzburg, S. Schwemmer, A.

---

[5] Any opinion, finding and conclusion or recommendation expressed in this material is hat of the authors, and the NRF does not accept any liability in this regard.

Shalchi, H. Sol, D. Spangler, Ł. Stawarz, R. Steenkamp, C. Stegmann, G. Superina, P.H. Tam, J.P. Tavernet, R. Terrier, C. van Eldik, G. Vasileiadis, C. Venter, J.P. Vialle, P. Vincent, M. Vivier, H.J. Völk, F. Volpe, S.J. Wagner, M. Ward, A.A. Zdziarski, An Exceptional Very High Energy Gamma-Ray Flare of PKS 2155-304. ApJ **664**, 71–74 (2007). doi:10.1086/520635

M.L. Ahnen, S. Ansoldi, L.A. Antonelli, P. Antoranz, A. Babic, B. Banerjee, P. Bangale, U. Barres de Almeida, J.A. Barrio, W. Bednarek, et al., Very High Energy γ-Rays from the Universe's Middle Age: Detection of the z = 0.940 Blazar PKS 1441+25 with MAGIC. ApJ **815**, 23 (2015). doi:10.1088/2041-8205/815/2/L23

M. Ajello, R.W. Romani, D. Gasparrini, M.S. Shaw, J. Bolmer, G. Cotter, J. Finke, J. Greiner, S.E. Healey, O. King, W. Max-Moerbeck, P.F. Michelson, W.J. Potter, A. Rau, A.C.S. Readhead, J.L. Richards, P. Schady, The Cosmic Evolution of Fermi BL Lacertae Objects. ApJ **780**, 73 (2014). doi:10.1088/0004-637X/780/1/73

J. Albert, E. Aliu, H. Anderhub, P. Antoranz, A. Armada, C. Baixeras, J.A. Barrio, H. Bartko, D. Bastieri, J.K. Becker, W. Bednarek, K. Berger, C. Bigongiari, A. Biland, R.K. Bock, P. Bordas, V. Bosch-Ramon, T. Bretz, I. Britvitch, M. Camara, E. Carmona, A. Chilingarian, J.A. Coarasa, S. Commichau, J.L. Contreras, J. Cortina, M.T. Costado, V. Curtef, V. Danielyan, F. Dazzi, A. De Angelis, C. Delgado, R. de los Reyes, B. De Lotto, E. Domingo-Santamaría, D. Dorner, M. Doro, M. Errando, M. Fagiolini, D. Ferenc, E. Fernández, R. Firpo, J. Flix, M.V. Fonseca, L. Font, M. Fuchs, N. Galante, R.J. García-López, M. Garczarczyk, M. Gaug, M. Giller, F. Goebel, D. Hakobyan, M. Hayashida, T. Hengstebeck, A. Herrero, D. Höhne, J. Hose, C.C. Hsu, P. Jacon, T. Jogler, R. Kosyra, D. Kranich, R. Kritzer, A. Laille, E. Lindfors, S. Lombardi, F. Longo, J. López, M. López, E. Lorenz, P. Majumdar, G. Maneva, K. Mannheim, O. Mansutti, M. Mariotti, M. Martínez, D. Mazin, C. Merck, M. Meucci, M. Meyer, J.M. Miranda, R. Mirzoyan, S. Mizobuchi, A. Moralejo, D. Nieto, K. Nilsson, J. Ninkovic, E. Oña-Wilhelmi, N. Otte, I. Oya, M. Panniello, R. Paoletti, J.M. Paredes, M. Pasanen, D. Pascoli, F. Pauss, R. Pegna, M. Persic, L. Peruzzo, A. Piccioli, E. Prandini, N. Puchades, A. Raymers, W. Rhode, M. Ribó, J. Rico, M. Rissi, A. Robert, S. Rügamer, A. Saggion, T. Saito, A. Sánchez, P. Sartori, V. Scalzotto, V. Scapin, R. Schmitt, T. Schweizer, M. Shayduk, K. Shinozaki, S.N. Shore, N. Sidro, A. Sillanpää, D. Sobczynska, A. Stamerra, L.S. Stark, L. Takalo, P. Temnikov, D. Tescaro, M. Teshima, D.F. Torres, N. Turini, H. Vankov, V. Vitale, R.M. Wagner, T. Wibig, W. Wittek, F. Zandanel, R. Zanin, J. Zapatero, Very High Energy Gamma-Ray Radiation from the Stellar Mass Black Hole Binary Cygnus X-1. ApJ **665**, 51–54 (2007). doi:10.1086/521145

J. Aleksić, L.A. Antonelli, P. Antoranz, M. Backes, J.A. Barrio, D. Bastieri, J. Becerra González, W. Bednarek, A. Berdyugin, K. Berger, E. Bernardini, A. Biland, O. Blanch, R.K. Bock, A. Boller, G. Bonnoli, D. Borla Tridon, I. Braun, T. Bretz, A. Cañellas, E. Carmona, A. Carosi, P. Colin, E. Colombo, J.L. Contreras, J. Cortina, L. Cossio, S. Covino, F. Dazzi, A. De Angelis, E. De Cea del Pozo, B. De Lotto, C. Delgado Mendez, A. Diago Ortega, M. Doert, A. Domínguez, D. Dominis Prester, D. Dorner, M. Doro, D. Elsaesser, D. Ferenc, M.V. Fonseca, L. Font, C. Fruck, R.J. García López, M. Garczarczyk, D. Garrido, G. Giavitto, N. Godinović, D. Hadasch, D. Häfner, A. Herrero, D. Hildebrand, D. Höhne-Mönch, J. Hose, D. Hrupec, B. Huber, T. Jogler, S. Klepser, T. Krähenbühl, J. Krause, A. La Barbera, D. Lelas, E. Leonardo, E. Lindfors, S. Lombardi, M. López, E. Lorenz, M. Makariev, G. Maneva, N. Mankuzhiyil, K. Mannheim, L. Maraschi, M. Mariotti, M. Martínez, D. Mazin, M. Meucci, J.M. Miranda, R. Mirzoyan, H. Miyamoto, J. Moldón, A. Moralejo, D. Nieto, K. Nilsson, R. Orito, I. Oya, D. Paneque, R. Paoletti, S. Pardo, J.M. Paredes, S. Partini, M. Pasanen, F. Pauss, M.A. Perez-Torres, M. Persic, L. Peruzzo, M. Pilia, J. Pochon, F. Prada, P.G. Prada Moroni, E. Prandini, I. Puljak, I. Reichardt, R. Reinthal, W. Rhode, M. Ribó, J. Rico, S. Rügamer, A. Saggion, K. Saito, T.Y. Saito, M. Salvati, K. Satalecka, V. Scalzotto, V. Scapin, C. Schultz, T. Schweizer, M. Shayduk, S.N. Shore, A. Sillanpää, J. Sitarek, D.

Sobczynska, F. Spanier, S. Spiro, A. Stamerra, B. Steinke, J. Storz, N. Strah, T. Surić, L. Takalo, F. Tavecchio, P. Temnikov, T. Terzić, D. Tescaro, M. Teshima, M. Thom, O. Tibolla, D.F. Torres, A. Treves, H. Vankov, P. Vogler, R.M. Wagner, Q. Weitzel, V. Zabalza, F. Zandanel, R. Zanin, MAGIC Collaboration, Y.T.Tanaka, D.L.Wood, S.Buson, MAGIC Discovery of Very High Energy Emission from the FSRQ PKS 1222+21. ApJ **730**, 8 (2011a). doi:10.1088/2041-8205/730/1/L8

J. Aleksić, L.A. Antonelli, P. Antoranz, M. Backes, J.A. Barrio, D. Bastieri, J. Becerra González, W. Bednarek, A. Berdyugin, K. Berger, E. Bernardini, A. Biland, O. Blanch, R.K. Bock, A. Boller, G. Bonnoli, D. Borla Tridon, I. Braun, T. Bretz, A. Cañellas, E. Carmona, A. Carosi, P. Colin, E. Colombo, J.L. Contreras, J. Cortina, L. Cossio, S. Covino, F. Dazzi, A. de Angelis, E. de Cea Del Pozo, B. de Lotto, C. Delgado Mendez, A. Diago Ortega, M. Doert, A. Domínguez, D. Dominis Prester, D. Dorner, M. Doro, D. Elsaesser, D. Ferenc, M.V. Fonseca, L. Font, C. Fruck, R.J. García López, M. Garczarczyk, D. Garrido, G. Giavitto, N. Godinović, D. Hadasch, D. Häfner, A. Herrero, D. Hildebrand, J. Hose, D. Hrupec, B. Huber, T. Jogler, S. Klepser, T. Krähenbühl, J. Krause, A. La Barbera, D. Lelas, E. Leonardo, E. Lindfors, S. Lombardi, M. López, E. Lorenz, P. Majumdar, M. Makariev, G. Maneva, N. Mankuzhiyil, K. Mannheim, L. Maraschi, M. Mariotti, M. Martínez, D. Mazin, M. Meucci, J.M. Miranda, R. Mirzoyan, H. Miyamoto, J. Moldón, A. Moralejo, D. Nieto, K. Nilsson, R. Orito, I. Oya, R. Paoletti, S. Pardo, J.M. Paredes, S. Partini, M. Pasanen, F. Pauss, M.A. Perez-Torres, M. Persic, L. Peruzzo, M. Pilia, J. Pochon, F. Prada, P.G. Prada Moroni, E. Prandini, I. Puljak, I. Reichardt, R. Reinthal, W. Rhode, M. Ribó, J. Rico, S. Rügamer, M. Rüger, A. Saggion, K. Saito, T.Y. Saito, M. Salvati, K. Satalecka, V. Scalzotto, V. Scapin, C. Schultz, T. Schweizer, M. Shayduk, S.N. Shore, A. Sillanpää, J. Sitarek, D. Sobczynska, F. Spanier, S. Spiro, A. Stamerra, B. Steinke, J. Storz, N. Strah, T. Surić, L. Takalo, F. Tavecchio, P. Temnikov, T. Terzić, D. Tescaro, M. Teshima, M. Thom, O. Tibolla, D.F. Torres, A. Treves, H. Vankov, P. Vogler, R.M. Wagner, Q. Weitzel, V. Zabalza, F. Zandanel, R. Zanin, MAGIC Observations and multiwavelength properties of the quasar 3C 279 in 2007 and 2009. A&A **530**, 4 (2011b). doi:10.1051/0004-6361/201116497

J. Aleksić, S. Ansoldi, L.A. Antonelli, P. Antoranz, A. Babic, P. Bangale, U. Barres de Almeida, J.A. Barrio, J. Becerra González, W. Bednarek, et al., MAGIC gamma-ray and multi-frequency observations of flat spectrum radio quasar PKS 1510-089 in early 2012. A&A **569**, 46 (2014). doi:10.1051/0004-6361/201423484

J. Aleksić, S. Ansoldi, L.A. Antonelli, P. Antoranz, A. Babic, P. Bangale, U. Barres de Almeida, J.A. Barrio, J. Becerra González, W. Bednarek, et al., Unprecedented study of the broadband emission of Mrk 421 during flaring activity in March 2010. A&A **578**, 22 (2015). doi:10.1051/0004-6361/201424811

T. Arlen, T. Aune, M. Beilicke, W. Benbow, A. Bouvier, J.H. Buckley, V. Bugaev, A. Cesarini, L. Ciupik, M.P. Connolly, W. Cui, R. Dickherber, J. Dumm, M. Errando, A. Falcone, S. Federici, Q. Feng, J.P. Finley, G. Finnegan, L. Fortson, A. Furniss, N. Galante, D. Gall, S. Griffin, J. Grube, G. Gyuk, D. Hanna, J. Holder, T.B. Humensky, P. Kaaret, N. Karlsson, M. Kertzman, Y. Khassen, D. Kieda, H. Krawczynski, F. Krennrich, G. Maier, P. Moriarty, R. Mukherjee, T. Nelson, A. O'Faoláin de Bhróithe, R.A. Ong, M. Orr, N. Park, J.S. Perkins, A. Pichel, M. Pohl, H. Prokoph, J. Quinn, K. Ragan, L.C. Reyes, P.T. Reynolds, E. Roache, D.B. Saxon, M. Schroedter, G.H. Sembroski, D. Staszak, I. Telezhinsky, G. Tešić, M. Theiling, K. Tsurusaki, A. Varlotta, S. Vincent, S.P. Wakely, T.C. Weekes, A. Weinstein, R. Welsing, D.A. Williams, B. Zitzer, VERITAS Collaboration, S.G.Jorstad, N.R.MacDonald, A.P.Marscher, P.S.Smith, R.C.Walker, T.Hovatta, J.Richards, W.Max-Moerbeck, A.Readhead, M.L.Lister, Y.Y.Kovalev, A.B.Pushkarev, M.A.Gurwell, A.Lähteenmäki, E.Nieppola, M.Tornikoski, E.Järvelä, Rapid TeV Gamma-Ray Flaring of BL Lacertae. ApJ **762**, 92 (2013). doi:10.1088/0004-637X/762/2/92

K. Asada, M. Nakamura, The Structure of the M87 Jet: A Transition from Parabolic

to Conical Streamlines. ApJ **745**, 28 (2012). doi:10.1088/2041-8205/745/2/L28

A.M. Atoyan, C.D. Dermer, Neutral Beams from Blazar Jets. ApJ **586**, 79–96 (2003). doi:10.1086/346261

S.A. Balbus, J.F. Hawley, Instability, turbulence, and enhanced transport in accretion disks. Reviews of Modern Physics **70**, 1–53 (1998). doi:10.1103/RevModPhys.70.1

D.L. Band, J.E. Grindlay, Synchrotron and inverse Compton emission from expanding sources in jets - Application to SS 433. ApJ **311**, 595–609 (1986). doi:10.1086/164799

M.G. Baring, Gamma - gamma Attenuation and Relativisitic Beaming in Gamma-Ray Bursts. ApJ **418**, 391 (1993). doi:10.1086/173398

U. Barres de Almeida, F. Tavecchio, N. Mankuzhiyil, Polarimetric tomography of blazar jets. MNRAS **441**, 2885–2890 (2014). doi:10.1093/mnras/stu744

K. Beckwith, J.F. Hawley, J.H. Krolik, The Influence of Magnetic Field Geometry on the Evolution of Black Hole Accretion Flows: Similar Disks, Drastically Different Jets. ApJ **678**, 1180–1199 (2008). doi:10.1086/533492

W. Bednarek, On the application of the mirror model for gamma-ray flare in 3C 279. A&A **336**, 123–129 (1998)

M.C. Begelman, A.C. Fabian, M.J. Rees, Implications of very rapid TeV variability in blazars. MNRAS **384**, 19–23 (2008). doi:10.1111/j.1745-3933.2007.00413.x

M.C. Begelman, B. Rudak, M. Sikora, Consequences of relativistic proton injection in active galactic nuclei. ApJ **362**, 38–51 (1990). doi:10.1086/169241

T.M. Belloni, States and Transitions in Black Hole Binaries, in *Lecture Notes in Physics, Berlin Springer Verlag*, ed. by T. Belloni. Lecture Notes in Physics, Berlin Springer Verlag, vol. 794, 2010, p. 53. doi:10.1007/978-3-540-76937-8-3

T. Belloni, M. Mendez, M. van der Klis, G. Hasinger, W.H.G. Lewin, J. van Paradijs, An Intermediate State of Cygnus X-1. ApJ **472**, 107 (1996). doi:10.1086/310369

A.M. Beloborodov, Plasma Ejection from Magnetic Flares and the X-Ray Spectrum of Cygnus X-1. ApJ **510**, 123–126 (1999)

V.S. Beskin, *MHD Flows in Compact Astrophysical Objects: Accretion, Winds and Jets* 2009

R.D. Blandford, A. Königl, Relativistic jets as compact radio sources. ApJ **232**, 34–48 (1979). doi:10.1086/157262

R.D. Blandford, A. Levinson, Pair cascades in extragalactic jets. 1: Gamma rays. ApJ **441**, 79–95 (1995). doi:10.1086/175338

R.D. Blandford, D.G. Payne, Hydromagnetic flows from accretion discs and the production of radio jets. MNRAS **199**, 883–903 (1982). doi:10.1093/mnras/199.4.883

R.D. Blandford, M.J. Rees, Some comments on radiation mechanisms in Lacertids, in *BL Lac Objects*, ed. by A.M. Wolfe, 1978, pp. 328–341

R.D. Blandford, R.L. Znajek, Electromagnetic extraction of energy from Kerr black holes. MNRAS **179**, 433–456 (1977). doi:10.1093/mnras/179.3.433

M. Błażejowski, M. Sikora, R. Moderski, G.M. Madejski, Comptonization of Infrared Radiation from Hot Dust by Relativistic Jets in Quasars. ApJ **545**, 107–116 (2000). doi:10.1086/317791

D. Blinov, V. Pavlidou, I. Papadakis, S. Kiehlmann, G. Panopoulou, I. Liodakis, O.G. King, E. Angelakis, M. Baloković, H. Das, R. Feiler, L. Fuhrmann, T. Hovatta, P. Khodade, A. Kus, N. Kylafis, A. Mahabal, I. Myserlis, D. Modi, B. Pazderska, E. Pazderski, I. Papamastorakis, T.J. Pearson, C. Rajarshi, A. Ramaprakash, P. Reig, A.C.S. Readhead, K. Tassis, J.A. Zensus, RoboPol: first season rotations of optical polarization plane in blazars. MNRAS **453**, 1669–1683 (2015). doi:10.1093/mnras/stv1723

D. Blinov, V. Pavlidou, I.E. Papadakis, T. Hovatta, T.J. Pearson, I. Liodakis, G.V. Panopoulou, E. Angelakis, M. Baloković, H. Das, P. Khodade, S. Kiehlmann, O.G. King, A. Kus, N. Kylafis, A. Mahabal, A. Marecki, D. Modi, I. Myserlis, E. Paleologou, I. Papamastorakis, B. Pazderska, E. Pazderski, C. Rajarshi, A. Ramaprakash, A.C.S. Readhead, P. Reig, K. Tassis, J.A. Zensus, RoboPol: optical polarization-plane rotations and flaring activity in blazars. MNRAS **457**,

2252–2262 (2016). doi:10.1093/mnras/stw158

G.R. Blumenthal, R.J. Gould, Bremsstrahlung, Synchrotron Radiation, and Compton Scattering of High-Energy Electrons Traversing Dilute Gases. Reviews of Modern Physics **42**, 237–271 (1970). doi:10.1103/RevModPhys.42.237

A. Bodaghee, J.A. Tomsick, K. Pottschmidt, J. Rodriguez, J. Wilms, G.G. Pooley, Gamma-Ray Observations of the Microquasars Cygnus X-1, Cygnus X-3, GRS 1915+105, and GX 339-4 with the Fermi Large Area Telescope. ApJ **775**, 98 (2013). doi:10.1088/0004-637X/775/2/98

M. Boettcher, P. Els, Gamma-Gamma Absorption in the Broad Line Region Radiation Fields of Gamma-Ray Blazars. (2016)

G. Bonnoli, G. Ghisellini, L. Foschini, F. Tavecchio, G. Ghirlanda, The γ-ray brightest days of the blazar 3C 454.3. MNRAS **410**, 368–380 (2011). doi:10.1111/j.1365-2966.2010.17450.x

S. Bonometto, A. Saggion, Polarization in Inverse Compton Scattering of Synchrotron Radiation. A&A **23**, 9 (1973)

V. Bosch-Ramon, G.E. Romero, J.M. Paredes, A broadband leptonic model for gamma-ray emitting microquasars. A&A **447**, 263–276 (2006). doi:10.1051/0004-6361:20053633

M. Böttcher, Modeling Intermediate BL Lac Objects Detected by Veritas. International Journal of Modern Physics D **19**, 873–878 (2010). doi:10.1142/S0218271810017135

M. Böttcher, J. Chiang, X-Ray Spectral Variability Signatures of Flares in BL Lacertae Objects. ApJ **581**, 127–142 (2002). doi:10.1086/344155

M. Böttcher, C.D. Dermer, On Compton Scattering Scenarios for Blazer Flares. ApJ **501**, 51–54 (1998). doi:10.1086/311458

M. Böttcher, C.D. Dermer, An Evolutionary Scenario for Blazar Unification. ApJ **564**, 86–91 (2002). doi:10.1086/324134

M. Böttcher, C.D. Dermer, Timing Signatures of the Internal-Shock Model for Blazars. ApJ **711**, 445–460 (2010). doi:10.1088/0004-637X/711/1/445

M. Böttcher, R. Schlickeiser, The pair production spectrum from photon-photon annihilation. A&A **325**, 866–870 (1997)

M. Böttcher, D.E. Harris, H. Krawczynski, *Relativistic Jets from Active Galactic Nuclei* 2012

M. Böttcher, H. Mause, R. Schlickeiser, γ-ray emission and spectral evolution of pair plasmas in AGN jets. I. General theory and a prediction for the GeV - TeV emission from ultrarelativistic jets. A&A **324**, 395–409 (1997)

M. Böttcher, A. Reimer, K. Sweeney, A. Prakash, Leptonic and Hadronic Modeling of Fermi-detected Blazars. ApJ **768**, 54 (2013). doi:10.1088/0004-637X/768/1/54

G.C. Bower, S. Markoff, J. Dexter, M.A. Gurwell, J.M. Moran, A. Brunthaler, H. Falcke, P.C. Fragile, D. Maitra, D. Marrone, A. Peck, A. Rushton, M.C.H. Wright, Radio and Millimeter Monitoring of Sgr A*: Spectrum, Variability, and Constraints on the G2 Encounter. ApJ **802**, 69 (2015). doi:10.1088/0004-637X/802/1/69

C. Brocksopp, R.P. Fender, G.G. Pooley, The orbital modulation in the radio emission of Cygnus X-1. MNRAS **336**, 699–704 (2002). doi:10.1046/j.1365-8711.2002.05813.x

G.R. Burbidge, On Synchrotron Radiation from Messier 87. ApJ **124**, 416 (1956). doi:10.1086/146237

B.J. Burn, On the depolarization of discrete radio sources by Faraday dispersion. MNRAS **133**, 67 (1966). doi:10.1093/mnras/133.1.67

A. Caccianiga, M.J.M. Marchã, The CLASS blazar survey: testing the blazar sequence. MNRAS **348**, 937–954 (2004). doi:10.1111/j.1365-2966.2004.07415.x

A. Cavaliere, V. D'Elia, The Blazar Main Sequence. ApJ **571**, 226–233 (2002). doi:10.1086/339778

M. Cerruti, C.D. Dermer, B. Lott, C. Boisson, A. Zech, Gamma-Ray Blazars near Equipartition and the Origin of the GeV Spectral Break in 3C 454.3. ApJ **771**, 4 (2013). doi:10.1088/2041-8205/771/1/L4

M. Cerruti, A. Zech, C. Boisson, S. Inoue, A hadronic origin for ultra-

high-frequency-peaked BL Lac objects. MNRAS **448**, 910–927 (2015). doi:10.1093/mnras/stu2691

X. Chen, M. Pohl, M. Böttcher, Particle diffusion and localized acceleration in inhomogeneous AGN jets - I. Steady-state spectra. MNRAS **447**, 530–544 (2015). doi:10.1093/mnras/stu2438

X. Chen, G. Fossati, E.P. Liang, M. Böttcher, Time-dependent simulations of multiwavelength variability of the blazar Mrk 421 with a Monte Carlo multizone code. MNRAS **416**, 2368–2387 (2011). doi:10.1111/j.1365-2966.2011.19215.x

X. Chen, M. Pohl, M. Böttcher, S. Gao, Particle diffusion and localized acceleration in inhomogeneous AGN jets - Part II: stochastic variation. MNRAS (2016). doi:10.1093/mnras/stw528

M. Chiaberge, G. Ghisellini, Rapid variability in the synchrotron self-Compton model for blazars. MNRAS **306**, 551–560 (1999). doi:10.1046/j.1365-8711.1999.02538.x

M. Chiaberge, A. Celotti, A. Capetti, G. Ghisellini, Does the unification of BL Lac and FR I radio galaxies require jet velocity structures? A&A **358**, 104–112 (2000)

M.J. Chodorowski, A.A. Zdziarski, M. Sikora, Reaction rate and energy-loss rate for photopair production by relativistic nuclei. ApJ **400**, 181–185 (1992). doi:10.1086/171984

R.T. Coogan, A.M. Brown, P.M. Chadwick, Localizing the γ-ray emission region during the 2014 June outburst of 3C 454.3. MNRAS **458**, 354–365 (2016). doi:10.1093/mnras/stw199

S. Corbel, R. Fender, Near-infrared synchrotron emission from the compact jet of gx 339-4. ApJ **573**, 35–39 (2002)

S. Corbel, R.P. Fender, A.K. Tzioumis, M. Nowak, V. McIntyre, P. Durouchoux, R. Sood, Coupling of the X-ray and radio emission in the black hole candidate and compact jet source GX 339-4. å **359**, 251–268 (2000)

S. Corbel, R.P. Fender, A.K. Tzioumis, J.A. Tomsick, J.A. Orosz, J.M. Miller, R. Wijnands, P. Kaaret, Large-Scale, Decelerating, Relativistic X-ray Jets from the Microquasar XTE J1550-564. Science **298**, 196–199 (2002). doi:10.1126/science.1075857

S. Corbel, M. Nowak, R.P. Fender, A.K. Tzioumis, S. Markoff, Radio/X-ray correlations in the low/hard state of GX 339−4. å **400**, 1007 (2003)

S. Corbel, M. Coriat, C. Brocksopp, A.K. Tzioumis, R.P. Fender, J.A. Tomsick, M.M. Buxton, C.D. Bailyn, The 'universal' radio/X-ray flux correlation: the case study of the black hole GX 339-4. MNRAS **428**, 2500–2515 (2013). doi:10.1093/mnras/sts215

H.D. Curtis, Descriptions of 762 Nebulae and Clusters Photographed with the Crossley Reflector. Publications of Lick Observatory **13**, 9–42 (1918)

T. Dauser, J. Garcia, J. Wilms, M. Böck, L.W. Brenneman, M. Falanga, K. Fukumura, C.S. Reynolds, Irradiation of an accretion disc by a jet: general properties and implications for spin measurements of black holes. MNRAS **430**, 1694–1708 (2013). doi:10.1093/mnras/sts710

C.D. Dermer, G. Menon, *High Energy Radiation from Black Holes: Gamma Rays, Cosmic Rays, and Neutrinos* 2009

C.D. Dermer, R. Schlickeiser, Model for the High-Energy Emission from Blazars. ApJ **416**, 458 (1993). doi:10.1086/173251

M. Díaz Trigo, J.C.A. Miller-Jones, S. Migliari, J.W. Broderick, T. Tzioumis, Baryons in the relativistic jets of the stellar-mass black-hole candidate 4U1630-47. Nature **504**, 260–262 (2013). doi:10.1038/nature12672

S. Dibi, S. Markoff, R. Belmont, J. Malzac, N.M. Barrière, J.A. Tomsick, Exploring plasma evolution during Sagittarius A* flares. MNRAS **441**, 1005–1016 (2014). doi:10.1093/mnras/stu599

S. Dibi, S. Markoff, R. Belmont, J. Malzac, J. Neilsen, G. Witzel, Using infrared/X-ray flare statistics to probe the emission regions near the event horizon of Sgr A. MNRAS(2016)

C. Diltz, M. Böttcher, Time dependent leptonic modeling of Fermi II processes in the jets of flat spectrum radio quasars. Journal of High Energy Astrophysics **1**,

63–70 (2014). doi:10.1016/j.jheap.2014.04.001

C. Diltz, M. Böttcher, G. Fossati, Time Dependent Hadronic Modeling of Flat Spectrum Radio Quasars. ApJ **802**, 133 (2015). doi:10.1088/0004-637X/802/2/133

D. Donato, G. Ghisellini, G. Tagliaferri, G. Fossati, Hard X-ray properties of blazars. A&A **375**, 739–751 (2001). doi:10.1051/0004-6361:20010675

L. Dondi, G. Ghisellini, Gamma-ray-loud blazars and beaming. MNRAS **273**, 583–595 (1995). doi:10.1093/mnras/273.3.583

A.C. Donea, R.J. Protheroe, Radiation fields of disk, BLR and torus in quasars and blazars: implications for /γ-ray absorption. Astroparticle Physics **18**, 377–393 (2003). doi:10.1016/S0927-6505(02)00155-X

J.B. Dove, J. Wilms, M. Maisack, M.C. Begelman, Self-Consistent Thermal Accretion Disk Corona Models for Compact Objects. ApJ **487**, 759 (1997). doi:10.1086/304647

J.S. Dunlop, J.A. Peacock, The Redshift Cut-Off in the Luminosity Function of Radio Galaxies and Quasars. MNRAS **247**, 19 (1990)

A.C. Fabian, M.J. Rees, L. Stella, N.E. White, X-ray fluorescence from the inner disc in Cygnus X-1. MNRAS **238**, 729–736 (1989). doi:10.1093/mnras/238.3.729

H. Falcke, P.L. Biermann, The jet-disk symbiosis. i. radio to x-ray emission models for quasars. å **293**, 665–682 (1995)

H. Falcke, E. Körding, S. Markoff, A Scheme to Unify Low-Power Accreting Black Holes. å **414**, 895 (2004)

R. Fender, Jets from X-ray binaries (Compact stellar X-ray sources, 2006), pp. 381–419

C.E. Fichtel, D.L. Bertsch, J. Chiang, B.L. Dingus, J.A. Esposito, J.M. Fierro, R.C. Hartman, S.D. Hunter, G. Kanbach, D.A. Kniffen, P.W. Kwok, Y.C. Lin, J.R. Mattox, H.A. Mayer-Hasselwander, L. McDonald, P.F. Michelson, C. von Montigny, P.L. Nolan, K. Pinkau, H.D. Radecke, H. Rothermel, P. Sreekumar, M. Sommer, E.J. Schneid, D.J. Thompson, T. Willis, The first energetic gamma-ray experiment telescope (EGRET) source catalog. ApJS **94**, 551–581 (1994). doi:10.1086/192082

J.D. Finke, Compton Dominance and the Blazar Sequence. ApJ **763**, 134 (2013). doi:10.1088/0004-637X/763/2/134

J.D. Finke, C.D. Dermer, On the Break in the Fermi-Large Area Telescope Spectrum of 3C 454.3. ApJ **714**, 303–307 (2010). doi:10.1088/2041-8205/714/2/L303

G. Fossati, L. Maraschi, A. Celotti, A. Comastri, G. Ghisellini, A unifying view of the spectral energy distributions of blazars. MNRAS **299**, 433–448 (1998). doi:10.1046/j.1365-8711.1998.01828.x

C.S. Froning, A.G. Cantrell, T.J. Maccarone, K. France, J. Khargharia, L.M. Winter, E.L. Robinson, R.I. Hynes, J.W. Broderick, S. Markoff, M.A.P. Torres, M. Garcia, C.D. Bailyn, J.X. Prochaska, J. Werk, C. Thom, S. Béland, C.W. Danforth, B. Keeney, J.C. Green, Multiwavelength Observations of A0620-00 in Quiescence. ApJ **743**, 26 (2011). doi:10.1088/0004-637X/743/1/26

E. Gallo, R.P. Fender, G.G. Pooley, A universal radio-X-ray correlation in low/hard state black hole binaries. MNRAS **344**, 60–72 (2003)

E. Gallo, R. Fender, C. Kaiser, D. Russell, R. Morganti, T. Oosterloo, S. Heinz, A dark jet dominates the power output of the stellar black hole Cygnus X-1. Nature **436**, 819–821 (2005). doi:10.1038/nature03879

E. Gallo, S. Migliari, S. Markoff, J.A. Tomsick, C.D. Bailyn, S. Berta, R. Fender, J.C.A. Miller-Jones, The Spectral Energy Distribution of Quiescent Black Hole X-Ray Binaries: New Constraints from Spitzer. ApJ **670**, 600–609 (2007). doi:10.1086/521524

E. Gallo, J.C.A. Miller-Jones, D.M. Russell, P.G. Jonker, J. Homan, R.M. Plotkin, S. Markoff, B.P. Miller, S. Corbel, R.P. Fender, The radio/X-ray domain of black hole X-ray binaries at the lowest radio luminosities. MNRAS **445**, 290–300 (2014). doi:10.1093/mnras/stu1599

P. Gandhi, A.W. Blain, D.M. Russell, P. Casella, J. Malzac, S. Corbel, P. D'Avanzo, F.W. Lewis, S. Markoff, M. Cadolle Bel, P. Goldoni, S. Wachter, D.

Khangulyan, A. Mainzer, A Variable Mid-infrared Synchrotron Break Associated with the Compact Jet in GX 339-4. ApJ **740**, 13 (2011). doi:10.1088/2041-8205/740/1/L13

M. Georganopoulos, F.A. Aharonian, J.G. Kirk, External Compton emission from relativistic jets in Galactic black hole candidates and ultraluminous X-ray sources. A&A **388**, 25–28 (2002). doi:10.1051/0004-6361:20020567

G. Ghisellini, P. Madau, On the origin of the gamma-ray emission in blazars. MNRAS **280**, 67–76 (1996). doi:10.1093/mnras/280.1.67

G. Ghisellini, F. Tavecchio, The blazar sequence: a new perspective. MNRAS **387**, 1669–1680 (2008). doi:10.1111/j.1365-2966.2008.13360.x

G. Ghisellini, F. Tavecchio, Canonical high-power blazars. MNRAS **397**, 985–1002 (2009). doi:10.1111/j.1365-2966.2009.15007.x

G. Ghisellini, F. Tavecchio, Fermi/LAT broad emission line blazars. MNRAS **448**, 1060–1077 (2015). doi:10.1093/mnras/stv055

G. Ghisellini, L. Maraschi, F. Tavecchio, The Fermi blazars' divide. MNRAS **396**, 105–109 (2009). doi:10.1111/j.1745-3933.2009.00673.x

G. Ghisellini, L. Maraschi, A. Treves, Inhomogeneous synchrotron-self-Compton models and the problem of relativistic beaming of BL Lac objects. A&A **146**, 204–212 (1985)

G. Ghisellini, F. Tavecchio, M. Chiaberge, Structured jets in TeV BL Lac objects and radiogalaxies. Implications for the observed properties. A&A **432**, 401–410 (2005). doi:10.1051/0004-6361:20041404

G. Ghisellini, A. Celotti, G. Fossati, L. Maraschi, A. Comastri, A theoretical unifying scheme for gamma-ray bright blazars. MNRAS **301**, 451–468 (1998). doi:10.1046/j.1365-8711.1998.02032.x

G. Ghisellini, F. Tavecchio, L. Foschini, G. Ghirlanda, L. Maraschi, A. Celotti, General physical properties of bright Fermi blazars. MNRAS **402**, 497–518 (2010). doi:10.1111/j.1365-2966.2009.15898.x

G. Ghisellini, F. Tavecchio, L. Foschini, T. Sbarrato, G. Ghirlanda, L. Maraschi, Blue Fermi flat spectrum radio quasars. MNRAS **425**, 1371–1379 (2012). doi:10.1111/j.1365-2966.2012.21554.x

G. Ghisellini, F. Tavecchio, L. Foschini, G. Bonnoli, G. Tagliaferri, The red blazar PMN J2345−1555 becomes blue. MNRAS **432**, 66–70 (2013). doi:10.1093/mnrasl/slt041

G. Ghisellini, F. Tavecchio, L. Maraschi, A. Celotti, T. Sbarrato, The power of relativistic jets is larger than the luminosity of their accretion disks. Nature **515**, 376–378 (2014). doi:10.1038/nature13856

D. Giannios, Reconnection-driven plasmoids in blazars: fast flares on a slow envelope. MNRAS **431**, 355–363 (2013). doi:10.1093/mnras/stt167

D. Giannios, D.A. Uzdensky, M.C. Begelman, Fast TeV variability in blazars: jets in a jet. MNRAS **395**, 29–33 (2009a). doi:10.1111/j.1745-3933.2009.00635.x

D. Giannios, D.A. Uzdensky, M.C. Begelman, Fast TeV variability in blazars: jets in a jet. MNRAS **395**, 29–33 (2009b). doi:10.1111/j.1745-3933.2009.00635.x

V.L. Ginzburg, On the Nature of the Radio Galaxies. AZh **38**, 380 (1961)

P. Giommi, P. Padovani, A simplified view of blazars: contribution to the X-ray and γ-ray extragalactic backgrounds. MNRAS **450**, 2404–2409 (2015). doi:10.1093/mnras/stv793

P. Giommi, P. Padovani, G. Polenta, A simplified view of blazars: the γ-ray case. MNRAS **431**, 1914–1922 (2013). doi:10.1093/mnras/stt305

P. Giommi, P. Padovani, G. Polenta, S. Turriziani, V. D'Elia, S. Piranomonte, A simplified view of blazars: clearing the fog around long-standing selection effects. MNRAS **420**, 2899–2911 (2012). doi:10.1111/j.1365-2966.2011.20044.x

T. Gleißner, J. Wilms, G.G. Pooley, M.A. Nowak, K. Pottschmidt, S. Markoff, S. Heinz, M. Klein-Wolt, R.P. Fender, R. Staubert, Long term variability of Cygnus X-1. III. Radio-X-ray correlations. å **425**, 1061–1068 (2004)

R.J. Gould, G.P. Schréder, Pair Production in Photon-Photon Collisions. Physical Review **155**, 1404–1407 (1967). doi:10.1103/PhysRev.155.1404

K. Gültekin, E.M. Cackett, J.M. Miller, T. Di Matteo, S. Markoff, D.O. Richstone, The Fundamental Plane of Accretion onto Black Holes with Dynamical Masses.

ApJ **706**, 404–416 (2009). doi:10.1088/0004-637X/706/1/404

F. Guo, X. Li, H. Li, W. Daughton, B. Zhang, N. Lloyd-Ronning, Y.H. Liu, H. Zhang, W. Deng, Efficient Production of High-energy Nonthermal Particles during Magnetic Reconnection in a Magnetically Dominated Ion-Electron Plasma. ApJ **818**, 9 (2016). doi:10.3847/2041-8205/818/1/L9

F. Haardt, Models for the X-ray emission from radio-quiet AGNs:. Mem. Soc. Astron. Italiana **68**, 73 (1997)

S. Heinz, Composition, Collimation, Contamination: The Jet of Cygnus X-1. ApJ **636**, 316–322 (2006). doi:10.1086/497954

S. Heinz, R.A. Sunyaev, The non-linear dependence of flux on black hole mass and accretion rate in core-dominated jets. MNRAS **343**, 59–64 (2003)

R.M. Hjellming, K.J. Johnston, Radio emission from conical jets associated with x-ray binaries. ApJ **328**, 600–609 (1988)

S. Hümmer, M. Rüger, F. Spanier, W. Winter, Simplified Models for Photohadronic Interactions in Cosmic Accelerators. ApJ **721**, 630–652 (2010). doi:10.1088/0004-637X/721/1/630

R.I. Hynes, C.W. Mauche, C.A. Haswell, C.R. Shrader, W. Cui, S. Chaty, The x-ray transient xte j1118+480: Multiwavelength observations of a low-state minioutburst. ApJ **539**, 37 (2000)

R.I. Hynes, C.A. Haswell, W. Cui, C.R. Shrader, K. O'Brien, S. Chaty, D.R. Skillman, J. Patterson, K. Horne, The remarkable rapid X-ray, ultraviolet, optical and infrared variability in the black hole XTE J1118+480. MNRAS **345**, 292–310 (2003)

M. Joshi, M. Böttcher, Time-dependent Radiation Transfer in the Internal Shock Model Scenario for Blazar Jets. ApJ **727**, 21 (2011). doi:10.1088/0004-637X/727/1/21

M. Kadler, F. Krauß, K. Mannheim, R. Ojha, C. Müller, R. Schulz, G. Anton, W. Baumgartner, T. Beuchert, S. Buson, B. Carpenter, T. Eberl, P.G. Edwards, D. Eisenacher Glawion, D. Elsässer, N. Gehrels, C. Gräfe, H. Hase, S. Horiuchi, C.W. James, A. Kappes, A. Kappes, U. Katz, A. Kreikenbohm, M. Kreter, I. Kreykenbohm, M. Langejahn, K. Leiter, E. Litzinger, F. Longo, J.E.J. Lovell, J. McEnery, C. Phillips, C. Plötz, J. Quick, E. Ros, F.W. Stecker, T. Steinbring, J. Stevens, D.J. Thompson, J. Trüstedt, A.K. Tzioumis, J. Wilms, J.A. Zensus, Coincidence of a high-fluence blazar outburst with a PeV-energy neutrino event. (2016)

M. Kalamkar, P. Casella, P. Uttley, K. O'Brien, D. Russell, T. Maccarone, M. van der Klis, F. Vincentelli, Detection of the first infra-red quasi periodic oscillation in a black hole X-ray binary. MNRAS, (2016). doi:10.1093/mnras/stw1211

M.M. Kaufman Bernadó, G.E. Romero, I.F. Mirabel, Precessing microblazars and unidentified gamma-ray sources. A&A **385**, 10–13 (2002). doi:10.1051/0004-6361:20020251

S.R. Kelner, F.A. Aharonian, Energy spectra of gamma rays, electrons, and neutrinos produced at interactions of relativistic protons with low energy radiation. Physical Review D **78**(3), 034013 (2008). doi:10.1103/PhysRevD.78.034013

S.R. Kelner, F.A. Aharonian, V.V. Bugayov, Energy spectra of gamma rays, electrons, and neutrinos produced at proton-proton interactions in the very high energy regime. Physical Review D **74**(3), 034018 (2006). doi:10.1103/PhysRevD.74.034018

C.F. Kennel, F.V. Coroniti, Magnetohydrodynamic model of Crab nebula radiation. ApJ **283**, 710–730 (1984). doi:10.1086/162357

J.G. Kirk, P. Duffy, TOPICAL REVIEW: Particle acceleration and relativistic shocks. Journal of Physics G Nuclear Physics **25**, 163–194 (1999). doi:10.1088/0954-3899/25/8/201

J.G. Kirk, F.M. Rieger, A. Mastichiadis, Particle acceleration and synchrotron emission in blazar jets. A&A **333**, 452–458 (1998)

K.I.I. Koljonen, D.M. Russell, J.A. Fernández-Ontiveros, S. Markoff, T.D. Russell, J.C.A. Miller-Jones, A.J. van der Horst, F. Bernardini, P. Casella, P.A. Curran, P. Gandhi, R. Soria, A Connection between Plasma Conditions near Black Hole Event Horizons and Outflow Properties. ApJ **814**, 139 (2015).

doi:10.1088/0004-637X/814/2/139

S.S. Komissarov, M.V. Barkov, N. Vlahakis, A. Königl, Magnetic acceleration of relativistic active galactic nucleus jets. MNRAS **380**, 51–70 (2007). doi:10.1111/j.1365-2966.2007.12050.x

H. Krawczynski, The Polarization Properties of Inverse Compton Emission and Implications for Blazar Observations with the GEMS X-Ray Polarimeter. ApJ **744**, 30 (2012). doi:10.1088/0004-637X/744/1/30

H.S. Krawczynski, D. Stern, F.A. Harrison, F.F. Kislat, A. Zajczyk, M. Beilicke, J. Hoormann, Q. Guo, R. Endsley, A.R. Ingram, H. Miyasaka, K.K. Madsen, K.M. Aaron, R. Amini, M.G. Baring, B. Beheshtipour, A. Bodaghee, J. Booth, C. Borden, M. Böttcher, F.E. Christensen, P.S. Coppi, R. Cowsik, S. Davis, J. Dexter, C. Done, L.A. Dominguez, D. Ellison, R.J. English, A.C. Fabian, A. Falcone, J.A. Favretto, R. Fernández, P. Giommi, B.W. Grefenstette, E. Kara, C.H. Lee, M. Lyutikov, T. Maccarone, H. Matsumoto, J. McKinney, T. Mihara, J.M. Miller, R. Narayan, L. Natalucci, F. Özel, M.J. Pivovaroff, S. Pravdo, D. Psaltis, T. Okajima, K. Toma, W.W. Zhang, X-ray polarimetry with the Polarization Spectroscopic Telescope Array (PolSTAR). Astroparticle Physics **75**, 8–28 (2016). doi:10.1016/j.astropartphys.2015.10.009

H. Krawczynski, S.B. Hughes, D. Horan, F. Aharonian, M.F. Aller, H. Aller, P. Boltwood, J. Buckley, P. Coppi, G. Fossati, N. Götting, J. Holder, D. Horns, O.M. Kurtanidze, A.P. Marscher, M. Nikolashvili, R.A. Remillard, A. Sadun, M. Schröder, Multiwavelength Observations of Strong Flares from the TeV Blazar 1ES 1959+650. ApJ **601**, 151–164 (2004). doi:10.1086/380393

J.H. Krolik, *Active galactic nuclei : from the central black hole to the galactic environment* 1999

J.P. Lasota, The disc instability model of dwarf novae and low-mass X-ray binary transients. New A Rev. **45**, 449–508 (2001). doi:10.1016/S1387-6473(01)00112-9

P. Laurent, J. Rodriguez, J. Wilms, M. Cadolle Bel, K. Pottschmidt, V. Grinberg, Polarized Gamma-Ray Emission from the Galactic Black Hole Cygnus X-1. Science **332**, 438 (2011). doi:10.1126/science.1200848

A. Lazarian, G.L. Eyink, E.T. Vishniac, G. Kowal, Magnetic Reconnection in Astrophysical Environments, in *Magnetic Fields in Diffuse Media*, ed. by A. Lazarian, E.M. de Gouveia Dal Pino, C. Melioli. Astrophysics and Space Science Library, vol. 407, 2015, p. 311. doi:10.1007/978-3-662-44625-612

A. Levinson, R. Blandford, Pair Cascades in Extragalactic Jets. II. The Beamed X-Ray Spectrum. ApJ **449**, 86 (1995). doi:10.1086/176034

A. Levinson, R. Blandford, On the Jets Associated with Galactic Superluminal Sources. ApJ **456**, 29 (1996). doi:10.1086/309851

A.P. Lightman, T.R. White, Effects of cold matter in active galactic nuclei - A broad hump in the X-ray spectra. ApJ **335**, 57–66 (1988). doi:10.1086/166905

K.R. Lind, R.D. Blandford, Semidynamical models of radio jets - Relativistic beaming and source counts. ApJ **295**, 358–367 (1985). doi:10.1086/163380

P. Lipari, M. Lusignoli, D. Meloni, Flavor composition and energy spectrum of astrophysical neutrinos. Physical Review D **75**(12), 123005 (2007). doi:10.1103/PhysRevD.75.123005

M.L. Lister, M.F. Aller, H.D. Aller, D.C. Homan, K.I. Kellermann, Y.Y. Kovalev, A.B. Pushkarev, J.L. Richards, E. Ros, T. Savolainen, MOJAVE. X. Parsec-scale Jet Orientation Variations and Superluminal Motion in Active Galactic Nuclei. AJ **146**, 120 (2013). doi:10.1088/0004-6256/146/5/120

H.T. Liu, J.M. Bai, Absorption of 10-200 GeV Gamma Rays by Radiation from Broad-Line Regions in Blazars. ApJ **653**, 1089–1097 (2006). doi:10.1086/509097

Y. Lyubarsky, Asymptotic Structure of Poynting-Dominated Jets. ApJ **698**, 1570–1589 (2009). doi:10.1088/0004-637X/698/2/1570

P. Magdziarz, A.A. Zdziarski, Angle-dependent Compton reflection of X-rays and gamma-rays. MNRAS **273**, 837–848 (1995)

D. Malyshev, A.A. Zdziarski, M. Chernyakova, High-energy gamma-ray emission from Cyg X-1 measured by Fermi and its theoretical implications. MNRAS **434**,

2380–2389 (2013). doi:10.1093/mnras/stt1184

N. Mankuzhiyil, S. Ansoldi, M. Persic, F. Tavecchio, The Environment and Distribution of Emitting Electrons as a Function of Source Activity in Markarian 421. ApJ **733**, 14 (2011). doi:10.1088/0004-637X/733/1/14

N. Mankuzhiyil, S. Ansoldi, M. Persic, E. Rivers, R. Rothschild, F. Tavecchio, Emitting Electrons and Source Activity in Markarian 501. ApJ **753**, 154 (2012). doi:10.1088/0004-637X/753/2/154

K. Mannheim, The proton blazar. A&A **269**, 67–76 (1993)

K. Mannheim, P.L. Biermann, Gamma-ray flaring of 3C 279 - A proton-initiated cascade in the jet? A&A **253**, 21–24 (1992)

L. Maraschi, F. Tavecchio, Spectral Energy Distributions of Blazars: Facts and Speculations, in *Blazar Demographics and Physics*, ed. by P. Padovani, C.M. Urry. Astronomical Society of the Pacific Conference Series, vol. 227, 2001, p. 40

L. Maraschi, G. Ghisellini, A. Celotti, A jet model for the gamma-ray emitting blazar 3C 279. ApJ **397**, 5–9 (1992). doi:10.1086/186531

A. Marcowith, G. Henri, G. Pelletier, Gamma-ray emission of blazars by a relativistic electron-positron beam. MNRAS **277**, 681–699 (1995). doi:10.1093/mnras/277.2.681

S. Markoff, From Multiwavelength to Mass Scaling: Accretion and Ejection in Microquasars and AGN, in *Lecture Notes in Physics, Berlin Springer Verlag*, ed. by T. Belloni. Lecture Notes in Physics, Berlin Springer Verlag, vol. 794, 2010, p. 143. doi:10.1007/978-3-540-76937-8-6

S. Markoff, M.A. Nowak, Constraining X-Ray Binary Jet Models via Reflection. ApJ **609**, 972–976 (2004)

S. Markoff, H. Falcke, R. Fender, A jet model for the broadband spectrum of XTE J1118+480. Synchrotron emission from radio to X-rays in the Low/Hard spectral state. A&A **372**, 25–28 (2001a). doi:10.1051/0004-6361:20010420

S. Markoff, M.A. Nowak, J. Wilms, Going with the Flow: Can the Base of Jets Subsume the Role of Compact Accretion Disk Coronae? ApJ **635**, 1203–1216 (2005a). doi:10.1086/497628

S. Markoff, M.A. Nowak, J. Wilms, Going with the Flow: Can the Base of Jets Subsume the Role of Compact Accretion Disk Coronae? ApJ **635**, 1203–1216 (2005b). doi:10.1086/497628

S. Markoff, H. Falcke, F. Yuan, P.L. Biermann, The nature of the 10 kilosecond flare in sgr a*. å **379**, 13–16 (2001b)

S. Markoff, M. Nowak, S. Corbel, R. Fender, H. Falcke, Exploring the Role of Jets in the Radio/X-ray Correlations of GX 339−4. å **397**, 645 (2003)

S. Markoff, M. Nowak, A. Young, H.L. Marshall, C.R. Canizares, A. Peck, M. Krips, G. Petitpas, R. Schödel, G.C. Bower, P. Chandra, A. Ray, M. Muno, S. Gallagher, S. Hornstein, C.C. Cheung, Results from an Extensive Simultaneous Broadband Campaign on the Underluminous Active Nucleus M81*: Further Evidence for Mass-scaling Accretion in Black Holes. ApJ **681**, 905–924 (2008). doi:10.1086/588718

S. Markoff, M.A. Nowak, E. Gallo, R. Hynes, J. Wilms, R.M. Plotkin, D. Maitra, C.V. Silva, S. Drappeau, As Above, So Below: Exploiting Mass Scaling in Black Hole Accretion to Break Degeneracies in Spectral Interpretation. ApJ **812**, 25 (2015). doi:10.1088/2041-8205/812/2/L25

A.P. Marscher, Relativistic jets and the continuum emission in QSOs. ApJ **235**, 386–391 (1980a). doi:10.1086/157642

A.P. Marscher, Spontaneous formation of knots in relativistic flows - A model for variability in compact synchrotron sources. ApJ **239**, 296–304 (1980b). doi:10.1086/158110

A.P. Marscher, Turbulent, Extreme Multi-zone Model for Simulating Flux and Polarization Variability in Blazars. ApJ **780**, 87 (2014). doi:10.1088/0004-637X/780/1/87

A.P. Marscher, W.K. Gear, Models for high-frequency radio outbursts in extragalactic sources, with application to the early 1983 millimeter-to-infrared flare of 3C 273. ApJ **298**, 114–127 (1985). doi:10.1086/163592

A.P. Marscher, S.G. Jorstad, F.D. D'Arcangelo, P.S. Smith, G.G. Williams, V.M. Larionov, H. Oh, A.R. Olmstead, M.F. Aller, H.D. Aller, I.M. McHardy, A. Lähteenmäki, M. Tornikoski, E. Valtaoja, V.A. Hagen-Thorn, E.N. Kopatskaya, W.K. Gear, G. Tosti, O. Kurtanidze, M. Nikolashvili, L. Sigua, H.R. Miller, W.T. Ryle, The inner jet of an active galactic nucleus as revealed by a radio-to-γ-ray outburst. Nature **452**, 966–969 (2008a). doi:10.1038/nature06895

A.P. Marscher, S.G. Jorstad, F.D. D'Arcangelo, P.S. Smith, G.G. Williams, V.M. Larionov, H. Oh, A.R. Olmstead, M.F. Aller, H.D. Aller, I.M. McHardy, A. Lähteenmäki, M. Tornikoski, E. Valtaoja, V.A. Hagen-Thorn, E.N. Kopatskaya, W.K. Gear, G. Tosti, O. Kurtanidze, M. Nikolashvili, L. Sigua, H.R. Miller, W.T. Ryle, The inner jet of an active galactic nucleus as revealed by a radio-to-γ-ray outburst. Nature **452**, 966–969 (2008b). doi:10.1038/nature06895

A.P. Marscher, S.G. Jorstad, V.M. Larionov, M.F. Aller, H.D. Aller, A. Lähteenmäki, I. Agudo, P.S. Smith, M. Gurwell, V.A. Hagen-Thorn, T.S. Konstantinova, E.G. Larionova, L.V. Larionova, D.A. Melnichuk, D.A. Blinov, E.N. Kopatskaya, I.S. Troitsky, M. Tornikoski, T. Hovatta, G.D. Schmidt, F.D. D'Arcangelo, D. Bhattarai, B. Taylor, A.R. Olmstead, E. Manne-Nicholas, M. Roca-Sogorb, J.L. Gómez, I.M. McHardy, O. Kurtanidze, M.G. Nikolashvili, G.N. Kimeridze, L.A. Sigua, Probing the Inner Jet of the Quasar PKS 1510-089 with Multi-Waveband Monitoring During Strong Gamma-Ray Activity. ApJ **710**, 126–131 (2010). doi:10.1088/2041-8205/710/2/L126

E. Massaro, P. Giommi, C. Leto, P. Marchegiani, A. Maselli, M. Perri, S. Piranomonte, S. Sclavi, Roma-BZCAT: a multifrequency catalogue of blazars. A&A **495**, 691–696 (2009). doi:10.1051/0004-6361:200810161

A. Mastichiadis, M. Petropoulou, S. Dimitrakoudis, Mrk 421 as a case study for TeV and X-ray variability in leptohadronic models. MNRAS **434**, 2684–2695 (2013). doi:10.1093/mnras/stt1210

J.E. McClintock, R.A. Remillard, Black hole binaries (Compact stellar X-ray sources, Eds. Walter Lewin & Michiel van der Klis. Cambridge Astrophysics Series, No. 39. Cambridge, UK: Cambridge University Press, 2006), pp. 157–213

J.E. McClintock, R. Narayan, J.F. Steiner, Black Hole Spin via Continuum Fitting and the Role of Spin in Powering Transient Jets. Space Sci. Rev. **183**, 295–322 (2014). doi:10.1007/s11214-013-0003-9

M.L. McConnell, A.A. Zdziarski, K. Bennett, H. Bloemen, W. Collmar, W. Hermsen, L. Kuiper, W. Paciesas, B.F. Phlips, J. Poutanen, J.M. Ryan, V. Schönfelder, H. Steinle, A.W. Strong, The Soft Gamma-Ray Spectral Variability of Cygnus X-1. ApJ **572**, 984–995 (2002). doi:10.1086/340436

I.M. McHardy, E. Koerding, C. Knigge, P. Uttley, R.P. Fender, Active galactic nuclei as scaled-up Galactic black holes. Nature **444**, 730–732 (2006). doi:10.1038/nature05389

J.C. McKinney, General relativistic magnetohydrodynamic simulations of the jet formation and large-scale propagation from black hole accretion systems. MNRAS **368**, 1561–1582 (2006). doi:10.1111/j.1365-2966.2006.10256.x

A. Merloni, A.C. Fabian, Coronal outflow dominated accretion discs: a new possibility for low-luminosity black holes? MNRAS **332**, 165–175 (2002)

A. Merloni, S. Heinz, T. di Matteo, A Fundamental Plane of black hole activity. MNRAS **345**, 1057–1076 (2003)

E.T. Meyer, G. Fossati, M. Georganopoulos, M.L. Lister, From the Blazar Sequence to the Blazar Envelope: Revisiting the Relativistic Jet Dichotomy in Radio-loud Active Galactic Nuclei. ApJ **740**, 98 (2011). doi:10.1088/0004-637X/740/2/98

S. Migliari, R. Fender, M. Méndez, Iron Emission Lines from Extended X-ray Jets in SS 433: Reheating of Atomic Nuclei. Science **297**, 1673–1676 (2002). doi:10.1126/science.1073660

G. Miniutti, A.C. Fabian, A light bending model for the X-ray temporal and spectral properties of accreting black holes. MNRAS **349**, 1435–1448 (2004)

I.F. Mirabel, L.F. Rodríguez, A superluminal source in the Galaxy. Nature **371**, 46–48 (1994). doi:10.1038/371046a0

I.F. Mirabel, L.F. Rodriguez, B. Cordier, J. Paul, F. Lebrun, A double-sided radio

jet from the compact Galactic Centre annihilator 1E1740.7-2942. Nature **358**, 215–217 (1992). doi:10.1038/358215a0

C. Motch, S.A. Ilovaisky, C. Chevalier, Discovery of fast optical activity in the X-ray source GX 339-4. å **109**, 1–4 (1982)

A. Mücke, R.J. Protheroe, A proton synchrotron blazar model for flaring in Markarian 501. Astroparticle Physics **15**, 121–136 (2001). doi:10.1016/S0927-6505(00)00141-9

A. Mücke, R. Engel, J.P. Rachen, R.J. Protheroe, T. Stanev, Monte Carlo simulations of photohadronic processes in astrophysics. Computer Physics Communications **124**, 290–314 (2000). doi:10.1016/S0010-4655(99)00446-4

A. Mücke, R.J. Protheroe, R. Engel, J.P. Rachen, T. Stanev, BL Lac objects in the synchrotron proton blazar model. Astroparticle Physics **18**, 593–613 (2003a). doi:10.1016/S0927-6505(02)00185-8

A. Mücke, R.J. Protheroe, R. Engel, J.P. Rachen, T. Stanev, BL Lac objects in the synchrotron proton blazar model. Astroparticle Physics **18**, 593–613 (2003b). doi:10.1016/S0927-6505(02)00185-8

R. Narayan, J.E. McClintock, Observational evidence for a correlation between jet power and black hole spin. MNRAS **419**, 69–73 (2012). doi:10.1111/j.1745-3933.2011.01181.x

R. Narayan, T. Piran, Variability in blazars: clues from PKS 2155-304. MNRAS **420**, 604–612 (2012). doi:10.1111/j.1365-2966.2011.20069.x

H. Netzer, Ionized gas in active galactic nuclei. New A Rev. **52**, 257–273 (2008). doi:10.1016/j.newar.2008.06.009

M.A. Nowak, M. Hanke, S.N. Trowbridge, S.B. Markoff, J. Wilms, K. Pottschmidt, P. Coppi, D. Maitra, J.E. Davis, F. Tramper, Corona, Jet, and Relativistic Line Models for Suzaku/RXTE/Chandra-HETG Observations of the Cygnus X-1 Hard State. ApJ **728**, 13 (2011). doi:10.1088/0004-637X/728/1/13

J.A. Orosz, J.E. McClintock, J.P. Aufdenberg, R.A. Remillard, M.J. Reid, R. Narayan, L. Gou, The Mass of the Black Hole in Cygnus X-1. ApJ **742**, 84 (2011). doi:10.1088/0004-637X/742/2/84

L. Pacciani, F. Tavecchio, I. Donnarumma, A. Stamerra, L. Carrasco, E. Recillas, A. Porras, M. Uemura, Exploring the Blazar Zone in High-energy Flares of FSRQs. ApJ **790**, 45 (2014). doi:10.1088/0004-637X/790/1/45

A.G. Pacholczyk, Faraday Rotation Effect in Extragalactic Radio Sources. Nature **200**, 765 (1963). doi:10.1038/200765a0

P. Padovani, P. Giommi, H. Landt, E.S. Perlman, The Deep X-Ray Radio Blazar Survey. III. Radio Number Counts, Evolutionary Properties, and Luminosity Function of Blazars. ApJ **662**, 182–198 (2007). doi:10.1086/516815

C. Pepe, G.S. Vila, G.E. Romero, Lepto-hadronic model for the broadband emission of Cygnus X-1. A&A **584**, 95 (2015). doi:10.1051/0004-6361/201527156

M. Petropoulou, A. Mastichiadis, On proton synchrotron blazar models: the case of quasar 3C 279. MNRAS **426**, 462–472 (2012). doi:10.1111/j.1365-2966.2012.21720.x

M. Petropoulou, S. Dimitrakoudis, P. Padovani, A. Mastichiadis, E. Resconi, Photohadronic origin of γ-ray BL Lac emission: implications for IceCube neutrinos. MNRAS **448**, 2412–2429 (2015). doi:10.1093/mnras/stv179

R.M. Plotkin, S.F. Anderson, W.N. Brandt, S. Markoff, O. Shemmer, J. Wu, The Lack of Torus Emission from BL Lacertae Objects: An Infrared View of Unification with WISE. ApJ **745**, 27 (2012a). doi:10.1088/2041-8205/745/2/L27

R.M. Plotkin, S. Markoff, B.C. Kelly, E. Körding, S.F. Anderson, Using the Fundamental Plane of black hole activity to distinguish X-ray processes from weakly accreting black holes. MNRAS **419**, 267–286 (2012b). doi:10.1111/j.1365-2966.2011.19689.x

R.M. Plotkin, E. Gallo, S. Markoff, J. Homan, P.G. Jonker, J.C.A. Miller-Jones, D.M. Russell, S. Drappeau, Constraints on relativistic jets in quiescent black hole X-ray binaries from broad-band spectral modelling. MNRAS **446**, 4098–4111 (2015). doi:10.1093/mnras/stu2385

R.M. Plotkin, E. Gallo, P.G. Jonker, J.C.A. Miller-Jones, J. Homan, T. Muñoz-Darias, S. Markoff, M. Armas Padilla, R. Fender, A.P. Rushton, D.M. Russell,

M.A.P. Torres, A clean sightline to quiescence: multiwavelength observations of the high Galactic latitude black hole X-ray binary Swift J1357.2-0933. MNRAS **456**, 2707–2716 (2016). doi:10.1093/mnras/stv2861

M. Pohl, R. Schlickeiser, On the conversion of blast wave energy into radiation in AGN and GRBs, in *American Institute of Physics Conference Series*, ed. by B.L. Dingus, M.H. Salamon, D.B. Kieda. American Institute of Physics Conference Series, vol. 515, 2000, pp. 249–252. doi:10.1063/1.1291375

P. Polko, D.L. Meier, S. Markoff, Determining the Optimal Locations for Shock Acceleration in Magnetohydrodynamical Jets. ApJ **723**, 1343–1350 (2010). doi:10.1088/0004-637X/723/2/1343

P. Polko, D.L. Meier, S. Markoff, Linking accretion flow and particle acceleration in jets - I. New relativistic magnetohydrodynamical jet solutions including gravity. MNRAS **428**, 587–598 (2013). doi:10.1093/mnras/sts052

P. Polko, D.L. Meier, S. Markoff, Linking accretion flow and particle acceleration in jets - II. Self-similar jet models with full relativistic MHD gravitational mass. MNRAS **438**, 959–970 (2014). doi:10.1093/mnras/stt2155

W.J. Potter, G. Cotter, Synchrotron and inverse-Compton emission from blazar jets - II. An accelerating jet model with a geometry set by observations of M87. MNRAS **429**, 1189–1205 (2013). doi:10.1093/mnras/sts407

J. Poutanen, Relativistic jets in blazars: Polarization of radiation. ApJS **92**, 607–609 (1994). doi:10.1086/192024

J. Poutanen, B. Stern, GeV Breaks in Blazars as a Result of Gamma-ray Absorption Within the Broad-line Region. ApJ **717**, 118–121 (2010). doi:10.1088/2041-8205/717/2/L118

J. Poutanen, J.H. Krolik, F. Ryde, The nature of spectral transitions in accreting black holes - The case of CYG X-1. MNRAS **292**, 21–25 (1997). doi:10.1093/mnras/292.1.L21

M.A. Prieto, J.A. Fernández-Ontiveros, S. Markoff, D. Espada, O. González-Martín, The central parsecs of M87: jet emission and an elusive accretion disc. MNRAS **457**, 3801–3816 (2016). doi:10.1093/mnras/stw166

J.P. Rachen, P.L. Biermann, Extragalactic Ultra-High Energy Cosmic-Rays - Part One - Contribution from Hot Spots in Fr-II Radio Galaxies. å **272**, 161 (1993)

C.M. Raiteri, A. Capetti, Testing the blazar sequence with the least luminous BL Lacertae objects. A&A **587**, 8 (2016). doi:10.1051/0004-6361/201527679

T.A. Rector, J.T. Stocke, E.S. Perlman, S.L. Morris, I.M. Gioia, The Properties of the X-Ray-selected EMSS Sample of BL Lacertae Objects. AJ **120**, 1626–1647 (2000). doi:10.1086/301587

M.J. Rees, Appearance of Relativistically Expanding Radio Sources. Nature **211**, 468–470 (1966). doi:10.1038/211468a0

M.M. Reynoso, G.E. Romero, Magnetic field effects on neutrino production in microquasars. A&A **493**, 1–11 (2009). doi:10.1051/0004-6361:200811004

M.M. Reynoso, M.C. Medina, G.E. Romero, A lepto-hadronic model for high-energy emission from FR I radiogalaxies. A&A **531**, 30 (2011). doi:10.1051/0004-6361/201014998

M.M. Reynoso, G.E. Romero, M.C. Medina, A two-component model for the high-energy variability of blazars. Application to PKS 2155-304. A&A **545**, 125 (2012). doi:10.1051/0004-6361/201219873

J. Rodriguez, S. Corbel, J.A. Tomsick, Spectral Evolution of the Microquasar XTE J1550-564 over Its Entire 2000 Outburst. ApJ **595**, 1032–1038 (2003). doi:10.1086/377478

J. Rodriguez, V. Grinberg, P. Laurent, M. Cadolle Bel, K. Pottschmidt, G. Pooley, A. Bodaghee, J. Wilms, C. Gouiffès, Spectral State Dependence of the 0.4-2 MeV Polarized Emission in Cygnus X-1 Seen with INTEGRAL/IBIS, and Links with the AMI Radio Data. ApJ **807**, 17 (2015). doi:10.1088/0004-637X/807/1/17

G.E. Romero, G.S. Vila, The proton low-mass microquasar: high-energy emission. A&A **485**, 623–631 (2008). doi:10.1051/0004-6361:200809563

G.E. Romero, G.S. Vila, *Introduction to Black Hole Astrophysics*. Lecture Notes in Physics, Berlin Springer Verlag, vol. 876 2014. doi:10.1007/978-3-642-39596-3

G.E. Romero, H.R. Christiansen, M. Orellana, Hadronic High-Energy Gamma-Ray Emission from the Microquasar LS I +61 303. ApJ **632**, 1093–1098 (2005). doi:10.1086/444446

G.E. Romero, J.A. Combi, H. Vucetich, Rapid Variability in the Southern Blazar PKS 0521-365. Ap&SS **225**, 183–204 (1995). doi:10.1007/BF00613234

G.E. Romero, F.L. Vieyro, S. Chaty, Coronal origin of the polarization of the high-energy emission of Cygnus X-1. A&A **562**, 7 (2014). doi:10.1051/0004-6361/201323316

G.E. Romero, F.L. Vieyro, G.S. Vila, Non-thermal processes around accreting galactic black holes. A&A **519**, 109 (2010). doi:10.1051/0004-6361/200913663

G.E. Romero, D.F. Torres, M.M. Kaufman Bernadó, I.F. Mirabel, Hadronic gamma-ray emission from windy microquasars. A&A **410**, 1–4 (2003). doi:10.1051/0004-6361:20031314-1

P. Rossi, A. Mignone, G. Bodo, S. Massaglia, A. Ferrari, Formation of dynamical structures in relativistic jets: the FRI case. A&A **488**, 795–806 (2008). doi:10.1051/0004-6361:200809687

A. Rushton, J. Miller-Jones, Z. Paragi, T. Maccarone, G. Pooley, V. Tudose, R. Fender, R. Spencer, V. Dhawan, M. Garrett, VLBI constraints on the "jet-line" of Cygnus X-1. (2011)

D.M. Russell, E. Gallo, R.P. Fender, Observational constraints on the powering mechanism of transient relativistic jets. MNRAS **431**, 405–414 (2013a). doi:10.1093/mnras/stt176

D.M. Russell, R.P. Fender, R.I. Hynes, C. Brocksopp, J. Homan, P.G. Jonker, M.M. Buxton, Global optical/infrared-X-ray correlations in X-ray binaries: quantifying disc and jet contributions. MNRAS **371**, 1334–1350 (2006). doi:10.1111/j.1365-2966.2006.10756.x

D.M. Russell, D. Maitra, R.J.H. Dunn, S. Markoff, Evidence for a compact jet dominating the broad-band spectrum of the black hole accretor XTE J1550-564. MNRAS **405**, 1759–1769 (2010). doi:10.1111/j.1365-2966.2010.16547.x

D.M. Russell, S. Markoff, P. Casella, A.G. Cantrell, R. Chatterjee, R.P. Fender, E. Gallo, P. Gandhi, J. Homan, D. Maitra, J.C.A. Miller-Jones, K. O'Brien, T. Shahbaz, Jet spectral breaks in black hole X-ray binaries. MNRAS **429**, 815–832 (2013b). doi:10.1093/mnras/sts377

T.D. Russell, R. Soria, J.C.A. Miller-Jones, P.A. Curran, S. Markoff, D.M. Russell, G.R. Sivakoff, The accretion-ejection coupling in the black hole candidate X-ray binary MAXI J1836-194. MNRAS **439**, 1390–1402 (2014). doi:10.1093/mnras/stt2498

G.B. Rybicki, A.P. Lightman, *Radiative processes in astrophysics* 1979

S. Sabatini, M. Tavani, E. Striani, A. Bulgarelli, V. Vittorini, G. Piano, E. Del Monte, M. Feroci, F. de Pasquale, M. Trifoglio, F. Gianotti, A. Argan, G. Barbiellini, P. Caraveo, P.W. Cattaneo, A.W. Chen, F. D'Ammando, E. Costa, G. De Paris, G. Di Cocco, I. Donnarumma, Y. Evangelista, A. Ferrari, M. Fiorini, F. Fuschino, M. Galli, A. Giuliani, M. Giusti, C. Labanti, F. Lazzarotto, P. Lipari, F. Longo, M. Marisaldi, S. Mereghetti, E. Morelli, E. Moretti, A. Morselli, L. Pacciani, A. Pellizzoni, F. Perotti, P. Picozza, M. Pilia, G. Pucella, M. Prest, M. Rapisarda, A. Rappoldi, A. Rubini, E. Scalise, P. Soffitta, A. Trois, E. Vallazza, S. Vercellone, A. Zambra, D. Zanello, C. Pittori, F. Verrecchia, P. Santolamazza, P. Giommi, S. Colafrancesco, L.A. Antonelli, L. Salotti, Episodic Transient Gamma-ray Emission from the Microquasar Cygnus X-1. ApJ **712**, 10–15 (2010). doi:10.1088/2041-8205/712/1/L10

S. Sabatini, M. Tavani, P. Coppi, G. Pooley, M. Del Santo, R. Campana, A. Chen, Y. Evangelista, G. Piano, A. Bulgarelli, P.W. Cattaneo, S. Colafrancesco, E. Del Monte, A. Giuliani, M. Giusti, F. Longo, A. Morselli, A. Pellizzoni, M. Pilia, E. Striani, M. Trifoglio, S. Vercellone, Gamma-Ray Observations of Cygnus X-1 above 100 MeV in the Hard and Soft States. ApJ **766**, 83 (2013). doi:10.1088/0004-637X/766/2/83

R.M. Sambruna, L. Maraschi, C.M. Urry, On the Spectral Energy Distributions of Blazars. ApJ **463**, 444 (1996). doi:10.1086/177260

R. Schlickeiser, Models of high-energy emission from active galactic nuclei. A&AS

120, 481–489 (1996)

R. Schlickeiser, *Cosmic Ray Astrophysics* 2002

M. Schmidt, 3C 273 : A Star-Like Object with Large Red-Shift. Nature **197**, 1040 (1963). doi:10.1038/1971040a0

T. Shahbaz, D.M. Russell, C. Zurita, J. Casares, J.M. Corral-Santana, V.S. Dhillon, T.R. Marsh, Evidence for quiescent synchrotron emission in the black hole X-ray transient Swift J1357.2-0933. MNRAS **434**, 2696–2706 (2013). doi:10.1093/mnras/stt1212

I.S. Shklovskii, Radio Galaxies. Soviet Ast. **4**, 885 (1961)

M. Sikora, G. Madejski, On Pair Content and Variability of Subparsec Jets in Quasars. ApJ **534**, 109–113 (2000). doi:10.1086/308756

M. Sikora, M.C. Begelman, M.J. Rees, Comptonization of diffuse ambient radiation by a relativistic jet: The source of gamma rays from blazars? ApJ **421**, 153–162 (1994). doi:10.1086/173633

L. Sironi, A. Spitkovsky, Relativistic Reconnection: An Efficient Source of Nonthermal Particles. ApJ **783**, 21 (2014). doi:10.1088/2041-8205/783/1/L21

L. Sironi, M. Petropoulou, D. Giannios, Relativistic jets shine through shocks or magnetic reconnection? MNRAS **450**, 183–191 (2015). doi:10.1093/mnras/stv641

P. Soffitta, X. Barcons, R. Bellazzini, J. Braga, E. Costa, G.W. Fraser, S. Gburek, J. Huovelin, G. Matt, M. Pearce, J. Poutanen, V. Reglero, A. Santangelo, R.A. Sunyaev, G. Tagliaferri, M. Weisskopf, R. Aloisio, E. Amato, P. Attiná, M. Axelsson, L. Baldini, S. Basso, S. Bianchi, P. Blasi, J. Bregeon, A. Brez, N. Bucciantini, L. Burderi, V. Burwitz, P. Casella, E. Churazov, M. Civitani, S. Covino, R.M. Curado da Silva, G. Cusumano, M. Dadina, F. D'Amico, A. De Rosa, S. Di Cosimo, G. Di Persio, T. Di Salvo, M. Dovciak, R. Elsner, C.J. Eyles, A.C. Fabian, S. Fabiani, H. Feng, S. Giarrusso, R.W. Goosmann, P. Grandi, N. Grosso, G. Israel, M. Jackson, P. Kaaret, V. Karas, M. Kuss, D. Lai, G.L. Rosa, J. Larsson, S. Larsson, L. Latronico, A. Maggio, J. Maia, F. Marin, M.M. Massai, T. Mineo, M. Minuti, E. Moretti, F. Muleri, S.L. O'Dell, G. Pareschi, G. Peres, M. Pesce, P.O. Petrucci, M. Pinchera, D. Porquet, B. Ramsey, N. Rea, F. Reale, J.M. Rodrigo, A. Różańska, A. Rubini, P. Rudawy, F. Ryde, M. Salvati, V.A. de Santiago, S. Sazonov, C. Sgró, E. Silver, G. Spandre, D. Spiga, L. Stella, T. Tamagawa, F. Tamborra, F. Tavecchio, T. Teixeira Dias, M. van Adelsberg, K. Wu, S. Zane, XIPE: the X-ray imaging polarimetry explorer. Experimental Astronomy **36**, 523–567 (2013). doi:10.1007/s10686-013-9344-3

A. Sokolov, A.P. Marscher, I.M. McHardy, Synchrotron Self-Compton Model for Rapid Nonthermal Flares in Blazars with Frequency-dependent Time Lags. ApJ **613**, 725–746 (2004). doi:10.1086/423165

M. Spada, G. Ghisellini, D. Lazzati, A. Celotti, Internal shocks in the jets of radio-loud quasars. MNRAS **325**, 1559–1570 (2001). doi:10.1046/j.1365-8711.2001.04557.x

H.C. Spruit, Theory of Magnetically Powered Jets, in *Lecture Notes in Physics, Berlin Springer Verlag*, ed. by T. Belloni. Lecture Notes in Physics, Berlin Springer Verlag, vol. 794, 2010, p. 233. doi:10.1007/978-3-540-76937-8

B.E. Stern, J. Poutanen, Variation of the $\gamma\gamma$ opacity by the He II Lyman continuum constrains the location of the γ-ray emission region in the blazar 3C 454.3. MNRAS **417**, 11–15 (2011). doi:10.1111/j.1745-3933.2011.01107.x

B.E. Stern, J. Poutanen, The Mystery of Spectral Breaks: Lyman Continuum Absorption by Photon-Photon Pair Production in the Fermi GeV Spectra of Bright Blazars. ApJ **794**, 8 (2014). doi:10.1088/0004-637X/794/1/8

A.M. Stirling, R.E. Spencer, C.J. de la Force, M.A. Garrett, R.P. Fender, R.N. Ogley, A relativistic jet from Cygnus X-1 in the low/hard X-ray state. MNRAS **327**, 1273–1278 (2001). doi:10.1046/j.1365-8711.2001.04821.x

E.J. Summerlin, M.G. Baring, Diffusive Acceleration of Particles at Oblique, Relativistic, Magnetohydrodynamic Shocks. ApJ **745**, 63 (2012). doi:10.1088/0004-637X/745/1/63

M. Tavani, V. Vittorini, A. Cavaliere, An Emerging Class of Gamma-ray Flares from Blazars: Beyond One-zone Models. ApJ **814**, 51 (2015). doi:10.1088/0004-

637X/814/1/51

F. Tavecchio, G. Ghisellini, Spine-sheath layer radiative interplay in subparsec-scale jets and the TeV emission from M87. MNRAS **385**, 98–102 (2008). doi:10.1111/j.1745-3933.2008.00441.x

F. Tavecchio, G. Ghisellini, On the magnetization of BL Lac jets. MNRAS **456**, 2374–2382 (2016). doi:10.1093/mnras/stv2790

F. Tavecchio, G. Ghisellini, D. Guetta, Structured Jets in BL Lac Objects: Efficient PeV Neutrino Factories? ApJ **793**, 18 (2014). doi:10.1088/2041-8205/793/1/L18

F. Tavecchio, L. Maraschi, G. Ghisellini, Constraints on the Physical Parameters of TeV Blazars. ApJ **509**, 608–619 (1998). doi:10.1086/306526

F. Tavecchio, L. Maraschi, E. Pian, L. Chiappetti, A. Celotti, G. Fossati, G. Ghisellini, E. Palazzi, C.M. Raiteri, R.M. Sambruna, A. Treves, C.M. Urry, M. Villata, A. Djannati-Ataï, Theoretical Implications from the Spectral Evolution of Markarian 501 Observed with BeppoSAX. ApJ **554**, 725–733 (2001). doi:10.1086/321394

F. Tavecchio, G. Ghisellini, G. Bonnoli, G. Ghirlanda, Constraining the location of the emitting region in Fermi blazars through rapid γ-ray variability. MNRAS **405**, 94–98 (2010). doi:10.1111/j.1745-3933.2010.00867.x

F. Tavecchio, J. Becerra-Gonzalez, G. Ghisellini, A. Stamerra, G. Bonnoli, L. Foschini, L. Maraschi, On the origin of the γ-ray emission from the flaring blazar PKS 1222+216. A&A **534**, 86 (2011). doi:10.1051/0004-6361/201117204

A. Tchekhovskoy, J.C. McKinney, R. Narayan, Simulations of ultrarelativistic magnetodynamic jets from gamma-ray burst engines. MNRAS **388**, 551–572 (2008). doi:10.1111/j.1365-2966.2008.13425.x

A. Tchekhovskoy, R. Narayan, J.C. McKinney, Magnetohydrodynamic simulations of gamma-ray burst jets: Beyond the progenitor star. New A **15**, 749–754 (2010). doi:10.1016/j.newast.2010.03.001

B.E. Tetarenko, G.R. Sivakoff, C.O. Heinke, J.C. Gladstone, WATCHDOG: A Comprehensive All-sky Database of Galactic Black Hole X-ray Binaries. ApJS **222**, 15 (2016). doi:10.3847/0067-0049/222/2/15

L. Titarchuk, Generalized Comptonization models and application to the recent high-energy observations. ApJ **434**, 570–586 (1994). doi:10.1086/174760

M.H. Ulrich, L. Maraschi, C.M. Urry, Variability of Active Galactic Nuclei. ARA&A **35**, 445–502 (1997). doi:10.1146/annurev.astro.35.1.445

C.M. Urry, P. Padovani, Unified Schemes for Radio-Loud Active Galactic Nuclei. PASP **107**, 803 (1995). doi:10.1086/133630

G.S. Vila, G.E. Romero, Leptonic/hadronic models for electromagnetic emission in microquasars: the case of GX 339-4. MNRAS **403**, 1457–1468 (2010). doi:10.1111/j.1365-2966.2010.16208.x

G.S. Vila, G.E. Romero, N.A. Casco, An inhomogeneous lepto-hadronic model for the radiation of relativistic jets. Application to XTE J1118+480. A&A **538**, 97 (2012). doi:10.1051/0004-6361/201118106

N. Vlahakis, A. Königl, Relativistic Magnetohydrodynamics with Application to Gamma-Ray Burst Outflows. I. Theory and Semianalytic Trans-Alfvénic Solutions. ApJ **596**, 1080–1103 (2003). doi:10.1086/378226

N. Vlahakis, K. Tsinganos, C. Sauty, E. Trussoni, A disc-wind model with correct crossing of all magnetohydrodynamic critical surfaces. MNRAS **318**, 417–428 (2000). doi:10.1046/j.1365-8711.2000.03703.x

M. Weidinger, F. Spanier, A self-consistent and time-dependent hybrid blazar emission model. Properties and application. A&A **573**, 7 (2015). doi:10.1051/0004-6361/201424159

J. Wilms, M.A. Nowak, K. Pottschmidt, G.G. Pooley, S. Fritz, Long term variability of Cygnus X-1. IV. Spectral evolution 1999-2004. å **447**, 245–261 (2006). doi:10.1051/0004-6361:20053938

D. Yan, L. Zhang, Understanding the TeV emission from a distant blazar PKS 1424+240 in a lepto-hadronic jet model. MNRAS **447**, 2810–2816 (2015). doi:10.1093/mnras/stu2551

F. Yuan, E. Quataert, R. Narayan, Nonthermal Electrons in Radiatively Inefficient

Accretion Flow Models of Sagittarius A*. ApJ **598**, 301–312 (2003)

R. Zanin, A. Fernández-Barral, E. de Oña-Wilhelmi, F. Aharonian, O. Blanch, V. Bosch-Ramon, D. Galindo, Detection of gamma rays of likely jet origin in Cygnus X-1. (2016)

A.A. Zdziarski, M. Böttcher, Hadronic models of blazars require a change of the accretion paradigm. MNRAS **450**, 21–25 (2015). doi:10.1093/mnrasl/slv039

A.A. Zdziarski, P. Lubiński, M. Sikora, The MeV spectral tail in Cyg X-1 and optically thin emission of jets. MNRAS **423**, 663–675 (2012). doi:10.1111/j.1365-2966.2012.20903.x

A.A. Zdziarski, Ł. Stawarz, P. Pjanka, M. Sikora, Jet models for black hole binaries in the hard spectral state. MNRAS **440**, 2238–2254 (2014). doi:10.1093/mnras/stu420

J.A. Zensus, T.J. Pearson (eds.), Superluminal radio sources; Proceedings of the Workshop, Pasadena, CA, Oct. 28-30, 1986, in *Superluminal Radio Sources* 1987

H. Zhang, M. Böttcher, X-Ray and Gamma-Ray Polarization in Leptonic and Hadronic Jet Models of Blazars. ApJ **774**, 18 (2013). doi:10.1088/0004-637X/774/1/18

H. Zhang, X. Chen, M. Böttcher, Synchrotron Polarization in Blazars. ApJ **789**, 66 (2014). doi:10.1088/0004-637X/789/1/66

H. Zhang, X. Chen, M. Böttcher, F. Guo, H. Li, Polarization Swings Reveal Magnetic Energy Dissipation in Blazars. ApJ **804**, 58 (2015). doi:10.1088/0004-637X/804/1/58

H. Zhang, W. Deng, H. Li, M. Böttcher, Polarization Signatures of Relativistic Magnetohydrodynamic Shocks in the Blazar Emission Region. I. Force-free Helical Magnetic Fields. ApJ **817**, 63 (2016). doi:10.3847/0004-637X/817/1/63